

Straylight as Additional Indicator for Visual Function Assessment and Clinical Decision Making

Maartje C.J. van Bree

Straylight as Additional Indicator for Visual Function Assessment and Clinical Decision Making

Maartje van Bree

The research leading to this thesis was financially supported by the 'Stichting Wetenschappelijk Onderzoek Oogziekenhuis (SWOO) - Prof.dr. H.J. Flieringa.

Printing of this thesis was financially supported by Abbott Medical Optics (AMO) Netherlands BV, Alcon Nederland BV, Allergan BV, Bausch & Lomb BV, Carl Zeiss BV, Laméris Ootech BV, Merck, Sharp & Dohme BV, Simovision BV, Théa Pharma, Ursapharm Benelux BV and Dutch Ophthalmic Research Center (D.O.R.C.) (International) BV.

ISBN 978-94-6169-353-2

© Maartje van Bree, 2013

All rights reserved. No parts of this thesis may be reproduced, stored in a retrieval system, or transmitted in any form or by any means, electronic, mechanical, photocopying, recording or otherwise, without the prior written permission of the corresponding journals or the author.

Cover illustration: M.J.P. & A.L.P. van Bree

Cover design: Optima Grafische Communicatie, Rotterdam, The Netherlands

Layout and printing: Optima Grafische Communicatie, Rotterdam, The Netherlands

Straylight as Additional Indicator for Visual Function Assessment and Clinical Decision Making

**Strooilicht als additionele indicator voor
beoordeling van de visuele functie en klinische besluitvorming**

Proefschrift

ter verkrijging van de graad van doctor aan de
Erasmus Universiteit Rotterdam
op gezag van de
rector magnificus
Prof.dr. H.G. Smidt
en volgens besluit van het College voor Promoties.

De openbare verdediging zal plaatsvinden op
woensdag 13 maart 2013 om 15:30 uur

door

Maartje Christina Johanna van Bree

geboren te Tilburg



PROMOTIECOMMISSIE

Promotor:

Prof.dr. J.C. van Meurs

Overige leden:

Prof.dr. N.M. Jansonius

Prof.dr. G. van Rij

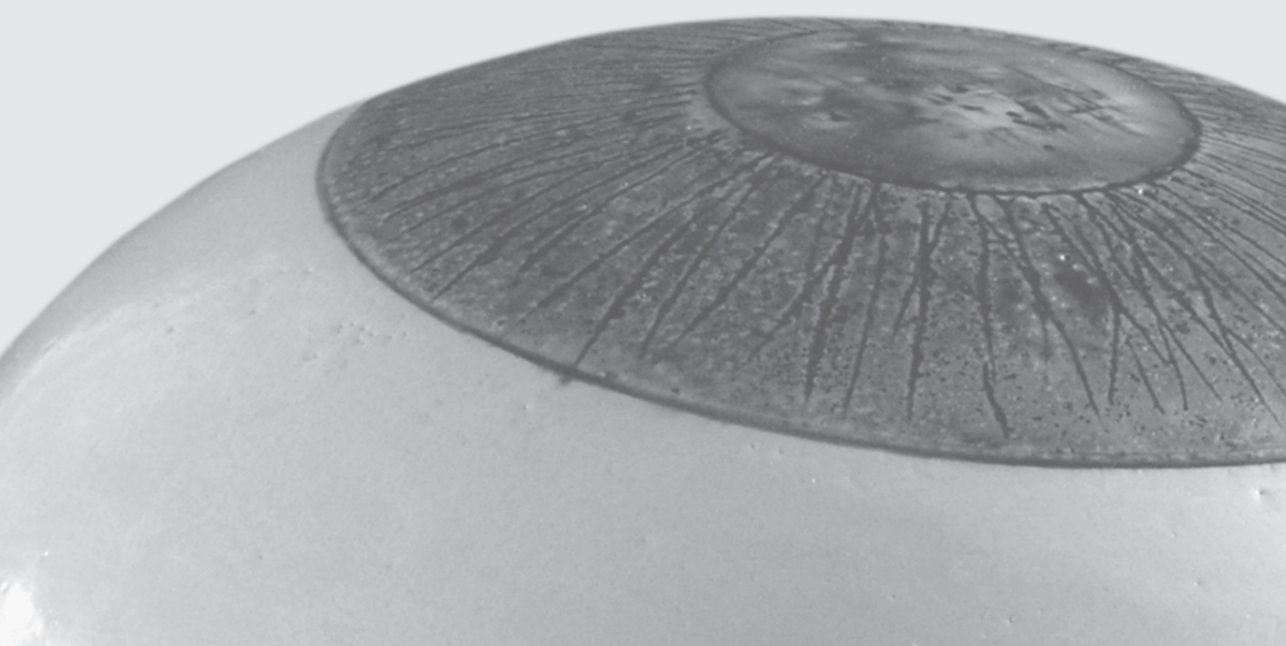
Dr. J. van der Steen

Copromotor:

Dr. T.J.T.P. van den Berg

Table of contents

Chapter 1	
General introduction	7
Chapter 2	
Aim and outline	21
Chapter 3	
Real-world scenes captured through PCO specimens: simulation of visual function deterioration experienced by PCO patients	29
Chapter 4	
Effect of Nd:YAG laser capsulotomy on retinal straylight values in patients with posterior capsule opacification	37
Chapter 5	
Posterior capsule opacification severity, assessed with straylight measurement, as main indicator of early visual function deterioration	51
Chapter 6	
Imaging of forward light-scatter by opacified posterior capsules isolated from pseudophakic donor eyes	83
Chapter 7	
In vitro recording of forward light-scatter by human lens capsules and different types of posterior capsule opacification	107
Chapter 8	
Straylight values after refractive surgery: screening for ocular fitness in demanding professions	125
Summary	145
Summary in Dutch - Samenvatting	151
Abbreviations	157
PhD portfolio	159
List of publications	161
Dankwoord	163
About the author	167



Chapter 1

General introduction



1.1 VISUAL FUNCTION

For decades, visual function (VF) was defined by visual acuity (VA) and visual field. VA is a measure of perception of fine detail. In ophthalmic practice, corrected distance visual acuity (CDVA) is routinely tested using a letter chart and appropriate spectacles or contact lenses. Visual field examination is used to determine retinal luminance sensitivity at various retinal locations, and to determine the boundaries of peripheral vision. Then it was realized that other aspects of VF are also important for visual performance in the “real world”: quite frequently, patients report subjective visual symptoms despite having good CDVA (and normal visual field). In other words, it was realized that good CDVA does not imply good VF. Ophthalmic interventions were usually evaluated using VA as an outcome parameter. Real-world visual scenes however, comprise complex combinations of contrasts with large luminance differences; including luminance differences that are more subtle than the high contrast letters used for CDVA testing. To evaluate this part of VF, contrast sensitivity (CS) tests were introduced. CS is a measure for the ability to detect luminance differences, in particular the ability to detect the luminance difference between an object and its surroundings. CS is tested using a chart with sinusoidal gratings or low contrast letters. However, the aspect of VF assessed with CS testing is quite similar to that assessed with VA testing. The more independent aspect of VF that could still not be adequately assessed is straylight (see “Straylight” section). Straylight causes glare sensitivity. Glare sensitivity can be described as loss of visual quality, or even loss of VF, that is particularly experienced in the presence of a distant bright light source and low-contrast surroundings. Glare symptoms include blinding, perception of halos (ring of light) around bright lights, “hazy vision”, and lowered contrast perception. Glare sensitivity enhanced scientific curiosity for straylight. After it was found that glare sensitivity is caused by intraocular straylight, glare sensitivity was officially defined as straylight. The straylight parameter was introduced as a well defined measure for this aspect of VF (see “Clinical straylight measurement” section). A typical example of glare sensitivity is the blinding effect of headlights of oncoming traffic during night driving (Figure 1).¹⁻³



Figure 1. The blinding effect of headlights of oncoming traffic during night driving: typical examples of glare sensitivity in a healthy, young eye (A), and an eye with increased intraocular straylight (B).

Figure 1A illustrates how a person with a healthy, young eye would see, whereas Figure 1B illustrates how a person with increased intraocular straylight would see. Luminance caused by the bright headlights spreads in all directions, acting as a veil of light covering the entire visual scene. Close to the bright headlights, the intensity of the light veil is high and it diminishes towards the periphery of the visual scene. The veil of light is called straylight, and reduces retinal contrast all over the visual scene.^{4,5} So, in low-intensity parts of the visual scene, it causes discrimination difficulties of objects. Note that large intensity differences exist in most normal visual scenes, especially during night driving. Because of its effect on perception of the entire visual scene, straylight is another important determinant of VF.

Through the years, various innovations reduced the risks and improved the outcomes of ophthalmic interventions for VF restoration. Although VF restoration remains important, current efforts are increasingly directed towards VF preservation. Accordingly, treatment of early-stage ophthalmic conditions has become more accepted. Especially in early treatment, effort should be made to determine at which stage treatment of a particular condition will be effective. For example, early-stage opacification of the crystalline lens (cataract) or posterior lens capsule (posterior capsule opacification [PCO], see “Straylight in posterior capsule opacification” section) may already cause VF deterioration. It should be assessed at which early stage of cataract or PCO, treatment can be expected to have functional benefit. Furthermore, for VF preservation it is essential to evaluate whether treatment of one aspect of VF does not adversely affect another aspect. In other words, iatrogenic conditions with undesirable visual symptoms should be avoided. For example, nowadays dependence on spectacles or contact lenses can be eliminated by surgical correction of refractive errors (see “Straylight in laser refractive surgery” section). However, refractive surgery should not only reduce refractive errors, but also glare sensitivity should recover to preoperative level. Up to now, ophthalmic interventions were usually evaluated using VA as an outcome parameter. However, VA represents only one aspect of VF. As described earlier in this section, straylight represents a distinct aspect of VF. So, when monitoring VF, the different aspects of VF should be assessed. In this thesis, it was evaluated whether straylight is a valuable, additional parameter for VF assessment.

1.2 OPTICAL QUALITY

The quality of an object’s retinal projection is determined by the quality of retinal projections of individual points that constitute the object.⁶ The optical quality of the human eye can be determined by assessing its response to a single point of light. In a perfect eye, the retinal image of the light point would be identical to the original stimulus. However, the optics of the human eye are not perfect. In the presence of optical imperfections, the imperfections will spread out the retinal image of the point of light, resulting in a bright light spot in the

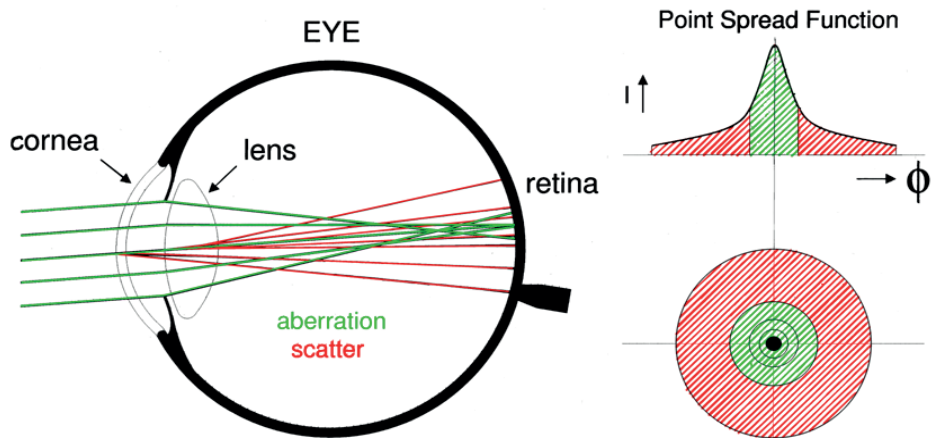


Figure 2. The two domains of the point spread function: the small angle domain (green) which is affected by aberrations, and the peripheral large angle domain (red) which is affected by light scatter. Diagram by TJTP van den Berg.

centre that is surrounded by a zone of light spreading with diminishing intensity.⁶ The eye's optical quality can be graphically represented by plotting the intensity of the projected light point as a function of its distribution (spreading) over the retina. Such a distribution of the retinal light originating from a point of light, is called the Point Spread Function (PSF). Figure 2 schematically illustrates the PSF. Precise functions have been defined by the Commission Internationale de l'Eclairage (CIE),⁷ which is an International Commission on standards in vision (see <http://www.cie.co.at>). The peak of the PSF, corresponding to the highest light intensity has a half width of 0.02 degrees, or 1 minute of arc, corresponding to a normal VA of 1 (decimal notation). The slope of the PSF is steep at small visual angles, and flattens at larger visual angles. The central and peripheral parts of the PSF are two distinct, functional domains.⁶ The central, small angle domain of the PSF is affected by aberrations in the eye's optical path, which results in a retinal image with decreased sharpness and contrast loss. The small angle domain can be functionally assessed by VA testing and contrast sensitivity (CS) testing (up to 0.3 degrees). The peripheral, large angle domain, with visual angles beyond 1 degree, is affected by light-scatter, resulting in blinding (glare), and hazy vision. The large angle domain can be functionally assessed by straylight measurement.⁶ So essentially, two different domains of vision, VA and straylight, contribute to VF.

1.3 STRAYLIGHT

The light entering the eye is refracted (bended) by the ocular media (e.g., cornea, crystalline lens), and used for retinal image formation. However, a small part of the light entering the

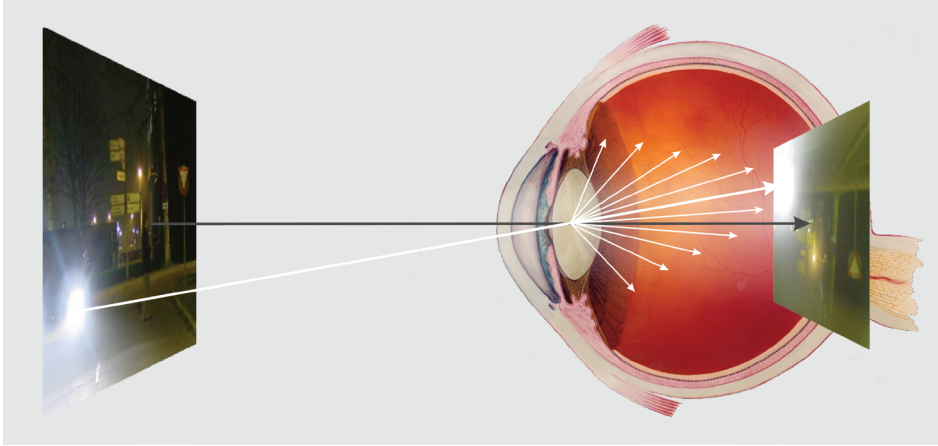


Figure 3. Imperfections of the optical media cause light scatter in all forward directions towards the retina, affecting the quality of the entire retinal image. Diagram from Van den Berg TJ, Franssen L, Coppens JE. Ocular Media Clarity and Straylight. In: DA Dartt, ed. *Encyclopedia of the Eye*. Oxford: Academic Press, Elsevier; 2010:173-83.

eye is scattered (spreaded) by ocular structures, causing a perceived veil of light projected over the retinal image that is called straylight (Figure 3).⁴ In healthy young eyes, 1/3 of the total amount of straylight is caused by the cornea, 1/3 by the crystalline lens and 1/3 by the iris, sclera and fundus.^{6,8} So, even in healthy young eyes, a small part of the light entering the eye is scattered. Loss of transparency of the ocular media, caused by certain eye conditions or aging, results in an increase in straylight. For instance, increased straylight can be found in patients with cataract.^{9,10} Straylight does not increase until approximately 40 years of age. At 65 years of age the amount of straylight is doubled as compared to healthy young eyes.^{9,10} An increase in straylight can also be encountered as a side-effect of ophthalmic treatment, such as PCO after cataract extraction ("Straylight in posterior capsule opacification" section), or in suboptimal wound-healing after refractive surgery (Straylight in laser refractive surgery" section). Imperfections of ocular structures cause light-scatter in all forward directions towards the retina. As a consequence, it can not be used for retinal image formation and degrades the image projected on the retina. So, more straylight results in lower quality of the retinal image. A comprehensive straylight overview has recently been published.⁶

1.4 STRAYLIGHT IN POSTERIOR CAPSULE OPACIFICATION

PCO is a long-term complication of cataract extraction. During cataract surgery, a circular opening is made in the anterior lens capsule for access to the opacified crystalline lens. The opacified crystalline lens, including lens epithelial cells (LECs), is removed. Its surrounding lens capsule remains in situ. Because it is impossible to remove all LECs, some of those will

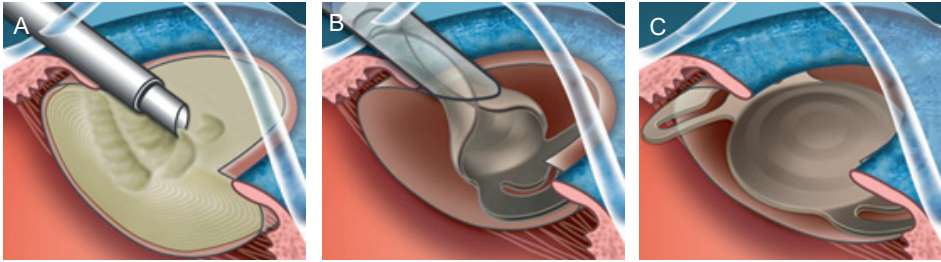


Figure 4. Cataract surgery. Removal of the opacified crystalline lens (phacoemulsification) (A), implantation of a folded intraocular lens (B), unfolded intraocular lens positioned in the lens capsule (C). Diagram from <http://i-cataract.com>.

also remain in situ. The anterior opening of the lens capsule is used to insert a clear, artificial intraocular lens (IOL) into the lens capsule (Figure 4). Mechanical trauma during cataract surgery causes a wound-healing response of the residual LECs. Wound-healing causes LECs to proliferate, to (trans)differentiate and to deposit extracellular matrix. Migration of LECs into the space between the IOL and the posterior part of the lens capsule causes opacification. This is called PCO (Figure 5). Actually, PCO (posterior capsule opacification) is a confusing misnomer: opacification is caused by the proliferated and (trans)differentiated LECs,^{11;12}

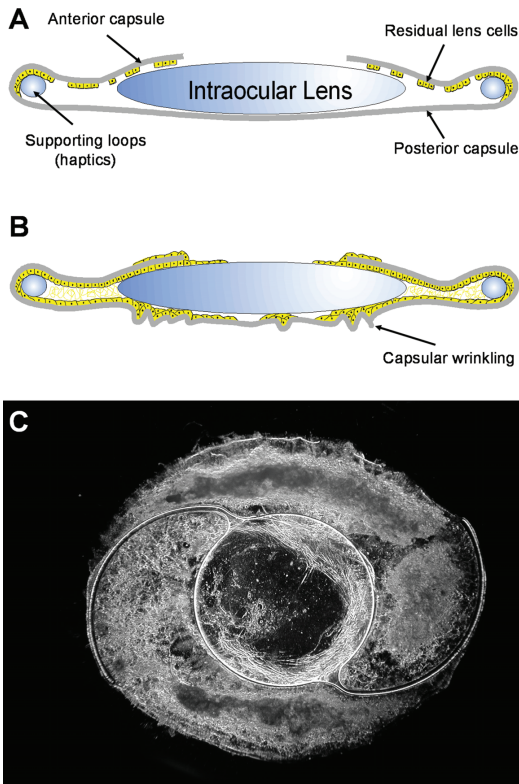


Figure 5. A schematic representation of a capsular bag with intraocular lens (IOL) and residual lens epithelial cells (A), and development of posterior capsule opacification (B). A darkfield photomicrograph of an opacified capsular bag with IOL obtained from a pseudophakic donor eye (C). Figure from Wormstone IM. Posterior capsule opacification: a cell biological perspective. *Exp. Eye Res.* 2002; 74:337-347.

whereas usually the posterior capsule (PC) itself remains transparent.¹³ Two morphologically different PCO types can be distinguished. Regeneratory PCO, or pearl-type PCO, generally has a lustrous appearance, and is thought to be caused by proliferation and swelling of LECs.¹³ Fibrotic PCO, generally has a whitish, matte appearance, and is thought to be caused by LEC transdifferentiation.^{11;12} PCO causes light entering the eye to be scattered, which reduces VF. VF can be restored by capsulotomy: opening the PC using a neodymium-doped yttrium aluminium garnet (Nd:YAG) laser.

1.5 STRAYLIGHT IN LASER REFRACTIVE SURGERY

Refractive problems are errors in the eye's ability to accurately refract and focus light rays, which causes blurring of an object's retinal projection. Refractive errors include (1) myopia (nearsightedness) which is an inability to clearly focus distant objects on the retina, (2) hyperopia (farsightedness), which is an inability to clearly focus near objects on the retina, and (3) astigmatism, which is an inability to focus light rays that propagate in two perpendicular planes, at a single point on the retina. In subjects with a desire to reduce or eliminate their dependence on spectacles or contact lenses, laser refractive surgery can be used to correct refractive errors by permanently altering the shape of the cornea. Unfortunately, suboptimal corneal wound healing after laser refractive surgery can cause corneal haze (clouding of the cornea) (Figure 6). Corneal haze may cause increased light-scatter, resulting in night vision problems and glare sensitivity.¹⁴⁻¹⁷

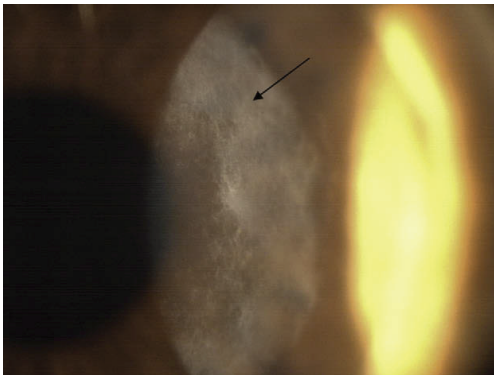


Figure 6. Corneal haze after laser refractive surgery. Photograph from Teus MA, De Benito-Llopis L, Alio JL. Mitomycin C in Corneal Refractive Surgery. *Surv Ophthalmol.* 2009;54(4):487-502.

1.6 CLINICAL STRAYLIGHT MEASUREMENT

In ophthalmic practice, intraocular straylight can be measured using an instrument called C-Quant (Oculus Optikgeräte GmbH, Wetzlar, Germany) (Figure 7A).¹⁸ The C-Quant instrument uses the Compensation Comparison (CC) method for straylight measurement, which is a psychophysical technique.¹⁹ The CC method uses a circular test field that is divided into two semicircles, and surrounded by a flickering annulus (Figure 7B). The flickering annulus serves as a straylight source. Light originating from the flickering annulus enters the eye of the observer, is scattered and projected on the retinal image of the circular test field. As a result, a flicker is perceived in the circular test field. The more intraocular light-scatter (straylight), the stronger the flicker perceived by the observer. The perceived flicker resulting from straylight can be extinguished (compensated) by presenting light in counter phase.¹⁹ In one of the semicircles such compensation light in counter phase is presented. The intensity of the compensation light can be adjusted, whereas the intensity of the flickering annulus is constant. If the amount of counter phase compensation light is equal to the amount of straylight, the flicker in the semicircle with compensation light is extinguished. So, if the amount of counter phase compensation light needed to extinguish the flicker is known, then the amount of intraocular straylight is known. Precise details of the test are explained elsewhere.¹⁹ The observer's task is to decide in which of the two semicircles the flicker is strongest, by pressing a button corresponding to that semicircle (Figure 7A). This is repeated for a series of stimuli with variable amounts of compensation light. The observer's responses are recorded and used for fitting a psychometric curve.¹⁹ This curve can be used to deduce the measurement result, which is the straylight parameter s , usually used with its logarithm ($\log[s]$).¹⁹ As mentioned earlier in this section, the CC method is a psychophysical technique, which indicates that the observer's responses to observed stimuli are used to quantify

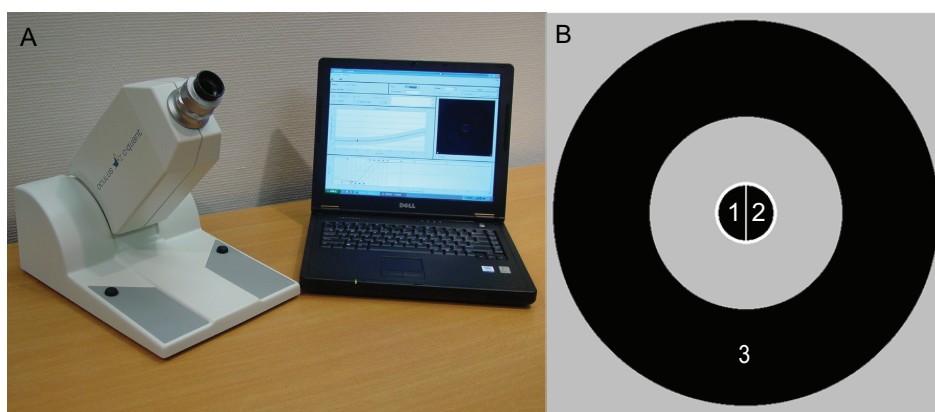


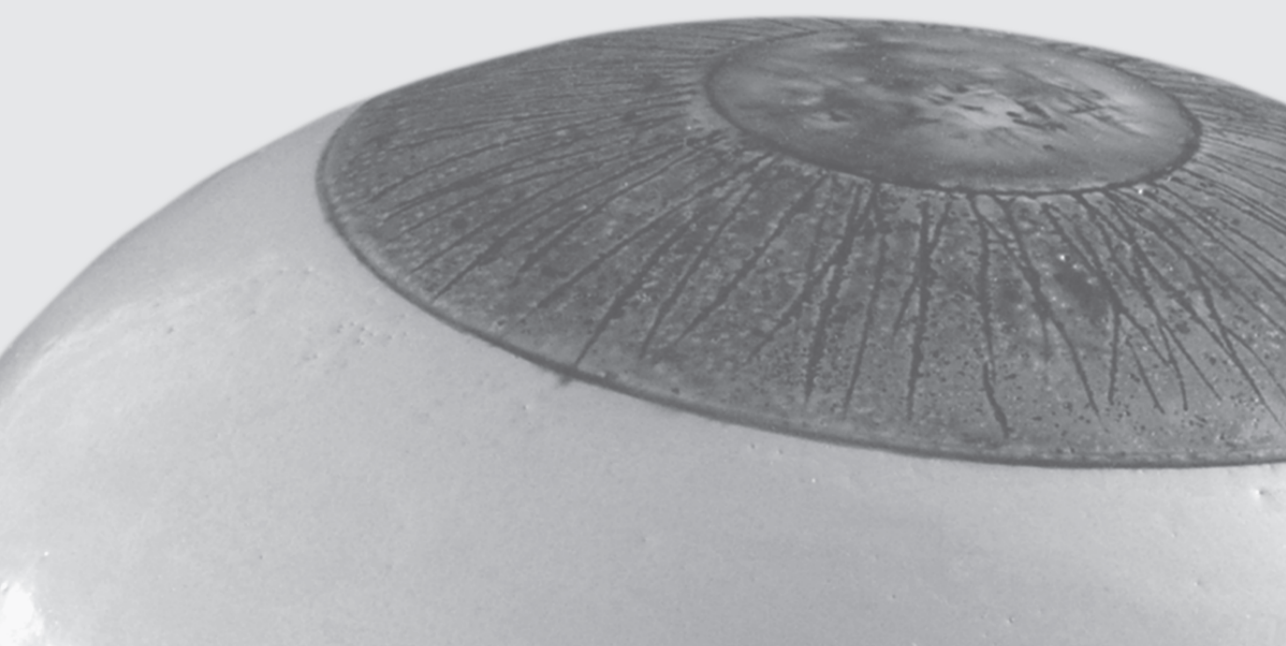
Figure 7. C-Quant instrument (A). Circular test field divided into two semicircles (1, 2) and surrounded by a flickering annulus (3) (B).

intraocular light-scatter. Therefore, the straylight parameter is a functional measure of VF. Because observation accuracy determines measurement reliability, the CC method provides reliability parameters for each individual straylight measurement.²⁰⁻²²

REFERENCE LIST

1. Assessment of visual function of driving-license holders 2003:17-52. EU project I-TREN E3 200/7/SI282826. Available at: http://www.glare.be/EU_report2002%20pdf. Accessed January 4, 2013.
2. Relevance of glare sensitivity and impairment of visual function among European drivers. 2005:41. EU project: SUBB27020B-E3-GLARE-2002-S07.1809. Available at: http://www.glare.be/Rapport2004_33_wo_articles.pdf. Accessed January 4, 2013.
3. van den Berg TJ, van Rijn LJ, Vonhoff DJ, et al. Disability glare in the aging eye. Assessment and impact on driving. *J Optom* 2009;2:112-8.
4. van den Berg TJ. Importance of pathological intraocular light scatter for visual disability. *Documenta Ophthalmologica* 1986;61:327-33.
5. van den Berg TJ. On the relation between glare and straylight. *Documenta Ophthalmologica* 1991;78:177-81.
6. van den Berg TJ, Franssen L, Coppens JE. Ocular Media Clarity and Straylight. In: DA Dartt, ed. *Encyclopedia of the Eye*. Oxford: Academic Press, Elsevier; 2010:173-83.
7. Vos JJ, van den Berg TJ. Report on disability glare. CIE collection 1999;135:1-9.
8. Vos JJ. Disability glare - a state of the art report. *Commission Internationale de l'Eclairage Journal* 1984;3/2:39-53.
9. van den Berg TJ. Analysis of intraocular straylight, especially in relation to age. *Optom Vis Sci* 1995;72:52-9.
10. van den Berg TJ, Van Rijn LJ, Michael R, et al. Straylight effects with aging and lens extraction. *American Journal of Ophthalmology* 2007;144:358-63.
11. Wormstone IM. Posterior capsule opacification: a cell biological perspective. *Exp Eye Res* 2002;74:337-47.
12. Wormstone IM, Wang L, Liu CS. Posterior capsule opacification. *Exp Eye Res* 2009;88:257-69.
13. Apple DJ, Solomon KD, Tetz MR, et al. Posterior capsule opacification. *Surv Ophthalmol* 1992;37:73-116.
14. Beerthuizen JJ, Franssen L, Landesz M, van den Berg TJ. Straylight values 1 month after laser in situ keratomileusis and photorefractive keratectomy. *Journal of Cataract and Refractive Surgery* 2007;33:779-83.
15. Lapid-Gortzak R, van der Linden JW, van der Meulen IJ, et al. Straylight measurements in laser in situ keratomileusis and laser-assisted subepithelial keratectomy for myopia. *Journal of Cataract and Refractive Surgery* 2010;36:465-71.
16. Rozema JJ, Coeckelbergh T, van den Berg TJ, et al. Straylight before and after LASEK in myopia: changes in retinal straylight. *Invest Ophthalmol Vis Sci* 2010;51:2800-4.
17. Vignal R, Tanzer D, Brunstetter T, Schallhorn S. [Scattered light and glare sensitivity after wavefront-guided photorefractive keratectomy (WFG-PRK) and laser in situ keratomileusis (WFG-LASIK)]. *J Fr Ophtalmol* 2008;31:489-93.

18. van den Berg TJ, Coppens JE, inventors; Konink NL Akademie van Wetens, applicant. Method and device for measuring retinal stray light. European patent EP 1659929. May 31, 2006.
19. Franssen L, Coppens JE, van den Berg TJ. Compensation comparison method for assessment of retinal straylight. *Invest Ophthalmol Vis Sci* 2006;47:768-76.
20. Cerviño A, Montes-Mico R, Hosking SL. Performance of the compensation comparison method for retinal straylight measurement: effect of patient's age on repeatability. *Br J Ophthalmol* 2008; 92:788-91.
21. Coppens JE, Franssen L, van Rijn LJ, van den Berg TJ. Reliability of the compensation comparison stray-light measurement method. *J Biomed Opt* 2006;11:34027.
22. Coppens JE, Franssen L, van den Berg TJ. Reliability of the compensation comparison method for measuring retinal stray light studied using Monte-Carlo simulations. *J Biomed Opt* 2006;11: 054010.



Chapter 2

Aim and outline



2.1 AIM

The aim of this thesis is to evaluate whether the straylight parameter may be suited as an additional VF indicator. Such an indicator should provide the ophthalmologist objective guidance in monitoring VF. In this thesis, two possible applications of the straylight parameter as an indicator of VF were studied.

First, it was evaluated whether the straylight parameter could be used as a predictor of beneficial treatment. In ophthalmic practice, predicting whether treatment will be beneficial can be complicated by several factors, such as heterogeneity of the condition. PCO is heterogeneous with respect to severity and morphology. Moreover, PCO severity can be differentiated into PCO density (PCO thickness), and PCO fraction (the extent to which the PC is covered by PCO). All these PCO characteristics (density, fraction and morphology) are expected to affect VF. This thesis contributes to the understanding of the effect of PCO on VF, by studying the relation between the PCO characteristics and their effect on the small (VA, CS testing) and large angle domain (straylight testing) of VF. In addition, the effect of PCO on the straylight domain was documented in detail, by studying light-scatter by PCO isolated from light-scatter by other ocular structures. An in-vitro set-up^{1,2} and PCO specimens obtained from donor eyes, allowed the detailed study of light-scatter by PCO. Moreover, light-scatter by isolated PCO areas of particular severity and morphology could be studied in-vitro. Improved understanding of the impact of PCO on different aspects of VF, derived from the in-vivo and in-vitro sections of this thesis, can be used in a clinical guide for appropriate capsulotomy referral of PCO patients.

Second, it was evaluated if straylight can be used as a visual quality standard for ocular fitness. As mentioned in Chapter 1, VF preservation has recently gained importance. A typical example is the increasing popularity of laser refractive surgery for the correction of refractive errors. Nowadays, laser refractive surgery is not only popular in persons who consider dependence on spectacles or contact lenses a burden, but also in applicants for demanding professions, e.g., military, pilots. Among applicants for demanding professions, refractive errors are a frequent disqualifying factor because applicants have to meet strict requirements for uncorrected distance VA. Laser refractive surgery should not only correct refractive errors, but should also preserve other aspects of VF, such as straylight, especially in applicants for demanding professions. In this thesis, straylight measurement was used as a screening method for ocular fitness in applicants for demanding professions and a history of laser refractive surgery.

2.2 OUTLINE

In **Chapter 3**, the impact of light-scatter by PCO on different aspects of visual function was illustrated by making pictures through PCO specimens obtained from donor eyes. Through the specimens, different scenes of the outer world were photographed: (1) a letter chart, (2) a traffic scene with headlight simulation of oncoming traffic. The pictures illustrate how patients with PCO may perceive these scenes.

In ophthalmic practice, the indication for posterior capsulotomy in PCO is usually based on VA testing and slit-lamp examination. However, there is often a discrepancy between those two assessments and subjective visual impairment experienced by the patient. The discrepancy might be caused by visual impairment due to increased straylight. In **Chapter 4**, the effect of PCO on the parameters straylight and VA, which represent distinct aspects of visual function, was studied in-vivo.

The extent to which PCO patients benefit from posterior capsulotomy is difficult to predict. Especially in clinically apparent, but less severe PCO. It would be useful to have a clinical guide for the prediction of postcapsulotomy VF improvement, based on precapsulotomy VF parameters. Benefit might depend on heterogeneous PCO characteristics, such as PCO severity and morphology. In **Chapter 5**, the effect of PCO severity and morphology on VF parameters (e.g., VA and straylight) is assessed. It was evaluated whether straylight can serve as a valuable, additional indicator for appropriate posterior capsulotomy referral.

In **Chapter 6**, light-scatter by PCO was studied isolated from light-scatter by other ocular structures, by isolating PCO specimens (opacified lens capsules including the IOL) from donor bulbi and documenting light-scatter with an in-vitro set-up.^{1,2} In most PCO cases, the central part of the PC is composed of several heterogeneous PCO areas, e.g., PCO areas of different severity. As a result, the straylight value measured in-vivo, is composed of mixed contributions of heterogeneous PCO areas. In Chapter 6, light-scatter was documented in correspondence to an in-vivo situation: light-scatter by the central part of the PCO specimens was documented. The PCO specimens had a fibrotic or regenerative appearance, and most of their central parts included both clear and opacified PC areas. Straylight was studied in detail, by documenting the optical characteristics of light scattered by PCO. The optical characteristics of scattered light, such as angular and wavelength dependence, can be used to assess the characteristic size of scattering PCO particles. Particles much larger than the wavelength of light, have weak or no wavelength dependence and strong angular dependence. They refract light, and are expected to predominantly affect the small-angle domain of VF. Particles much smaller than the wavelength of light, have strong wavelength dependence and weak or no angular dependence. They scatter light, and are expected to predominantly affect the large-

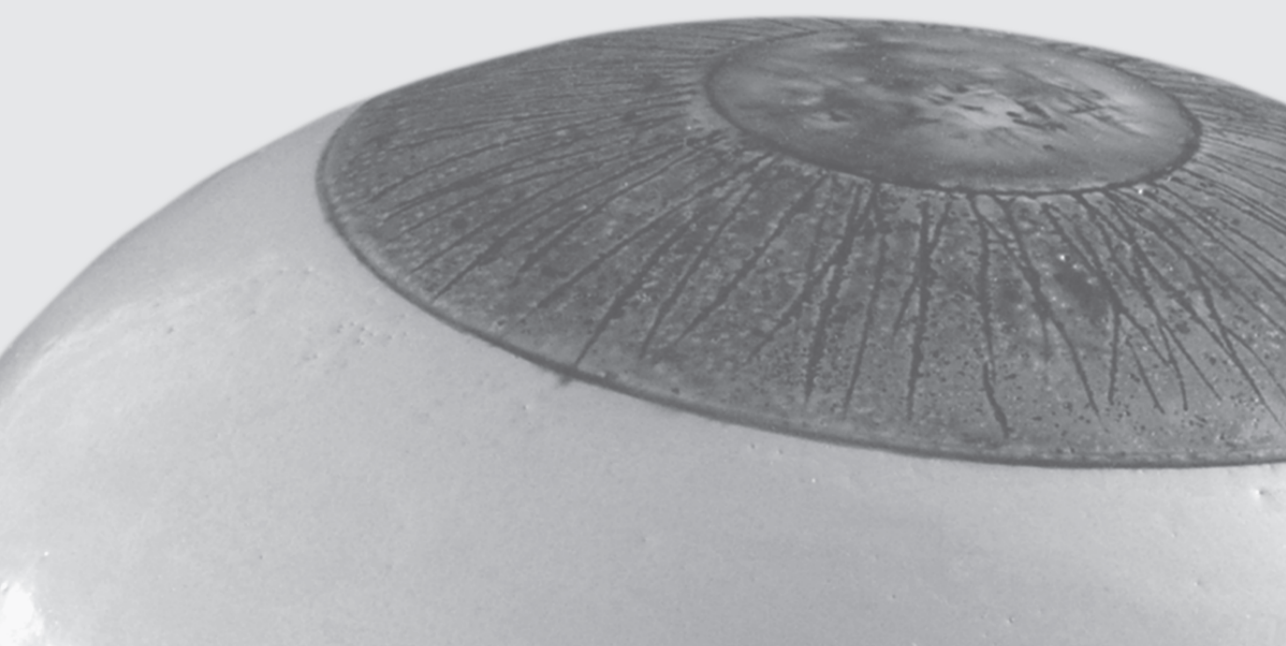
angle domain of VF. Depending on the ratio between small and larger PCO particles, PCO is expected to predominantly affect the small or the large angle domain of VF. In Chapter 6, the optical characteristics of light scattered by different PCO types were documented to elucidate the effect of PCO morphology on the large angle (straylight) domain of VF.

In addition, the PCO specimens and in-vitro set-up^{1,2} were used to study light-scatter by specific, capsule areas, *i.e.*, anterior capsule (AC) areas, clear PC areas, areas of fibrotic PCO and areas of regenerative PCO. The capsule areas studied in **Chapter 7** were either clear or opacified, and the opacified areas had different morphology and severity. The isolated study of scatter characteristics of specific, homogeneous capsule areas adds to a better understanding of (in-vivo) light-scatter experienced by the PCO patient, in which the contribution of heterogeneous capsule areas is combined.

In this thesis it was also evaluated if straylight can be used as a visual quality standard for ocular fitness. Poor uncorrected distance VA is a frequent reason for medical disqualification of applicants for demanding professions. Medical disqualification may be prevented by correction of refractive errors, using laser refractive surgery. However, approval of laser refractive surgery in demanding professions is controversial, because of possible postoperative complications. Suboptimal postoperative wound healing may lead to corneal haze, resulting in increased glare sensitivity caused by straylight. So, although laser refractive surgery may improve uncorrected distance VA (small angle domain of VF), postoperative VF can be impaired by increased glare sensitivity (large angle domain of VF). Increased glare sensitivity may reduce visual performance in difficult conditions, such as night time military operations. Therefore, for proper assessment of ocular fitness, different VF domains should be tested. In **Chapter 8** the possible introduction of the straylight parameter as an additional ocular fitness criterion in demanding professions was evaluated.

REFERENCE LIST

1. van den Berg TJ, IJspeert JK. Light scattering in donor lenses. *Vision Res* 1995;35:169-77.
2. van den Berg TJ. Depth-dependent forward light scattering by donor lenses. *Invest Ophthalmol Vis Sci* 1996;37:1157-66.



Chapter 3

Real-world scenes captured through PCO specimens: simulation of visual function deterioration experienced by PCO patients

Maartje C.J. van Bree, Bastiaan Kruijt, Thomas J.T.P. van den Berg

Journal of Cataract & Refractive Surgery 2013;39(1):144-7



INTRODUCTION

Light entering the eye is refracted by the ocular media, and used for retinal image formation. A small part of light is scattered by media imperfections, causing perception of light spreading around bright light sources, called straylight.¹ Straylight is an important aspect of visual function (VF), because scattered light is lost for image formation and degrades the image. For example, VF deterioration due to straylight by posterior capsule opacification (PCO). Straylight causes glare: VF loss experienced in the presence of a distant bright light source and low-contrast surroundings. Besides blinding, straylight symptoms include “hazy vision”, halo’s and lowered contrast.¹

VF has distinct functional domains: (1) a small-angle domain affected by aberrations causing blur, assessed by visual acuity (VA) and contrast sensitivity tests, and (2) a large-angle domain affected by light-scatter, assessed by straylight measurement. Ocular conditions such as PCO, may affect the domains to a different extent. In real-world settings, PCO patients are frequently hindered by straylight, despite of good VA: good VA does not imply good optical quality.² Proper assessment of the impact of PCO requires testing of all VF parameters, representing different functional domains.^{2,3}

A recent study evaluated how the impact of PCO on VF is related to PCO severity.³ PCO “severity” includes PCO density (thickness) and fraction (coverage), i.e. the fraction of the Posterior Capsule (PC) covered by PCO. Based on physics theory⁴ it can be expected that straylight is affected by PCO density and fraction, whereas VA is mainly affected by PCO fraction. Straylight reflects the fraction of light entering the eye that is scattered. The scattered fraction is expected to increase linearly in proportion to PCO density and fraction. However, VA is expected to remain unaffected until the PCO fraction becomes large: in early PCO (small PCO fraction, large clear PC fraction) a large fraction of light is still adequately projected on the retina, resulting in an unaffected, sharp image of high-intensity, whereas in severe PCO (large PCO fraction, small clear PC fraction) only a small part of light is adequately projected (the remainder is scattered), resulting in VA loss. Consistent with these theoretical expectations, a proportionate effect of PCO severity on straylight and a nonproportionate effect on VA was found.³

By capturing images of real-world scenes through PCO specimens, this study tries to mimic visual deterioration experienced by PCO patients. It may give clinicians a general impression of the impact of PCO on different VF domains.

METHODS

Specimens comprising an opacified PC with intraocular lens (IOL) were dissected from human donor bulbi (preparation, fixation⁵). The specimen was positioned between a microscope camera (at its posterior side) and a chart depicting real-world scenes (at its anterior side). The camera served as an in-vitro counterpart of in-vivo retinal photoreceptors, and captured real-world scenes through the specimen. Two scenes were used: a Landolt C chart (Figure 1, A), representing VA testing in ophthalmic practice, and a traffic scene at night with headlight simulation of oncoming traffic (Figure 1, B), a typical example of glare experienced in daily life.

RESULTS

Scenes captured through a clear IOL, mimic visual perception without media and retinal pathology: good VA (Figure 2, 2.1B) and nonpathological glare (Figure 2, 2.1C-D). Scenes captured through PCO specimens mimic visual perception by patients with PCO of different severity (assuming normal retinal function). As expected from physics theory, VA (Figure 2, 2.2B and 2.3B) remains good if a large area of the PC is clear (Figure 2, 2.2A, 2.3A). With increasing PCO coverage, the image's intensity diminishes (Figure 2, 2.4B), eventually resulting in VA loss (Figure 2, 2.5B). Glare gradually increases with increasing PCO severity, (Figure 2, first and third columns). Glare gradually increases with increasing pupil diameter if the exposed part of the PC covered by PCO is enlarged (e.g. Figure 2, 2.4A and 2.4C-D, as opposed to 2.5A and 2.5C-D). In-vitro recorded straylight values ranged from $\log(s)=0.86$ (Figure 2, 2.2A) to 1.70 (Figure 2, 2.5D) ($\log(s)$ = logarithm of the straylight parameter s), and represent light-scatter by the opacified PC-IOL complex (4mm pupil).⁵ In-vivo straylight values would be somewhat higher: they represent the amount of straylight in the eye as a whole, including light-scatter by other ocular structures.

COMMENT

Previous studies found that straylight is more sensitive to the functional effect of slight PCO than VA,^{3,6} which is reemphasized by the present research. The impact of PCO on different VF aspects was illustrated by capturing real-world scenes through PCO specimens. The results demonstrate the added value of straylight for proper, objective VF assessment. Note that the dynamic range of luminance recorded by a camera is much smaller than that perceived by the human visual system, resulting in images with brighter highlights and darker shadows than perceived by the eye. The scenes in the present report serve only as an approximation of human visual perception.

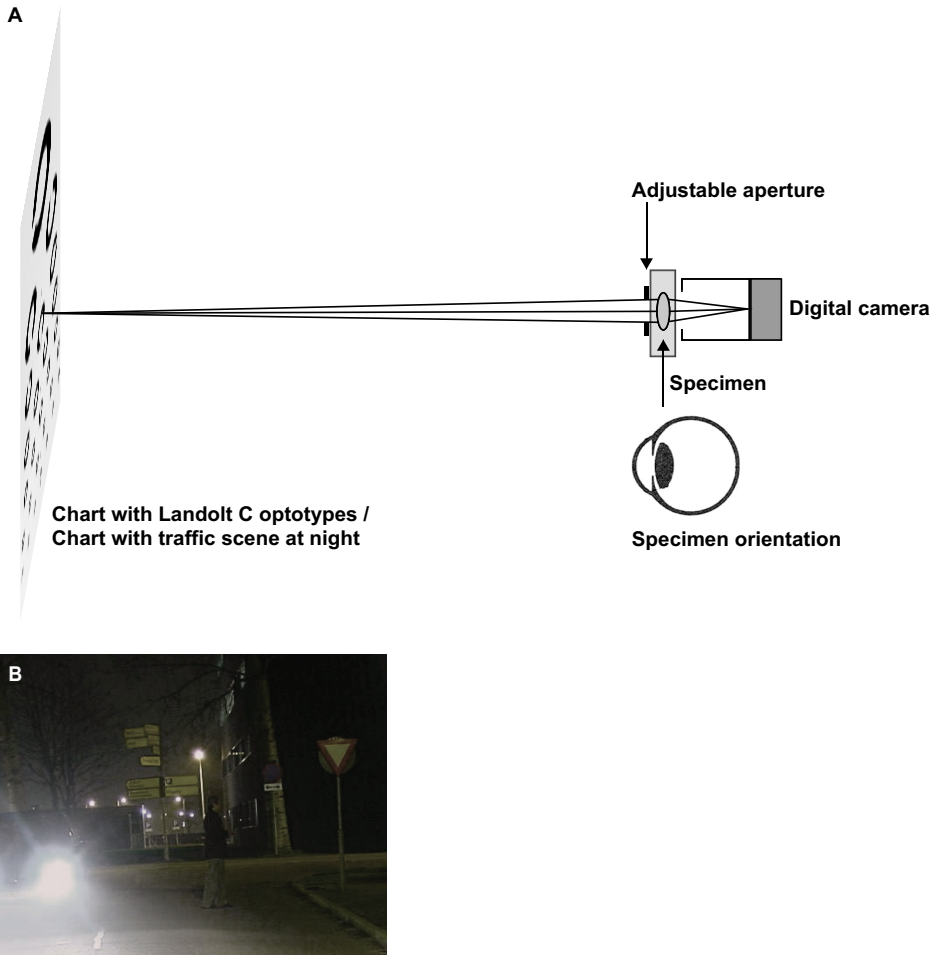


Figure 1. A simplified eye model was used: the specimen, an opacified PC-intraocular lens complex, was immersed in a cell with phosphate-buffered saline. The specimen was placed in the imaging setup (A) (schematic side view, not to scale), with its posterior part oriented towards a digital camera (Qimaging Evolution MP), and its anterior part towards a chart depicting real-world scenes. To obtain sharp images through IOLs with varying dioptric power, the focal distance was adjusted by moving the cell forward and backward on a rail system. The white balance of the camera was carefully set (Image Pro Plus v6.3 software). Aperture diameters of 3mm and 5mm were used to mimic natural pupil diameter under ambient and scotopic lighting. Images of real-world scenes were a chart with Landolt C optotypes, and a chart with a picture of a traffic scene at night (B). At the position of the headlight of the oncoming car in the picture, an opening was made in the chart. A light source was placed in the chart opening and served as headlight simulation.

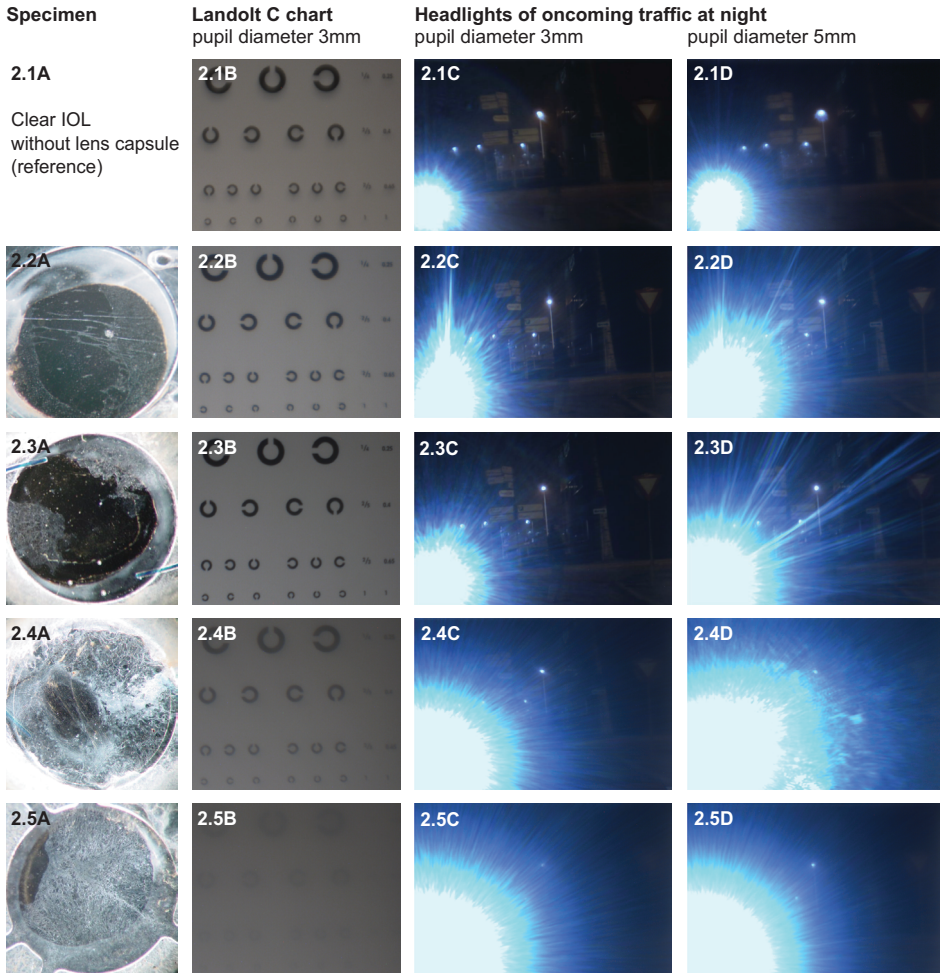
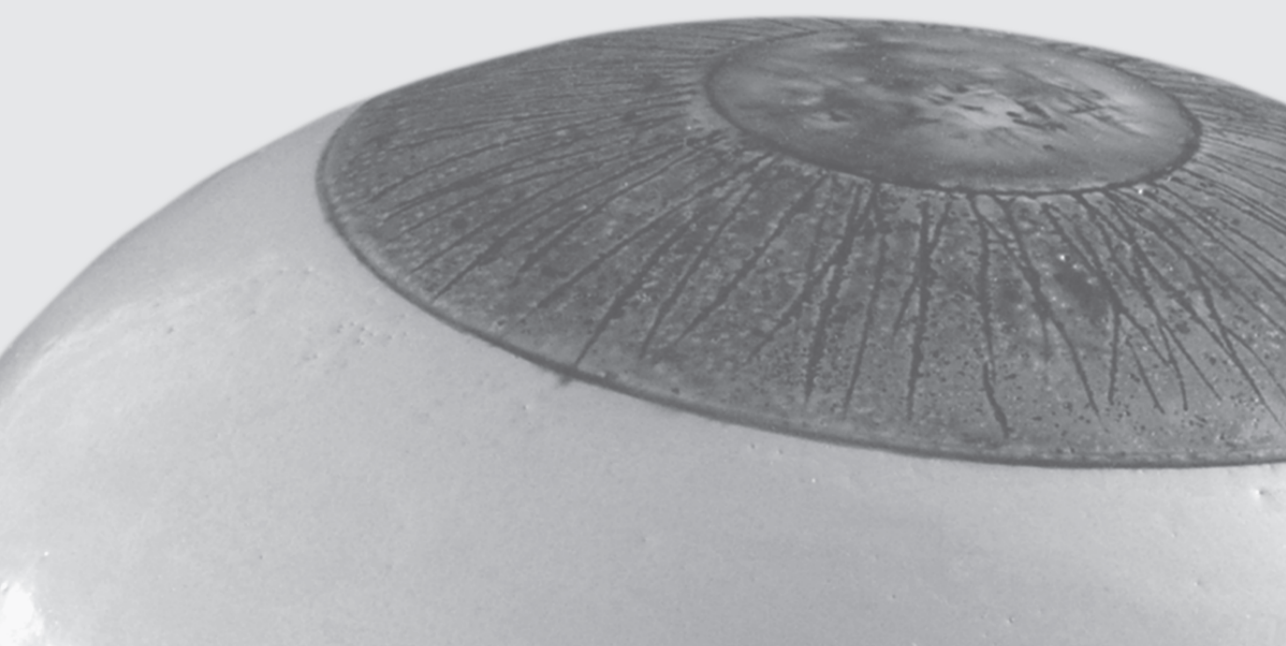


Figure 2. PCO specimens of different severity (A) and images of real-world scenes captured through specimens: a Landolt C chart (3mm aperture) (B), and a traffic scene at night with headlight simulation of oncoming traffic, captured using a 3mm (C) and a 5mm aperture (D). The real-world scenes are arranged on the same row as the PCO specimen they were captured through, e.g. images 2.2B-2.2D are captured through PCO specimen 2.2A. Images 2.1B-D were captured through a clear IOL without capsular bag, and serve as a reference for the images of real-world scenes captured through specimens (2.2B-D to 2.5B-D).

REFERENCE LIST

1. van den Berg TJ, Franssen L, Coppens JE. Ocular Media Clarity and Straylight. In: DA Dartt, ed. *Encyclopedia of the Eye*. Oxford: Academic Press, Elsevier; 2010:173-83.
2. van Bree MC, Zijlmans BL, van den Berg TJ. Effect of neodymium:YAG laser capsulotomy on retinal straylight values in patients with posterior capsule opacification. *J Cataract Refract Surg* 2008;34:1681-6.
3. van Bree MC, van den Berg TJ, Zijlmans BL. Posterior capsule opacification severity assessed with straylight, as main indicator of early visual function deterioration. *Ophthalmology* 2012; in press.
4. Kruijt B, van den Berg TJ. Optical scattering measurements of laser induced damage in the intraocular lens. *PLoS One* 7[2], e31764. 2012.
5. van Bree MC, van der Meulen IJ, Franssen L, et al. Imaging of forward light-scatter by opacified posterior capsules isolated from pseudophakic donor eyes. *Invest Ophthalmol Vis Sci* 2011;52: 5587-97.
6. Meacock WR, Spalton DJ, Boyce J, Marshall J. The effect of posterior capsule opacification on visual function. *Invest Ophthalmol Vis Sci* 2003;44:4665-9.



Chapter 4

Effect of Nd:YAG laser capsulotomy on retinal straylight values in patients with posterior capsule opacification

Maartje C.J. van Bree, Bart L.M. Zijlmans, Thomas J.T.P. van den Berg

Journal of Cataract & Refractive Surgery 2008;34(10):1681-6



ABSTRACT

Purpose: To determine the effect of neodymium-doped yttrium aluminium garnet (Nd:YAG) laser capsulotomy on retinal straylight values in patients with posterior capsule opacification (PCO).

Methods: This prospective study comprised 35 patients with PCO scheduled to have Nd:YAG capsulotomy. Before and after capsulotomy, the best corrected visual acuity (BCVA) was determined, a slit-lamp examination was performed, and retinal straylight was measured. The straylight measurements were performed using the C-Quant instrument, utilizing the compensation comparison method. Based on the median BCVA before capsulotomy (0.40 logarithm of the minimum angle of resolution [logMAR]), patients were divided into 2 groups: those with visual acuity (VA) better than 0.40 logMAR (good VA group) and those with an acuity of 0.40 logMAR or worse (poor VA group).

Results: The BCVA and the straylight values improved significantly after capsulotomy. The improvement in the straylight value was statistically significant in the good and poor VA group. The BCVA and straylight values behaved independently from each other. Before capsulotomy, the BCVA and the straylight value were moderately correlated. After capsulotomy, there was no significant correlation between the 2 parameters. Also, the improvement in the 2 parameters after capsulotomy was unrelated.

Conclusions: After capsulotomy, both BCVA and straylight values improved significantly. There was no uniform relation between BCVA and retinal straylight. Straylight must be considered an independent entry criterion for capsulotomy.

INTRODUCTION

Posterior capsule opacification (PCO) is the most common complication of cataract extraction with intraocular lens (IOL) implantation. Opening the posterior capsule by neodymium-doped yttrium aluminium garnet (Nd:YAG) laser capsulotomy relieves PCO symptoms. In the clinical setting, the indication for capsulotomy is generally based on visual acuity (VA) testing and the morphological appearance of PCO at the slit-lamp. However, there is often a discrepancy between these 2 guiding principles and the degree of the patient's visual impairment.¹⁻⁶ Many PCO patients have disability glare, which is defined as a reduction in visual capacity resulting from a nearby glare source and is the result of forward intraocular light-scatter. The international standards committee Commission Internationale de l'Eclairage quantifies disability glare as straylight.⁷⁻¹¹ The straylight value reflects the quantity of light entering the eye that is not focused by the optical media to form a retinal image but instead is scattered by disturbances in internal optical elements. This causes a veil of light over the retina and leads to a reduction in retinal image contrast.⁸ The greater the intraocular straylight, the more reduced the visual capacity.

A study using the direct compensation method showed significant decreases in straylight values after cataract surgery.¹⁰ However, the straylight values in these pseudophakic eyes were not normalized and remained a factor 2 above those of healthy phakic subjects. These relatively high straylight values were attributed to the presence of PCO, the contribution of which was not evaluated.^{2,6} One study¹ reported the unlikely finding that capsulotomy had no effect on straylight. Another group^{12,13} used a modified direct compensation method to study the effect of capsulotomy size. They found significant reductions in straylight values only in cases in which wide capsulotomies were performed with dilated pupils, not in cases with small central capsulotomies. The roles of PCO remnants and IOL pitting were not taken into account. In addition, the reliability of the modified direct compensation method used in the study was not evaluated. The C-Quant instrument (Oculus GmbH), which uses the compensation comparison (CC) method, provides a reliable method of measuring forward light-scatter.¹⁴⁻¹⁹ In this study, we used this method to quantify retinal straylight before and after capsulotomy to determine straylight changes after treatment. In addition, we evaluated whether the straylight values of PCO patients with poor VA and PCO patients with good VA improved after capsulotomy.

METHODS

This prospective study comprised pseudophakic patients with a complaint of visual disability and clinically observable PCO, scheduled for capsulotomy at The Rotterdam Eye Hospital

from November 2006 to February 2007. All patients had had uneventful cataract extraction with IOL implantation at the hospital from January 2002 to October 2006.

Exclusion criteria were media opacities other than PCO (e.g., insufficient tear film, contact lenses, cornea pathology, anterior capsule remnants, vitreous turbidity), peripheral iridectomy, iris atrophy, astigmatism greater than 3.0 diopters, macular pathology, and a history of laser refractive surgery.²⁰ Patients with complicated capsulotomy (e.g., central IOL pitting, IOL dislocation, retinal detachment, inflammatory reaction, cystoid macular edema) or a best corrected visual acuity (BCVA) worse than 1.00 LogMAR after capsulotomy were also excluded. Only patients with reliable measurements based on the reliability parameters expected standard deviation (ESD) and quality (Q), were included.²¹

Before and after capsulotomy, the BCVA was determined, slit-lamp examination was performed, and retinal straylight was measured using the C-Quant instrument, utilizing the CC method. The method has been described in detail.¹⁶ Briefly, patients are instructed to concentrate on a test field of 2 semicircles. The test field is surrounded by a flickering annular straylight source that the patient is asked to ignore. Due to intraocular light-scatter, a weak flicker is induced in the test field. In 1 semicircle, a compensation flicker in counter phase is added. The amount of intraocular straylight is equal to the amount of compensation light needed for the flicker in that semicircle to disappear, the so-called equivalent luminance concept.¹¹ Patients are asked to assess which of the 2 semicircles flickers the strongest by pressing 1 of the 2 buttons corresponding to the 2 semicircles. Each measurement consists of a series of trials at various levels of compensation. The measurement result is expressed as log (straylight parameter), or log(s). For example, a change in the log(s) value from 1.90 to 1.30 corresponds to a straylight parameter change from 79 to 20, or an improvement by a factor of 4 (6 lines if compared to VA).^{15;16} The average log(s) value in young, healthy eyes is 0.87. Intraocular straylight increases with age, even in eyes with excellent VA. The mean log(s) value in healthy eyes at 70 years and 80 years is 1.20 and 1.40, respectively; the value increases significantly when cataract develops. A log(s) value greater than 1.47 indicates serious visual restriction. Two reliability parameters are used, the ESD (requirement ≤ 0.08) and the Q (requirement > 1.0).²¹ Straylight measurements were performed with undilated pupils to allow assessment of functional hindrance under normal daylight conditions.

Based on the median BCVA before capsulotomy, patients were divided into 2 groups for analysis. The good VA group comprised patients with VA better than 0.40 logarithm of the minimum angle of resolution (logMAR). The poor VA group comprised patients with VA of 0.40 logMAR or worse. Before capsulotomy, all patients received tropicamide 0.5% and fenylephrine 10% for mydriasis. All capsulotomies were performed by the same ophthalmologist (B.L.M.Z.) using a YAG 3000LE laser (Alcon, Inc.). With an energy level between

0.22 mJ and 1.88 mJ, punctures were made in a cruciate pattern. In all cases, this resulted in an opening in the posterior capsule with a minimum diameter of 4.0 mm around the visual axis. Because capsulotomy openings have a tendency to enlarge and then stabilize 1 month postoperatively,²² patients were reexamined at 1 month. The examination included BCVA, slit-lamp evaluation, and straylight measurement.

Statistical analysis was performed using SPSS for Windows (version 14.0, SPSS, Inc.). To guarantee an independent sample, only 1 eye per patient was included. For analysis, decimal Snellen VA was converted to a logMAR scale.²³ Paired *t* tests were applied to data that could be described by normal distribution. A 2-tailed probability less than 0.05 was considered statistically significant. Pearson correlation coefficients (*r*) were also determined.

RESULTS

Of the 44 patients included in the study, 5 were lost to follow up, 3 had an incomplete data set, and 1 had capsulotomy complicated by retinal detachment. The mean age of the remaining 35 patients was 69 years (range of 46 to 86 years). Forty-six percent of patients were in the good VA group and 54% in the poor VA group. Preoperatively, the mean BCVA was 0.52 logMAR and the median BCVA was 0.40 logMAR. The mean straylight value before capsulotomy was 1.55 log units in all patients, 1.45 log units in the good VA group and 1.64 log units in the poor VA group. Twelve patients (34%) had a log unit value greater than 1.47 (i.e. had serious visual restriction). Eight (67%) of the 12 patients were in the good VA group. Thus, 50% of patients in the good VA group and 21% in the poor VA group had serious visual restriction.

Table 1 shows the BCVA and straylight values before and after capsulotomy. In all patients, the mean BCVA improved significantly after capsulotomy ($p < .0005$, paired *t* test; 95% confidence interval [CI] -0.55 to -0.28 logMAR). After capsulotomy, there was a statistically significant log(*s*) decrease (mean decrease 0.34 log units) in all patients ($p < .0005$, paired *t*

Table 1. Mean BCVA and log(*s*) before and after capsulotomy

	Precapsulotomy			Postcapsulotomy		
	All patients (n= 35)	Good VA group (n= 16)	Poor VA group (n= 19)	All patients (n= 35)	Good VA group (n= 16)	Poor VA group (n= 19)
Mean BCVA	0.52	0.20	0.80	0.10	0.06	0.14
Mean log(<i>s</i>)	1.55	1.45	1.64	1.21	1.15	1.27

BCVA= best corrected visual acuity, LogMAR= logarithm of the Minimum Angle of Resolution, VA= visual acuity, log(*s*)= logarithm of the straylight parameter *s*

test; 95% CI -0.45 to -0.24 log units). The log(*s*) improvement was statistically significant in the good VA group ($p < .0005$, *t* test; 95% CI -0.42 to -0.18 log units) and the poor VA group ($p < .0005$, *t* test; 95% CI -0.55 to -0.20 log units). The straylight value improved less in the good VA group than in the poor VA group (mean improvement -0.30 and -0.37 log units, respectively) (Table 1); however, the difference between the 2 groups was not statistically significant ($p > .05$).

After capsulotomy, there was no straylight improvement in 3 eyes (8%) (Figures 1 and 2) and no BCVA improvement in 4 eyes (11%). The straylight value was below the 95% CI of the normal population in 5 eyes (13%) before capsulotomy and in 8 eyes (23%) after capsulotomy. In 3 eyes (8%) the straylight value decreased after capsulotomy but remained above 1.47 log(*s*) (Figure 1).

Before capsulotomy, there was a moderate correlation between BCVA and straylight ($r = .48$, $p < .005$) (Figure 3). Subgroup analysis showed no significant correlation between good BCVA and straylight ($r = .17$, $p > .05$), and a moderate correlation between poor BCVA and straylight ($r = .48$, $p < .05$). After capsulotomy, there was no significant correlation between the 2 parameters in any eye ($r = .20$, $p > .05$) (Figure 3). Subgroup analysis showed no significant correlation between straylight and good BCVA ($r = .10$, $p > .5$) or poor BCVA ($r = -.18$, $p = .5$). There was also no significant correlation between log(*s*) and logMAR improvement after capsulotomy ($r = -.30$, $p > .05$).

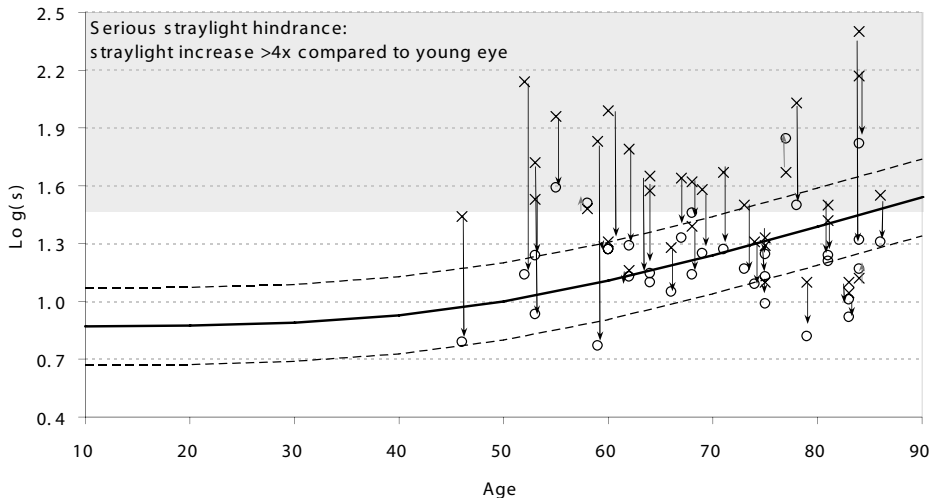


Figure 1. Straylight values before and after capsulotomy as a function of patient age, in relation to the psychophysical function of the straylight parameter *s* and its 95% confidence interval. The gray rectangle at the top of the graph indicates straylight values greater than 1.47 (i.e. serious visual restriction). The black arrows indicate individual straylight decreases after capsulotomy. The gray arrows represent 3 eyes without straylight improvement after capsulotomy.

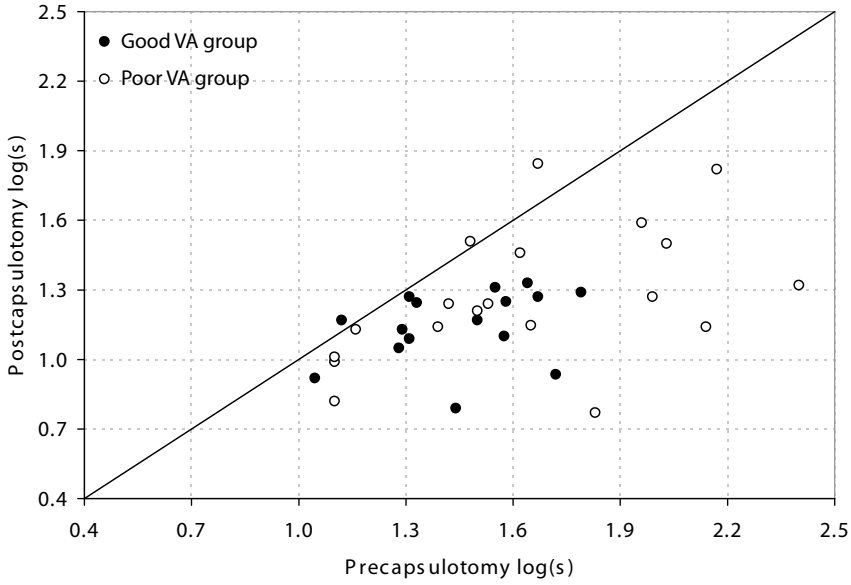


Figure 2. Straylight values before and after capsulotomy by subgroup. Dots below the equality line represent improved straylight values; dots above the equality line represent unimproved straylight values.

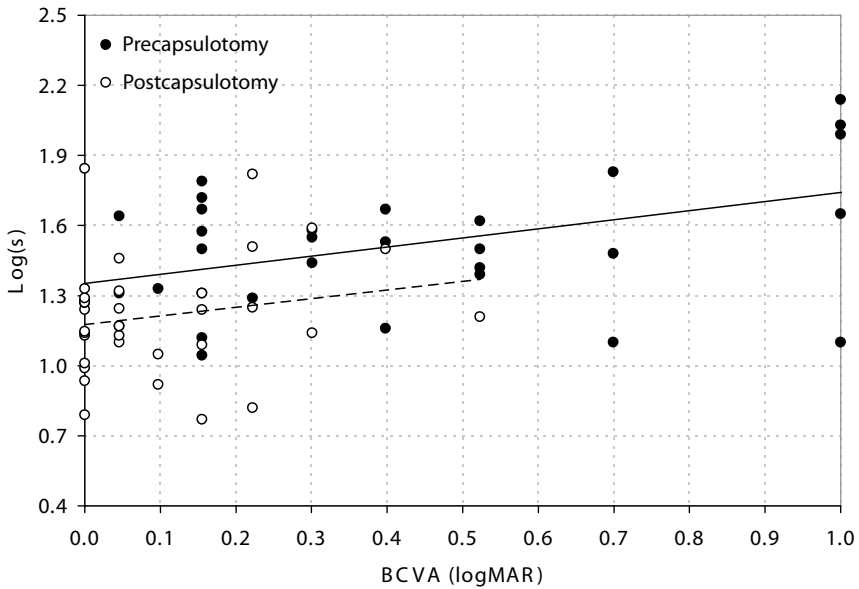


Figure 3. Straylight values in relation to best corrected visual acuity (BCVA) in PCO patients, before and after capsulotomy.

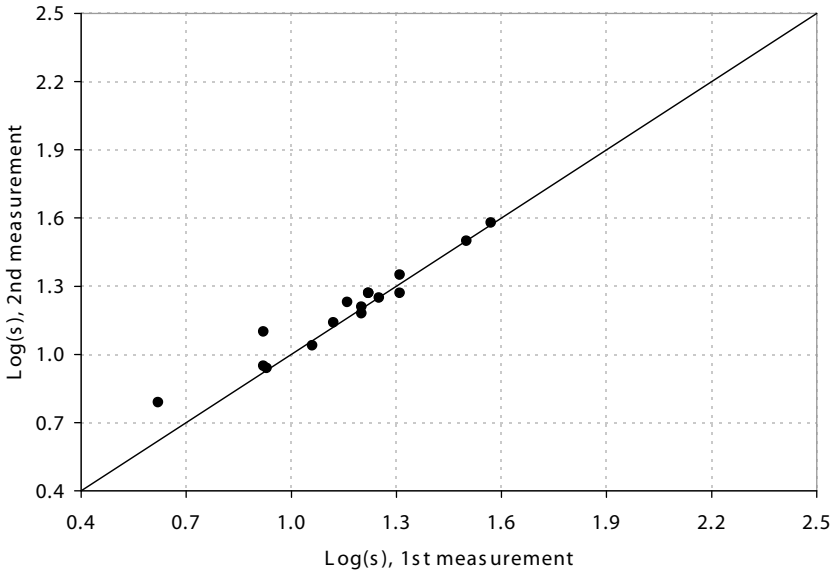


Figure 4. Repeated straylight measurements. The straylight value of the first measurement is plotted against the straylight value of the second measurement.

Figure 4 shows the results of 2 sequential straylight measurements during the same session in a subgroup of 17 randomly selected patients (half the sample). The overall repeated-measures standard deviation of the measurements was 0.05 log unit. The calculated within-group variance was 0.003 log unit and the repeatability 0.150 log unit. Thus, a decrease of more than 0.15 log unit could, with 95% confidence, be considered a treatment effect.

DISCUSSION

This study found that retinal straylight decreased significantly after capsulotomy in PCO patients. There were 2 other significant results. The 5 eyes (13%) with a precapsulotomy straylight value below the 95% CI of the normal population, had less disturbance from intraocular straylight than expected in the best eyes in their age group. However, after capsulotomy straylight improved in 4 out of 5 eyes. After capsulotomy, straylight was below the 95% CI of the normal population in 8 cases (23%). Van den Berg et al.²⁴ provide explanations for these 'super-normal results of pseudophakics' that apply to our findings. Second, 3 eyes (8%) had no straylight improvement after capsulotomy. These patients had a slit-lamp reexamination, which showed no signs of operative complications, severe media opacities, or other ocular pathology. In 3 eyes (8%) straylight improved after capsulotomy, but remained above 1.47 log(s). Further study is required to determine why some patients had less than expected, or no straylight improvement and why others did not have improved BCVA. Perhaps different

quantitative or qualitative aspects of PCO are to blame. For example, light scattered by posterior capsular pearls or by fibrosis could have a different effect. Thus, all PCO characteristics should be taken into consideration. Furthermore, straylight effects of the implanted IOLs are unknown.¹⁵ Pupil size is not a probable confounder because straylight is weakly dependent on pupil diameters between 2.0 and 7.0 mm.²⁵ Nevertheless, the effect on straylight values may be greater in eyes with optical media disturbances.²⁴ The same applies to eyes with little pigmentation.²⁶

One limitation of this study is that the normal control group, which was used to plot the psychophysical function of the straylight parameter and its 95% CI (Figure 1), was derived from data in the literature. This data set, however, was large and of multicenter origin. As discussed earlier, a remarkable finding is that straylight values in pseudophakics can be better than in same-aged normal eyes.²⁴ Thus, in some cases, surgery could decrease straylight values even further, back to the levels of youth. Close inspection of Figure 1 shows that some eyes in our study achieved this goal, a finding that should be evaluated further. Second, the localization of PCO in relation to the visual axis, the fraction of the involved capsule, and PCO morphology were not recorded. Further studies should classify PCO characteristics using a PCO scoring system to determine the relation between different PCO scores and their corresponding straylight values. Third, although all capsulotomies had a diameter of 4.0 mm around the visual axis, exact capsulotomy sizes were not measured. In future studies, it would be desirable to clarify the relationship between capsulotomy size and the straylight values.

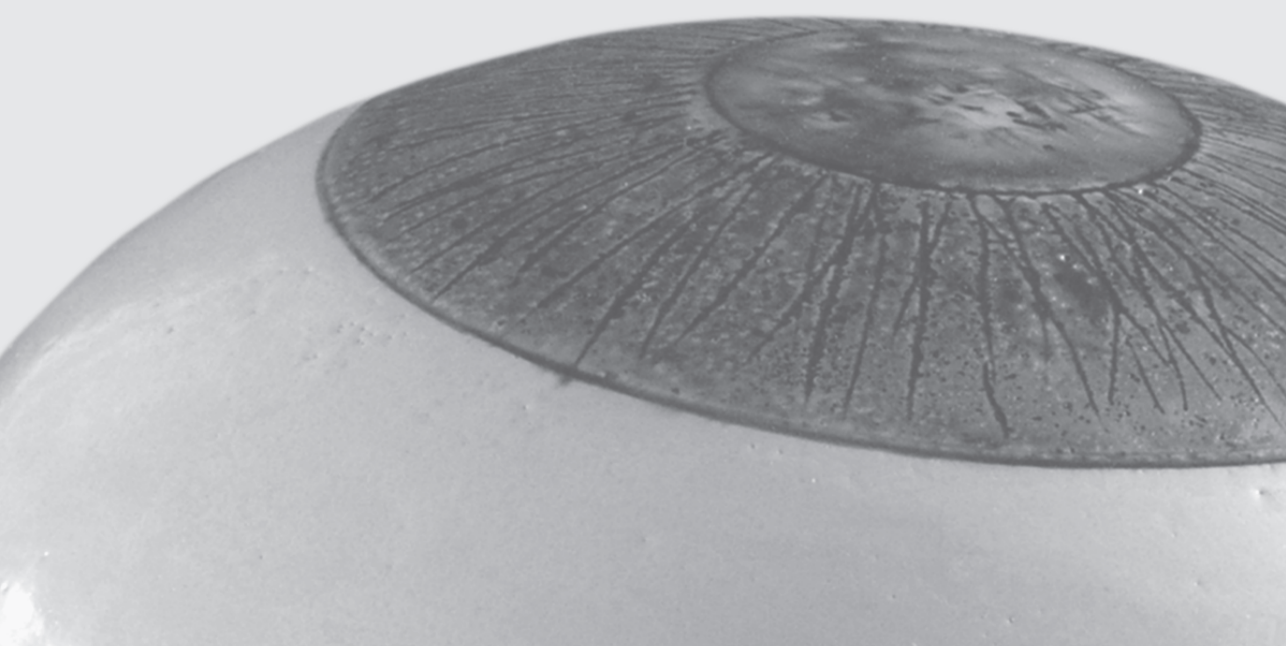
In conclusion, using the C-Quant instrument and the CC method, we quantified the effect of capsulotomy on retinal straylight in pseudophakic patients with PCO. In addition, we compared the effect of capsulotomy on the straylight value in patients with good and poor BCVA. Four conclusions can be deduced from this study. First, after capsulotomy, both BCVA and the straylight values improved significantly. Second, before capsulotomy 50% of eyes in the good VA group had straylight values greater than 1.47 (i.e., had serious visual restriction), and both subgroups significantly benefited from capsulotomy. Third, before capsulotomy the BCVA in the poor VA group was moderately correlated with the straylight value. After capsulotomy, no significant correlation existed between the BCVA and the straylight value, indicating that some patients benefited in 1 parameter of visual function and other patients benefited in the other parameter. Straylight measurement should serve as a clinical guideline for better assessment of capsulotomy indication, particularly in patients with glare symptoms and good visual quality. Fourth, further research on the relationship between the straylight parameter and relevant data, e.g., PCO score, pupil diameter, eye pigmentation, straylight effects of IOLs, contrast sensitivity, self-assessed visual function, is required. Performing clinical straylight measurements may improve the prediction of visual benefits of PCO patients

after capsulotomy. In addition, it may be a tool to assess the discrepancy between visual impairment experienced in daily life and BCVA or PCO characteristics, particularly in patients reporting disability glare.

REFERENCE LIST

1. Claesson M, Klaren L, Beckman C, Sjostrand J. Glare and contrast sensitivity before and after Nd: YAG laser capsulotomy. *Acta Ophthalmol (Copenh)* 1994;72:27-32.
2. Hard AL, Beckman C, Sjostrand J. Glare measurements before and after cataract surgery. *Acta Ophthalmol (Copenh)* 1993;71:471-6.
3. Hayashi K, Hayashi H, Nakao F, Hayashi F. Correlation between posterior capsule opacification and visual function before and after Neodymium: YAG laser posterior capsulotomy. *Am J Ophthalmol* 2003;136:720-6.
4. Knighton RW, Slomovic AR, Parrish RK 2nd. Glare measurements before and after neodymium-YAG laser posterior capsulotomy. *Am J Ophthalmol* 1985;100:708-13.
5. Sunderraj P, Villada JR, Joyce PW, Watson A. Glare testing in pseudophakes with posterior capsule opacification. *Eye (Lond)* 1992;6 (Pt 4):411-3.
6. Witmer FK, van den Brom HJ, Kooijman AC, Blanksma LJ. Intra-ocular light scatter in pseudophakia. *Doc Ophthalmol* 1989;72:335-40.
7. Jose RM, Bender LE, Boyce JF, Heatley C. Correlation between the measurement of posterior capsule opacification severity and visual function testing. *J Cataract Refract Surg* 2005;31:534-42.
8. van den Berg TJ. Importance of pathological intraocular light scatter for visual disability. *Doc Ophthalmol* 1986;61:327-33.
9. van den Berg TJ. On the relation between glare and straylight. *Doc Ophthalmol* 1991;78:177-81.
10. van den Berg TJ. Analysis of intraocular straylight, especially in relation to age. *Optom Vis Sci* 1995;72:52-9.
11. Vos JJ. Disability glare - a state of the art report. *Commission Internationale de l'Eclairage Journal* 1984;3/2:39-53.
12. Goble RR, O'Brart DP, Lohmann CP, et al. The role of light scatter in the degradation of visual performance before and after Nd:YAG capsulotomy. *Eye (Lond)* 1994;8 (Pt 5):530-4.
13. Lohmann CP, Goble RR, O'Brart DP, et al. [Sensitivity to glare before and after Nd:YAG capsulotomy. Comparison between small and large capsulotomy]. *Klin Monbl Augenheilkd* 1994;205: 65-9.
14. Elliott DB, Bullimore MA. Assessing the reliability, discriminative ability, and validity of disability glare tests. *Invest Ophthalmol Vis Sci* 1993;34:108-19.
15. Franssen L, Coppens JE. Straylight at the retina. Scattered papers. Thesis/Dissertation 2007; ISBN 978-90-808705-4-3. University of Amsterdam, Amsterdam, The Netherlands.
16. Franssen L, Coppens JE, van den Berg TJ. Compensation comparison method for assessment of retinal straylight. *Invest Ophthalmol Vis Sci* 2006;47:768-76.

17. Tan JC, Spalton DJ, Arden GB. Comparison of methods to assess visual impairment from glare and light scattering with posterior capsule opacification. *J Cataract Refract Surg* 1998;24:1626-31.
18. van den Berg TJ, Hagenouw MP, Coppens JE. The ciliary corona: physical model and simulation of the fine needles radiating from point light sources. *Invest Ophthalmol Vis Sci* 2005;46:2627-32.
19. van Rijn LJ, Nischler C, Gamer D, et al. Measurement of stray light and glare: comparison of Nyk-totest, Mesotest, stray light meter, and computer implemented stray light meter. *Br J Ophthalmol* 2005;89:345-51.
20. Beerthuizen JJ, Franssen L, Landesz M, van den Berg TJ. Straylight values 1 month after laser in situ keratomileusis and photorefractive keratectomy. *J Cataract Refract Surg* 2007;33:779-83.
21. Coppens JE, Franssen L, van den Berg TJ. Reliability of the compensation comparison method for measuring retinal stray light studied using Monte-Carlo simulations. *J Biomed Opt* 2006;11:054010.
22. Hu CY, Woung LC, Wang MC. Change in the area of laser posterior capsulotomy: 3 month follow-up. *J Cataract Refract Surg* 2001;27:537-42.
23. Holladay JT. Visual acuity measurements. *J Cataract Refract Surg* 2004;30:287-90.
24. van den Berg TJ, van Rijn LJ, Michael R, et al. Straylight effects with aging and lens extraction. *Am J Ophthalmol* 2007;144:358-63.
25. Franssen L, Taberner J, Coppens JE, van den Berg TJ. Pupil size and retinal straylight in the normal eye. *Invest Ophthalmol Vis Sci* 2007;48:2375-82.
26. IJspeert JK, de Waard PW, van den Berg TJ, de Jong PT. The intraocular straylight function in 129 healthy volunteers; dependence on angle, age and pigmentation. *Vision Res* 1990;30:699-707.



Chapter 5

Posterior capsule opacification severity, assessed with straylight measurement, as main indicator of early visual function deterioration

Maartje C.J. van Bree, Thomas J.T.P. van den Berg, Bart L.M. Zijlmans

Ophthalmology 2012;in press



ABSTRACT

Purpose: To study the effect of posterior capsule opacification (PCO) morphology and severity on different aspects of visual function (VF): the small-angle domain (visual acuity [VA], contrast sensitivity [CS]) and large-angle domain (straylight; logarithm of the straylight parameter s , $\log[s]$). To evaluate whether straylight is a valuable additional indicator for appropriate posterior capsulotomy referral.

Methods: For the study population, 240 pseudophakic eyes with PCO and a capsulotomy indication were selected. For the reference population, 99 pseudophakic eyes without PCO were selected. The relation between PCO morphology and PCO severity on one hand and pre- and postcapsulotomy logarithm of the minimum angle of resolution (logMAR), logarithm of CS ($\log[CS]$) and $\log(s)$ values on the other hand was determined. PCO severity was assessed with retro illumination, using evaluation of posterior capsule opacification (EPCO) software. Precapsulotomy logMAR and $\log(s)$ values were used to predict functionally significant logMAR and $\log(s)$ improvement after capsulotomy. LogMAR, $\log[CS]$ and $\log(s)$ improvements of ≥ 0.20 log units were considered functionally significant (i.e., treatment effect). Precapsulotomy logMAR and $\log(s)$ values, above which a treatment effect (improvement ≥ 0.20 log units) can be expected with $\geq 50\%$ probability, were determined and called cutoff values.

Results: Postcapsulotomy VF improvement was related to precapsulotomy VF values: postcapsulotomy improvement was largest in cases with substantially impaired precapsulotomy VF parameters. VF deterioration was related to PCO severity, rather than PCO morphology. PCO severity (EPCO score) assessed with retro illumination has a progressive, linear relation with $\log(s)$ and a curvilinear relation with logMAR. Reflected light examination is expected to overestimate functional PCO severity. The precapsulotomy cutoff value was ≥ 1.44 for $\log(s)$ and ≥ 0.21 for logMAR.

Conclusions: The linear relation between retro illumination PCO severity and $\log(s)$ indicates that $\log(s)$ is sensitive to low PCO severity, whereas the curvilinear relation between PCO severity and logMAR indicates that logMAR is unaffected by low PCO severity. Straylight is a sensitive, additional indicator for capsulotomy referral, especially in less severe cases of PCO. In ophthalmic practice, the precapsulotomy $\log(s)$ cutoff value of 1.44 can be used as an indicator for beneficial capsulotomy referral.

INTRODUCTION

In clinical practice, it is difficult to predict how much a patient with posterior capsule opacification (PCO) will benefit from neodymium-doped yttrium aluminium garnet (Nd:YAG) laser posterior capsulotomy, especially in less severe cases. A clinical guide for the prediction of benefits of capsulotomy, based on visual function (VF) parameters before capsulotomy would be useful. However, such a clinical guide is lacking. The present study evaluates whether straylight can be used as an additional, objective VF parameter in a clinical guide for appropriate posterior capsulotomy referral.

Visual acuity (VA) testing is affected by ocular media opacities and macular function (e.g., cystoid macular edema, age-related macular degeneration). Unlike VA, the straylight parameter is only affected by ocular media opacities,¹⁻³ thus straylight can be used to differentiate between VF impairment caused by media opacities and macular pathology. In addition, straylight measurement can be used to assess a distinct aspect of VF. For proper assessment of the effect of PCO on VF, parameters relating to different aspects of VF should be tested. VF has two distinct domains: (1) a small angle domain affected by aberrations and causing blur that can be assessed by VA and contrast sensitivity (CS) tests, and (2) a large angle domain affected by light-scatter that can be assessed by straylight measurement.^{3,4} An earlier study confirmed that PCO can affect the two VF domains to a different extent: elevated straylight values were found in PCO patients with good VA.⁵ In this study, the effect of PCO on the small-angle domain of VF was assessed by VA and CS tests, and the effect of PCO on the large-angle domain of VF was assessed by straylight measurement.

The effect of PCO on VF is expected to be related to PCO severity and morphology. It should be noted that PCO "severity" can be defined (1) as PCO density (PCO thickness), or (2) as PCO fraction (PCO coverage), that is, the fraction of the posterior capsule (PC) covered by PCO. Suppose that PCO density is not taken into account (i.e., PCO density is assumed to be constant), then a monotonous relation between PCO fraction and VF is expected: with increasing PCO fraction, increasing VF impairment is expected. However, we expect the exact relation to be different for straylight and VA. The straylight parameter reflects the fraction of light entering the eye that is scattered. The fraction of scattered light is expected to increase linearly in proportion to PCO fraction. In case of early PCO with a small PCO fraction, a small fraction of the light is scattered, and therefore a small straylight increase is expected. In case of a larger PCO fraction (of equal PCO density), a larger fraction of the light is scattered, and therefore a larger straylight increase is expected. Unlike straylight, VA is unaffected in cases with early PCO. Although the latter is well known to ophthalmologists, the underlying mechanism might not be well understood. In early PCO, with a small PCO fraction and a large clear PC fraction, a large fraction of the light entering the eye can still be adequately

projected on the retina, resulting in an unaffected, sharp retinal image of high-intensity. However, in case of a large PCO fraction and a small clear PC fraction, only a small part of the light is adequately projected on the retina (the remainder is scattered), resulting in a sharp retinal image of diminished intensity, and therefore VA loss. So, we expect VA to remain unaffected, until the PCO fraction becomes large. Given the assumption of constant PCO density, the relation between PCO fraction and straylight is expected to be linear, whereas the relation between PCO fraction and VA is expected to be nonlinear. In the present study, these theoretic relations were tested.

Two morphologically different PCO-types can be distinguished. Regenerative PCO has a lustrous, pearl-like appearance on reflected light examination, and is thought to be caused by proliferation and swelling of residual lens epithelial cells (LECs).⁶ Fibrotic PCO has a whitish, matte appearance on reflected light examination, and is thought to be caused by LEC transdifferentiation.^{7,8} As mentioned previously in this section, the effect of PCO on VF is expected not only to be related to PCO severity, but also to PCO morphology. The effect of PCO morphology on the small-angle domain of VF, has been addressed in few clinical studies.^{9,10} It was found that mean postcapsulotomy VA and CS improvement was larger in regenerative PCO than in fibrotic PCO.^{9,10} However, glare sensitivity was tested using a CS test with and without a brightness acuity tester glare source,⁹ a technique with limited discriminative ability and validity.¹¹ With the introduction of the C-Quant instrument (Oculus Optikgeräte GmbH, Wetzlar, Germany), using the compensation comparison (CC) method,¹² straylight (glare) measurement has become valid, reliable and objective.¹³ Although the effect of PCO on the straylight (large-angle) domain of VF has been assessed,^{5,14} clinical studies on effect of PCO morphology on straylight are lacking. Recently, the effect of PCO morphology on the straylight domain was studied in-vitro, in specimens obtained from pseudophakic donor eyes.^{3,15} In the present study, the effect of PCO morphology on VA, CS and straylight was tested.

By assessing the effect of PCO severity and morphology on the small-angle domain of VF (VA and CS measurement) and the large-angle domain (straylight measurement), the present study evaluates whether straylight measurement can serve as a valuable additional indicator for appropriate posterior capsulotomy referral, to be used as a clinical guide.

METHODS

Participants

The study protocol adhered to the tenets of the Declaration of Helsinki and was approved by the Institutional Review Board/Ethics Committee of the Erasmus Medical Center (Rotterdam,

The Netherlands). From March 2008 to July 2010 participants were prospectively enrolled at the Cataract Department of the Rotterdam Eye Hospital (Rotterdam, The Netherlands). Written informed consent was obtained before participation. One hundred pseudophakics without PCO were selected for the reference population. Two hundred and fifty pseudophakics with PCO were selected for the study population. Eligibility criterion for the study population was an indication for Nd:YAG capsulotomy, based on biomicroscopically observable PCO, VA testing and subjective symptoms of visual disability. Indication decisions were made by one of the ophthalmologists of the Cataract Department of the Rotterdam Eye Hospital, and reflect routine practice developed over previous years. VA was not considered a sole selection criterion, because it had been realized that VF can be impaired despite unimpaired VA.⁵ For the study population, exclusion criteria were corrected distance visual acuity (CDVA)¹⁶ worse than 0.8 logarithm of the minimum angle of resolution (logMAR), media opacities other than PCO (e.g., cornea pathology), contact lenses,¹⁷ iris diaphany, peripheral iridectomy, complicated cataract extraction, multifocal intra ocular lenses (IOLs), IOL related factors (e.g., severe dislocation, glistenings), capsulorrhexis visible in the natural pupil area,¹⁸ history of ophthalmic surgery (e.g., laser refractive surgery,¹⁹⁻²³ vitrectomy), history of intravitreal drug administration, macular pathology, and unreliable straylight measurement. These criteria and the presence of PCO, were exclusion criteria used for the reference population. For the study population, complicated capsulotomy (e.g., severe central IOL pitting) was an additional exclusion criterion. Because the amount of intraocular straylight is age-dependent,^{24,25} the study and reference population were matched for age. One eye per participant was included to ascertain independent analysis.

Visual function assessment

All VF parameters mentioned in this subsection were obtained in the study and reference population. In the study population, the parameters were obtained twice: before and one month after capsulotomy.

CDVA was measured with a rear-lighted early treatment diabetic retinopathy study (ETDRS) chart (Precision Vision, La Salle, Illinois, USA) on a logMAR scale, according to the modified ETDRS protocol.^{26,27} CS was measured using the Pelli-Robson contrast sensitivity chart (Haag-Streit, Köniz, Switzerland) with a range from 0.00 to 2.25 log(CS). As recommended by Elliott et al., participants were encouraged to observe triplets for at least 20 seconds, for proper perception of characters near the participant's contrast threshold.²⁸ Participants were encouraged to guess until 2 or 3 characters of a triplet were reported incorrectly. CS was scored by character and reported as log(CS).²⁸ Scoring was not adjusted for the "C" for "O" effect described by Elliott et al.²⁸

Sensitivity to glare was objectively quantified by measuring intraocular straylight with the C-Quant instrument. Straylight was measured using the psychophysical CC method,¹² and the measurement result was reported as the logarithm of the straylight parameter s , $\log(s)$. Increased glare sensitivity corresponds to an increased $\log(s)$ value. In a young and healthy eye, approximately 1/3 of the total amount of straylight is caused by the crystalline lens and 2/3 by other ocular structures (e.g., cornea, iris, vitreous, sclera, fundus).²⁹ Straylight is age-dependent: it increases due to aging of ocular structures.^{24;25} In particular, a crystalline lens subject to cataract formation strongly increases the total amount of straylight.²⁵ The C-Quant instrument provides a phakic reference curve and normal limits, based on normative data obtained from a population study on phakic eyes without comorbid conditions over a large age range.²⁵ Because the present study focuses on $\log(s)$ values in pseudophakics, the phakic reference curve provided by the C-Quant instrument, which includes the $\log(s)$ increase due to aging of the crystalline lens, could not be used. Therefore, a pseudophakic reference curve was determined and used instead.

For each individual straylight measurement, the C-Quant instrument provides two reliability parameters: the expected standard deviation (ESD) and quality parameter (Q).¹³ The ESD is considered the most important reliability parameter, because it is predictive of the repeated-measures standard deviation. Individual straylight measurements with an ESD >0.10 were considered unreliable and excluded. Repeated straylight measurements were performed; in case of two reliable repeated measurements the average $\log(s)$ value was used, otherwise only the reliable $\log(s)$ value was used.

To allow assessment of functional glare sensitivity under daytime light conditions, straylight measurement was performed under daytime light conditions and with natural pupil size. Under identical lighting conditions, the natural pupil diameter was determined using a Rosenbaum Pocket Eye Chart (Western Ophthalmics Corporation, Lynnwood, Washington) with accuracy steps of 0.5mm.

Participants subjectively self-assessed their VF by completing the VFQ-25/NL, the Dutch consensus translation³⁰ of the 25-item visual function questionnaire (VFQ) of the National Eye Institute (NEI), including optional items.³¹ VFQ-25/NL questionnaire answers were recoded according to the NEI VFQ-25 scoring algorithm.³² As recommended by the scoring algorithm, the general health subscale was excluded from the composite score. Furthermore, the ocular pain, near activities, color vision and peripheral vision subscales were not considered relevant for the purpose of the present study and were also excluded.³² VFQ-25/NL composite scores were calculated by averaging the question scores from the remaining 7 out of 11 subscales. Composite scores range from 0 to 100; higher scores indicate better self-perceived VF.

Slit-lamp photography of PCO

In the study population, the posterior lens capsule was documented using a photoslit-lamp (BX900®, Haag-Streit AG, Köniz, Switzerland) with reflected light and retro illumination. The following settings were used for reflected light images: magnification 16x, flash intensity high, background illumination 10%, aperture 2 (corresponding to an aperture diameter of 6.3mm), beam height 8mm, beam width 5mm, oblique illumination angle of 45 to 60 degrees. And for retro illumination images: magnification 16x, flash intensity high, background illumination 0%, aperture 2, beam height 8 mm, beam width 2 mm, slightly oblique illumination angle, projected near the pupil margin. Maximal mydriasis was obtained with tropicamide 0.5% and phenylephrine 10%.

PCO severity assessment

PCO severity was assessed in a subgroup of the study population, comprising the first 100 PCO cases that were enrolled. For PCO severity assessment, retro illumination images of PCO were analyzed with evaluation of posterior capsule opacification (EPCO) software (<http://www.epco2000.de>, accessed January 4, 2013).³³ In each retro illumination image, a region of interest (ROI) was indicated using the EPCO software. We used the central posterior capsule (PC) area, corresponding to the individual's natural pupil diameter under daytime light conditions, as the ROI. Within the ROI, areas of different PCO density were indicated. Then, the PCO fraction of each area was determined by the software. The PCO fraction is the fraction of the ROI covered by PCO, that is, a PCO fraction of 0.50 corresponds to a PCO area covering half of the ROI. PCO density (PCO thickness) was subjectively assessed and categorized, using an EPCO reference set.³³ There were 5 density categories, with (discrete) values ranging from 0 (no opacification) to 4 (severe opacification). For each PCO area, the PCO density score was multiplied by its corresponding PCO fraction. The EPCO score is the sum of these terms.³³ For example, a ROI with two different PCO areas, an PCO area with a density score of 2 and a fraction of 0.30, and an PCO area with a density score of 3 and a fraction of 0.70, results in an EPCO score of $(2 \times 0.30) + (3 \times 0.70) = 2.70$. The EPCO score ranges from 0 (no opacification within the ROI) to 4 (severe opacification of the entire ROI).³³

PCO fraction assessment

In addition to the PCO fractions assessed with retro illumination, which were used for EPCO score calculation, PCO fractions were also assessed with reflected light. PCO fractions were divided into a 4-category grading scale (category 1: 0.00 to <0.25, category 2: 0.25 to <0.50, category 3: 0.50 to <0.75, and category 4: 0.75 to 1.00).

PCO morphology assessment

PCO morphology was qualitatively classified, based on morphological appearance of the central 3mm zone of the posterior capsule, observed with slit-lamp examination. PCO with

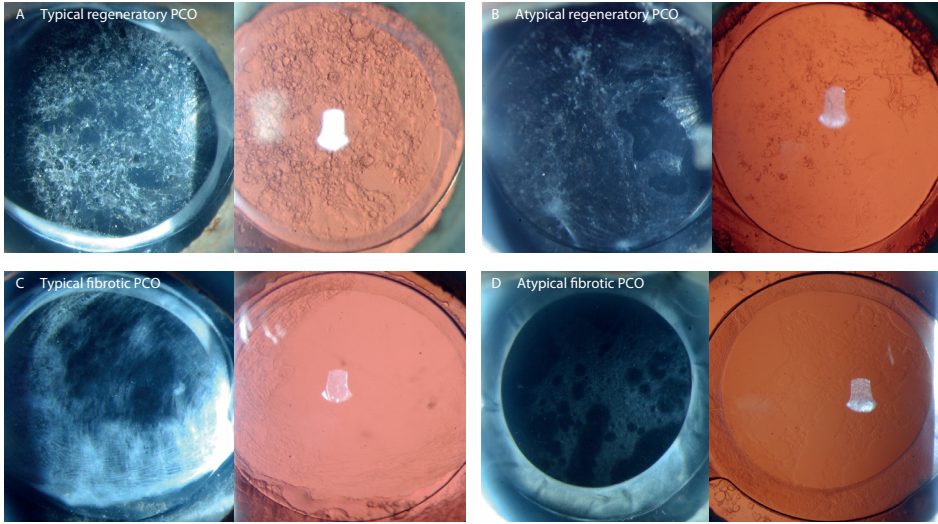


Figure 1. Representative examples of posterior capsule opacification (PCO). PCO with a lustrous appearance was classified as typical regenerative (Elschnig's pearls) (A), or atypical regenerative (B). PCO with a whitish, matte appearance was classified as typical fibrotic (C), or atypical fibrotic (D).

a generally lustrous appearance on reflected light examination was classified as regenerative PCO. Regenerative PCO was further subdivided into those with a typical regenerative appearance (Elschnig's pearls), and those with a more atypical regenerative appearance (Figure 1). The atypical regenerative PCO category was heterogeneous, including morphologic structures that have been described as cheese holes, plates, islands and traces by Neumayer et al.³⁴ PCs with a generally whitish, matte appearance on reflected light examination were classified as fibrotic. Fibrotic PCO was subdivided into those with a typical fibrotic appearance, and those with a more atypical fibrotic appearance, e.g., cheese hole structures with a whitish, matte appearance (Figure 1). PCs with a central 3mm zone of fibrotic and regenerative PCO were classified as PCO with mixed morphology (e.g., whitish, matte PCs combined with lustrous islands). Mixed morphology PCO was subdivided into those with an equal fibrotic-regenerative PCO ratio, those with a ratio in favour of regenerative PCO and those with a ratio in favour of fibrotic PCO. PC's whose appearance could not be fitted into the regenerative, fibrotic or mixed categories, were labelled as unclassified.

Nd:YAG laser posterior capsulotomy

All posterior capsulotomies were performed by the same ophthalmologist (B.L.M.Z.), with a 3000LE Nd:YAG laser (Alcon Inc., Fort Worth, Texas). After mydriasis, punctures were made from the peripheral to the central region of the PC in a cruciate pattern, resulting in a centred PC opening >4mm.¹⁸

PCO remnants after capsulotomy

The earlier mentioned study population subgroup, was screened for the presence of post-capsulotomy PCO remnants within the natural pupil area. If remnants were present after capsulotomy, the fraction of the natural pupil area covered by PCO remnants (remnant fraction) was determined with the EPCO software.³³

Secondary capsulotomy

A secondary capsulotomy was performed (B.L.M.Z.) in postcapsulotomy cases with PC remnants within the natural pupil area and persistent subjective visual symptoms. One month after secondary capsulotomy, all study parameters were obtained once again, and were used for final analysis.

Definition of functionally significant improvement

A postcapsulotomy CDVA change ≥ 0.20 log units (corresponding to 10 characters), a postcapsulotomy CS change ≥ 0.20 log units (corresponding to 4 characters), and a post-capsulotomy straylight change ≥ 0.20 log units at follow-up were considered functionally significant changes (i.e., treatment effect).

RESULTS

One hundred pseudophakics without PCO were selected for the reference population, of whom 1 was excluded because of repeated unreliable straylight measurements. Two hundred and fifty pseudophakics with PCO were selected for the study population, of whom 5 were excluded because of repeated unreliable straylight measurements, 2 were excluded because of severe central IOL pitting and 3 were excluded because of IOL glistenings that were revealed after capsulotomy. For final analysis, 99 pseudophakics without PCO were included in the reference population and 240 pseudophakics with PCO were included in the study population.

Several IOL materials and designs were included in the study and reference population. In the reference population the majority (93/99 [94%]) were hydrophobic acrylic IOLs, whereas in the study population 116/240 (48%) were polymethylmethacrylate (PMMA) IOLs, 82/240 (34%) were hydrophobic acrylic IOLs, and 25/240 (10%) were hydrophilic acrylic IOLs. Differences in IOL material and design might have affected PCO development in the study population.^{35,36}

Repeated straylight measurements

The repeated-measures standard deviation was 0.09 for the reference population, 0.09 for the precapsulotomy study population, and 0.07 for the postcapsulotomy study population (Figure 2).

Pseudophakic reference curve for straylight

As detailed in the Methods section, the age-dependence of straylight in a pseudophakic eye is different from that in a phakic eye. Therefore, a pseudophakic reference curve for straylight, based on data obtained from the present pseudophakic reference population, was determined. The pseudophakic reference curve shows a modestly age-dependent, linear log(s) increase according to $0.61 + 0.007 \times \text{age}$ (Figure 3). There were no statistically significant age-differences between the study population and the age-matched reference population (Table 1).

Visual function

After capsulotomy, all VF values (CDVA, CS, straylight, VFQ25/NL) improved statistically significantly (Table 1). However, all postcapsulotomy VF values (CDVA, CS, straylight, VFQ25/NL) were statistically significantly worse than the corresponding VF values in the reference population (Table 1). For example, in the study population the average precapsulotomy log(s) value of 1.38 improved statistically significantly, and was 1.21 after capsulotomy. However, the average postcapsulotomy log(s) value was statistically significantly higher than the average log(s) value of 1.12 in the reference population (Table 1; Figure 3).

EPCO score for PCO severity

As mentioned in the "Methods" section, EPCO scores for PCO severity (PCO density \times PCO fraction)³³ were determined in a subgroup of the study population ($n=100$). Three of the 100 pseudophakics were excluded due to precapsulotomy retro illumination images of suboptimal quality. The remaining 97 pseudophakics included 27 pseudophakics with regenerative PCO and 70 pseudophakics with fibrotic PCO.

Straylight and CDVA were found to worsen with increasing EPCO score (Figure 4). A linear relation between log(s) and EPCO score was found ($\log[s]=1.18 + 0.16 \times \text{EPCO score}$) (Figure 4A), whereas a curvilinear relation between logMAR and EPCO score was found ($\log\text{MAR}=0.053 + \log(1+[\text{EPCO score}/2.17]^2)^{14}$) (Figure 4B). The latter curve is rather flat at low EPCO scores and increases at moderate to high EPCO scores. The curves illustrate that EPCO score has a proportionate effect on log(s), and a nonproportionate effect on logMAR. That means that low PCO severity (a low EPCO score) causes straylight to increase, whereas it has no or minimal effect on CDVA. EPCO scores ≥ 1.24 cause a functionally significant log(s) effect, whereas EPCO scores of ≥ 1.66 cause a functionally significant CDVA effect (in both cases defined as ≥ 0.20 log units).

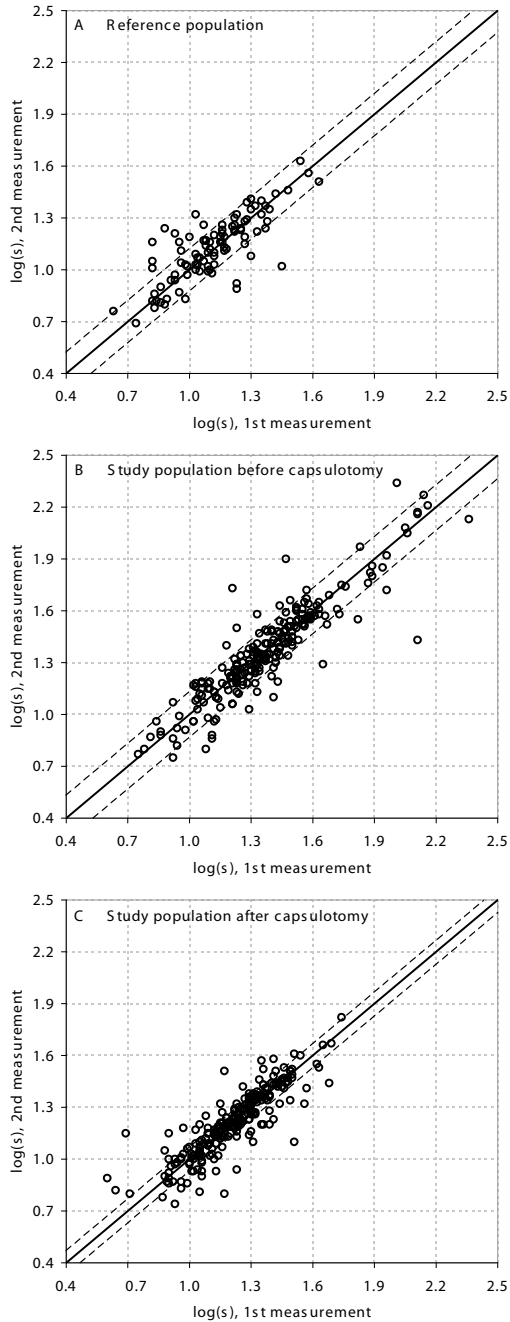


Figure 2. Repeated straylight [logarithm of the straylight parameter s , $\log(s)$] measurements obtained in the reference population (A), precapsulotomy study population (B) and postcapsulotomy study population (C). The equality line $y = x$ is indicated by the solid line and the standard deviation (SD) of differences is indicated by the dashed lines. The figures indicate the absence of systematic differences, e.g., no learning effect, between first and second straylight measurements.

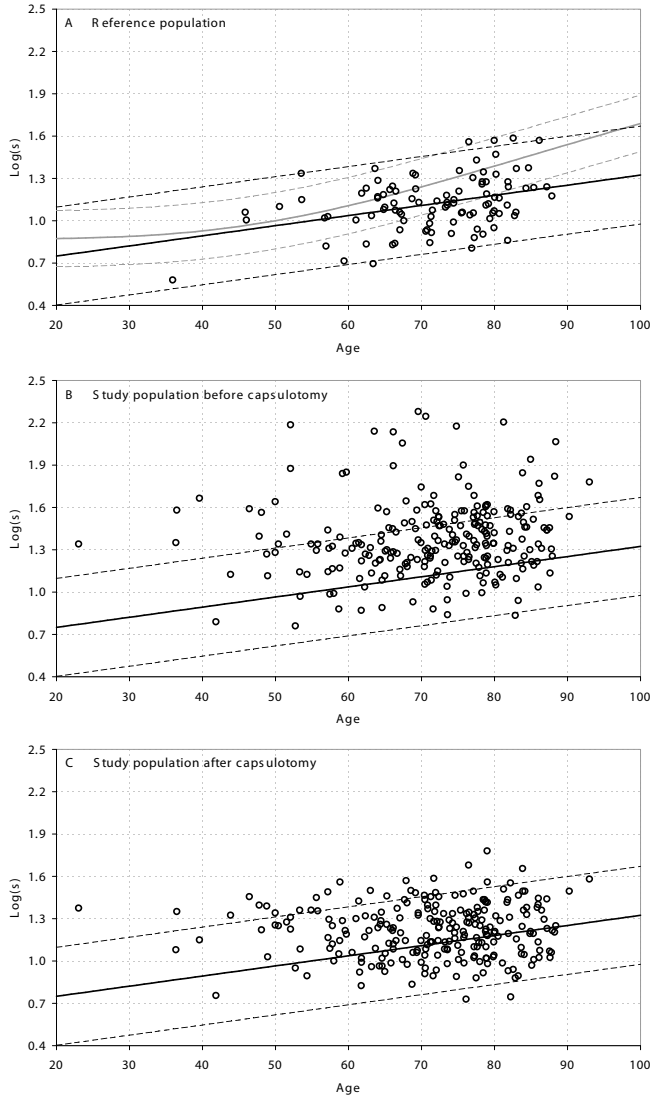


Figure 3. Precapsulotomy straylight [logarithm of the straylight parameter s , $\log(s)$] as a function of age for the reference population (A), precapsulotomy study population (B), and postcapsulotomy study population (C). The phakic reference curve provided by the C-Quant instrument is indicated by the solid, gray curve. Its 95% confidence interval (CI) of ± 0.20 log units is indicated by the dashed, gray curves (A). The phakic reference curve shows an age-dependent $\log(s)$ increase according to $0.87 + \log(1 + [\text{age}/65]^4)$. In the reference population, $\log(s)$ values and age are correlated (Spearman's ρ [99] = .32, $p < .001$). Accordingly, the pseudophakic reference curve shows a modestly age-dependent, linear $\log(s)$ increase according to $0.61 + 0.007 \times \text{age}$. The pseudophakic reference curve is indicated by the solid, black curve, and was found by least squares fitting. Its 95% CI of ± 0.35 log units is indicated by the dashed, black curves (A-C), and was calculated as $\pm 1.96 \times \text{age-corrected standard deviation (SD)}$. To calculate the age-corrected SD, $\log(0.007 \times \text{age})$ was subtracted from individual $\log(s)$ values in the reference population. Then the SD of the individual age-corrected $\log(s)$ values was calculated, which was 0.18. The age effect in the precapsulotomy (Spearman's ρ [240] = .14, $p = .025$) and postcapsulotomy (Spearman's ρ [240] = .039, $p = .55$) study population is small.

Table 1. Age and visual function parameters in the study and reference population

	Study population before capsulotomy (n=240)	Study population after capsulotomy (n=240)	Reference Population (n=99)	Statistical significance test; p-value*	
				Precapsulotomy versus postcapsulotomy study population	Reference population versus postcapsulotomy study population
Age (years)					
Distribution	Non-normal	Non-normal	Non-normal	-	Mann-Whitney Test;
Mean; SD	71.5; 11.3	71.5; 11.3	71.7; 9.74		p= .988
Median; Range	73.2; 23.0 to 93.0	73.1; 23.0 to 93.0	73.5; 35.9 to 87.9		
Log(s)					
Distribution	Non-normal	Normal	Normal	Wilcoxon Test;	T-Test;
Mean; SD	1.38; 0.27	1.21; 0.19	1.12; 0.19	p< .001	p< .001
Median; Range	1.34; 0.76 to 2.28	1.22; 0.73 to 1.78	1.11; 0.58 to 1.59		
CDVA (LogMAR)					
Distribution	Non-normal	Non-normal	Non-normal	Wilcoxon Test;	Mann-Whitney Test;
Mean; SD	0.20; 0.23	0.001; 0.12	-0.026; 0.12	p< .001	p= .003
Median; Range	0.14; 1.04 to -0.28	0.000; 0.50 to -0.27	0.000; 0.50 to -0.36		
Log(CS)					
Distribution	Non-normal	Non-normal	Non-normal	Wilcoxon Test;	Mann-Whitney Test;
Mean; SD	1.56; 0.24	1.73; 0.14	1.77; 0.12	p< .001	p= .005
Median; Range	1.64; 0.74 to 1.95	1.79; 1.04 to 1.95	1.79; 1.49 to 1.95		
VFQ-25/NL score					
Distribution	Non-normal	Non-normal	Non-normal	Wilcoxon Test;	Mann-Whitney Test;
Mean; SD	80.1; 13.5	86.6; 10.5	91.2; 8.6	p< .001	p< .001
Median; Range	83.4; 32.0 to 98.7	89.6; 33.6 to 100.0	93.5; 53.6 to 100.0		

*A two-tailed probability < .05 was considered statistically significant. SD= Standard Deviation, log(s)= logarithm of the straylight parameter *s*, CDVA= Corrected Distance Visual Acuity, LogMAR= logarithm of the Minimum Angle of Resolution, Log(CS)= logarithm of Contrast Sensitivity, VFQ-25/NL= dutch consensus translation of the 25-item Visual Function Questionnaire

The linear relation between EPCO score and log(*s*), and the curvilinear relation between EPCO score and logMAR, was almost identical for fibrotic and regenerative PCO (Figure 4). However, EPCO scores found in fibrotic PCO (median 0.89, range 0.01 to 2.21) were statistically significantly lower than those found in regenerative PCO (median 2.28, range 0.25 to 2.94) (Mann-Whitney U test, *p*< .001).

PCO fraction

Analysis of PCO fractions resulted in two findings. First, PCO fractions assessed with retro illumination were lower in fibrotic PCO than in regenerative PCO: in fibrotic PCO 56% (88/158) of the fractions was <0.5, whereas in regenerative PCO only 9% (4/45) of the fractions was <0.5. Second, the PCO fraction assessed with retro illumination differed from that assessed with reflected light. Such a PCO fraction discrepancy was found in 56% (89/158) of the cases with fibrotic PCO (Table 2) and in 18% (8/45) of the cases with regenerative PCO (Table 3). Close inspection of the discrepancies, revealed that they were mainly caused by a higher PCO

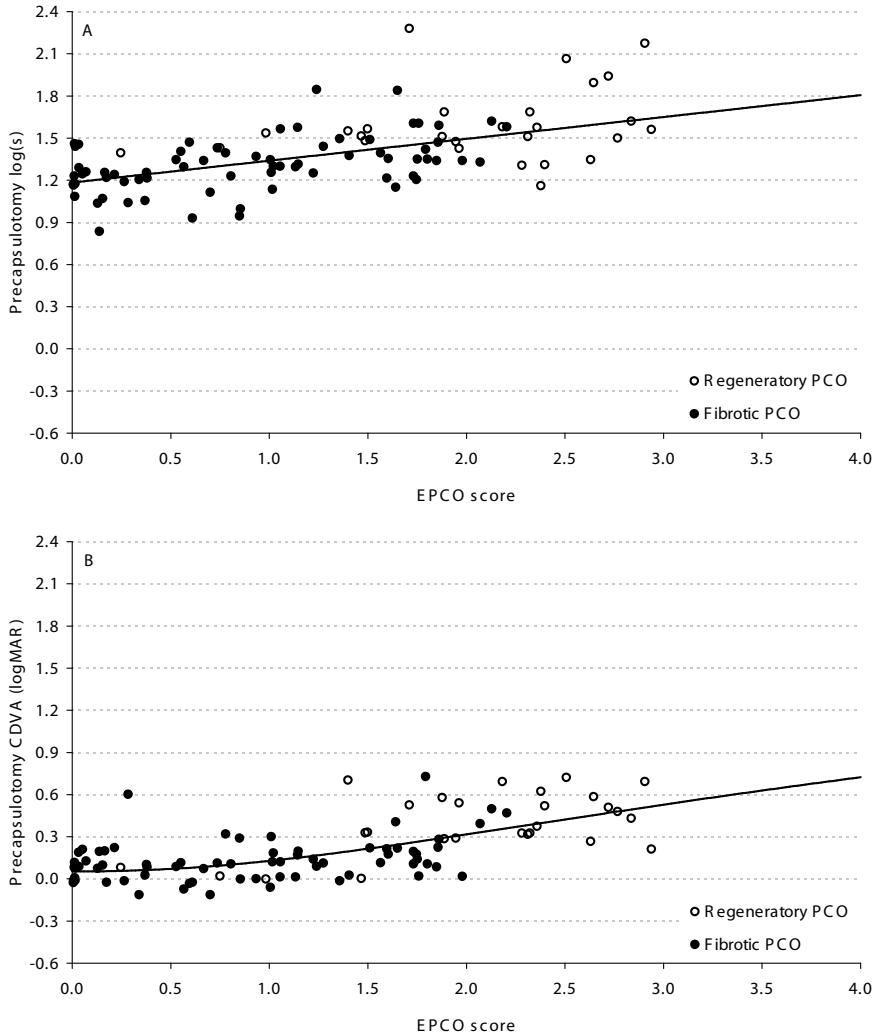


Figure 4. Precapsulotomy straylight as a function of Evaluation of Posterior Capsule Opacification (EPCO) score, which shows a linear relation (A), and precapsulotomy Corrected Distance Visual Acuity (CDVA) as a function of EPCO score, which shows a curvilinear relation (B). The curves were found by least squares fitting. The curvilinear model (unadjusted $R^2 = .46$; adjusted $R^2 = .45$) fitted the data statistically significantly better than a simple linear model ($r^2 = .37$). Correlation coefficients: Spearman's ρ [97] = .59, $p < .001$ for straylight, and Spearman's ρ [97] = .63, $p < .001$ for CDVA. PCO = Posterior Capsule Opacification, log(s) = logarithm of the straylight parameter s , logMAR = logarithm of the Minimum Angle of Resolution.

fraction observed with reflected light as compared to that observed with retro illumination: in 92% (82/89) of the fibrotic cases with a discrepancy, and in 100% (8/8) of the regenerative cases with a discrepancy. Among the 82 fibrotic cases with a discrepancy, were 47 cases with a grade 1 retro illumination PCO fraction (0.00 to 0.25). Their corresponding reflected light PCO fraction was 1 category discrepant in 23% (11/47), 2 categories discrepant in 30%

Table 2. PCO fraction discrepancies in fibrotic PCO, assessed using retro illumination and reflected light

	Reflected light			
	Grade 1	Grade 2	Grade 3	Grade 4
Retro illumination				
Grade 1	15% (23/158)	7% (11/158)	9% (14/158)	14% (22/158)
Grade 2	1% (2/158)	1% (2/158)	1% (2/158)	8% (13/158)
Grade 3	0% (0/158)	0% (0/158)	5% (8/158)	13% (20/158)
Grade 4	0% (0/158)	0% (0/158)	3% (5/158)	23% (36/158)

Grade 1: opacified fraction 0.00 to <0.25, Grade 2: opacified fraction 0.25 to <0.50,

Grade 3: opacified fraction 0.50 to <0.75, Grade 4: opacified fraction 0.75 to 1.00

Table 3 PCO fraction discrepancies in regenerative PCO, assessed using retro illumination and reflected light

	Reflected light			
	Grade 1	Grade 2	Grade 3	Grade 4
Retro illumination				
Grade 1	0% (0/45)	0% (0/45)	4% (2/45)	0% (0/45)
Grade 2	0% (0/45)	0% (0/45)	2% (1/45)	2% (1/45)
Grade 3	0% (0/45)	0% (0/45)	2% (1/45)	9% (4/45)
Grade 4	0% (0/45)	0% (0/45)	0% (0/45)	80% (36/45)

Grade 1: opacified fraction 0.00 to <0.25, Grade 2: opacified fraction 0.25 to <0.50,

Grade 3: opacified fraction 0.50 to <0.75, Grade 4: opacified fraction 0.75 to 1.00

(14/47), and 3 categories discrepant in 47% (22/47) (Table 2). Thus, especially in fibrotic cases the reflected light PCO fraction was considerably higher than the retro illumination PCO fraction.

PCO morphology

The study population of 240 cases was classified into different morphological categories: 45 PCs were classified as regenerative PCO, of which 20 with a typical pearl appearance and 25 with a more atypical regenerative appearance; 158 were classified as fibrotic PCO, of which 96 with a typical fibrotic appearance and 62 with a more atypical fibrotic appearance. Twenty-seven PCs were classified as mixed morphology, of whom 9 were classified as an equal mix, 6 as a mix with predominantly regenerative PCO and 12 as a mix with predominantly fibrotic PCO. Ten PCs had a morphological appearance that could not be fitted into the classification and were labeled as unclassified.

Average precapsulotomy log(s) values were different in the two PCO types: they were higher in regenerative PCO than in fibrotic PCO. In regenerative PCO, the average precapsulotomy log(s) value was 1.74 in the typical cases (range 1.34 to 2.28), and 1.55 in the atypical cases (range 1.16 to 2.18) (Figure 5, 5A-5B). In fibrotic PCO, the average precapsulotomy log(s)

value was 1.24 in the typical cases (range 0.76 to 1.85) and 1.31 in the atypical cases (range 0.89 to 1.84) (Figure 5, 5C-5D). A functionally significant log(s) improvement, defined as ≥ 0.20 log units, was found in 38% (89/240) of all PCO cases. Such a functionally significant log(s) improvement was found in the majority of regenerative PCO cases (typical cases 95%, 19/20; atypical cases 76%, 19/25), and in the minority of fibrotic PCO cases (typical cases 15%, 14/96; atypical cases 23%, 14/62) (Table 4). The percentage functionally significant logMAR and log(CS) improvements was also higher in the regenerative PCO categories than in the fibrotic PCO categories (Figure 6, Table 4). VFQ-25/NL score improvement was largest in typical regenerative PCO (Table 4).

Effect of PCO severity and morphology on visual function

As mentioned in the previous subsection, the functional effect of capsulotomy was larger in regenerative PCO than in fibrotic PCO. If only the relation between VF parameters and PCO morphology would have been assessed, it could have been falsely concluded that VF impairment is related to PCO morphology, and that the functional impairment caused by regenerative PCO is worse than that caused by fibrotic PCO. However, after assessment of PCO severity with the EPCO method, it was found that EPCO scores in regenerative PCO were statistically significantly higher than those in fibrotic PCO (subsection "EPCO score for PCO severity"). Higher EPCO scores were related to more severely impaired precapsulotomy VF values, and larger postcapsulotomy VF improvement. If both PCO types are equated on the basis of EPCO score, they have similar effect on log(s) (Figure 4A) and logMAR (Figure 4B). So, VF impairment was related to PCO severity (EPCO score). As can be expected, postcapsulotomy VF improvement was related to precapsulotomy VF values.

Precapsulotomy log(s) cutoff limits

Because postcapsulotomy log(s) improvement was found to be related to precapsulotomy log(s), precapsulotomy log(s) can be used to predict postcapsulotomy log(s) improvement. The precapsulotomy cutoff value above which a treatment effect (defined as ≥ 0.20 log units) can be expected with $\geq 50\%$ probability, can be deduced from the intersection point of the regression function and the horizontal $y = 0.20$ line ($\Delta \log[s] = 0.20$) in Figure 7. The cutoff value is 1.40 in regenerative PCO (Figure 7A) and 1.48 in fibrotic PCO (Figure 7B), and the average log[s] cutoff value is 1.44. Likewise, the precapsulotomy log(s) value with a $\geq 50\%$ probability for absent log(s) improvement ($\Delta \log[s] = 0.00$) can be deduced, which is 1.22 in regenerative PCO (Figure 7A) and 1.21 in fibrotic PCO (Figure 7B) (average log[s] cutoff value of 1.22). The average cutoff values of 1.44 (treatment effect) and 1.22 (no improvement), can be used as indicators for capsulotomy referral in ophthalmic practice. It should be noted that an adverse effect of capsulotomy can be expected if precapsulotomy log(s) values are low: capsulotomy in cases with a precapsulotomy log(s) value ≤ 0.95 , results in a paradoxical log(s) increase ≥ 0.20 log units, with a probability $\geq 50\%$ (Figure 7B; intersection point of the

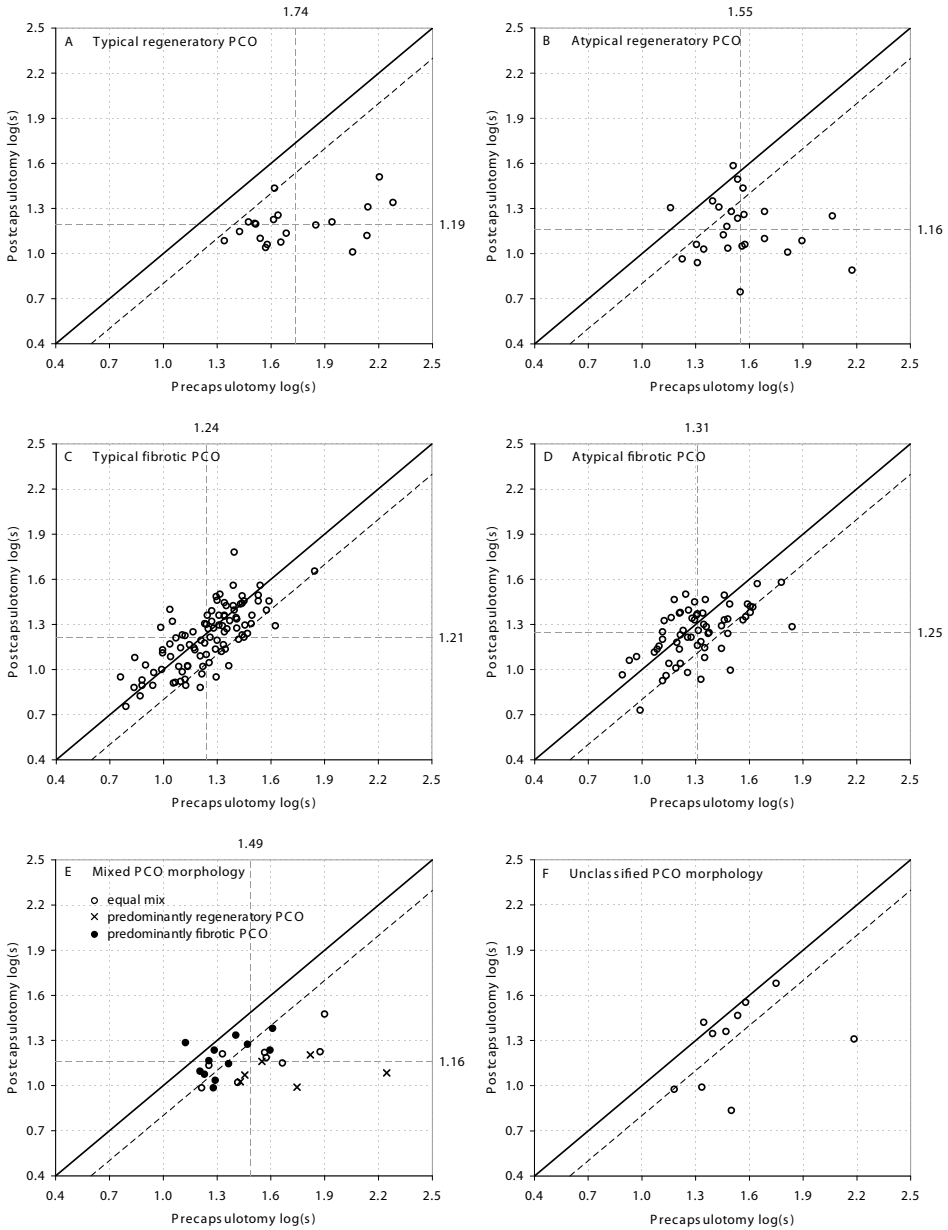


Figure 5. Postcapsulotomy straylight [logarithm of the straylight parameter s , $\log(s)$] as a function of precapsulotomy straylight, for the typical regenerative category (A), atypical regenerative category (B), typical fibrotic category (C), atypical fibrotic category (D), mixed Posterior Capsule Opacification (PCO) categories (E) and unclassified PCO (F). The number above the vertical, dashed line indicates the average precapsulotomy $\log(s)$ value, and the number next to the horizontal, dashed line indicates the average postcapsulotomy $\log(s)$ value. The diagonal, solid line represents the equality line $y=x$ indicating no change after capsulotomy. The diagonal, dashed line indicates functionally significant straylight improvement of 0.20 log units (treatment effect).

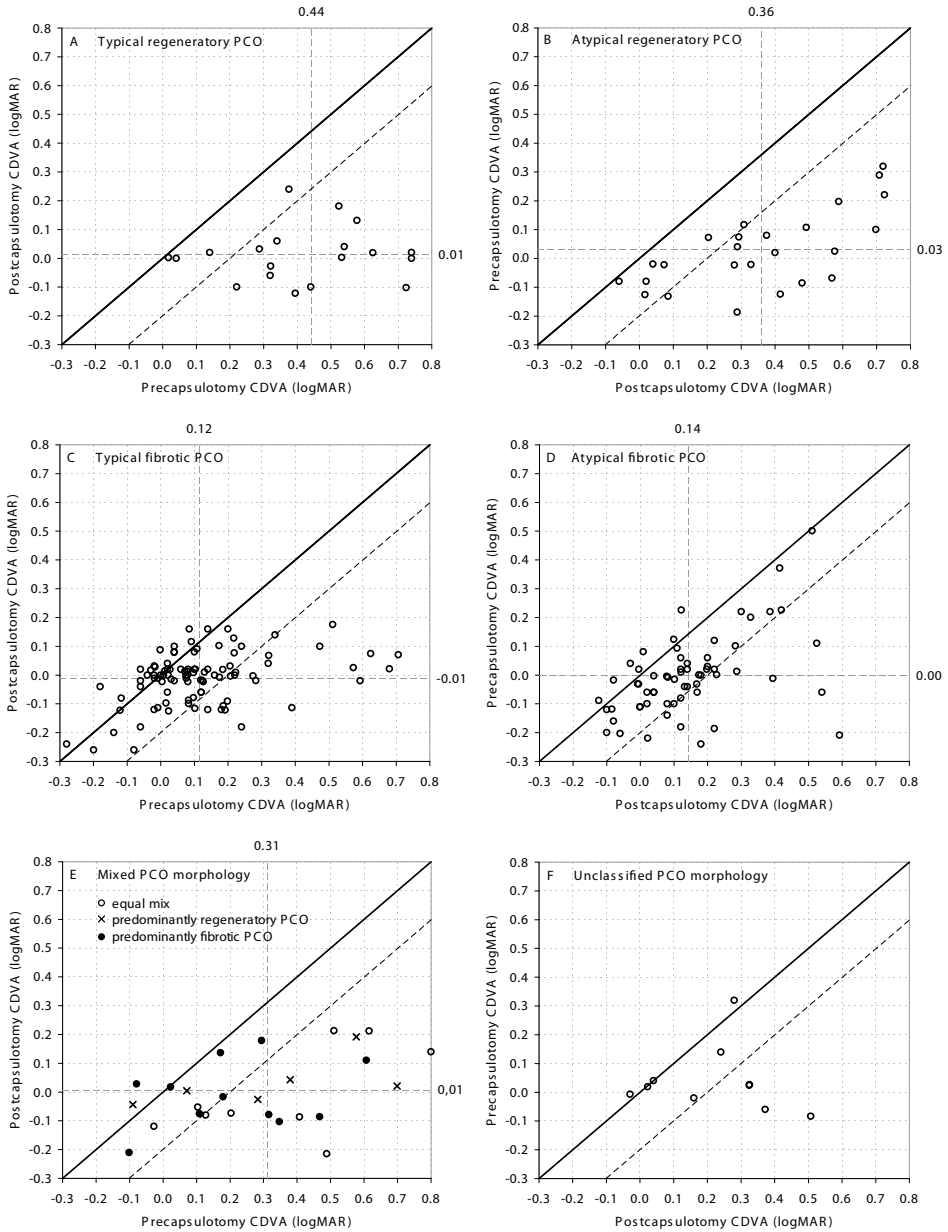


Figure 6. Postcapsulotomy Corrected Distance Visual Acuity (CDVA) [logarithm of the Minimum Angle of Resolution, logMAR] as a function of precapsulotomy CDVA, for the typical regenerative category (A), atypical regenerative category (B), typical fibrotic category (C), atypical fibrotic category (D), mixed Posterior Capsule Opacification (PCO) categories (E) and unclassified PCO (F). The number above the vertical, dashed line indicates the average precapsulotomy logMAR value, and the number next to the horizontal, dashed line indicates the average postcapsulotomy logMAR value. The diagonal, solid line represents the equality line $y = x$ and indicates no change. The diagonal, dashed line indicates functionally significant logMAR improvement of 0.20 log units (treatment effect).

Table 4. Capsulotomy effect on visual function parameters, classified by morphological appearance

	Regenerative PCO		Fibrotic PCO	
	Typical regenerative appearance (pearl PCO) (n=20)	Atypical regenerative appearance (n=25)	Typical fibrotic appearance (n=96)	Atypical fibrotic appearance (n=62)
Log(s)				
Mean before capsulotomy	1.74	1.55	1.24	1.31
Mean after capsulotomy	1.19	1.16	1.21	1.25
Δ^{\dagger}				
Distribution	Normal	Normal	Normal	Normal
Mean; SD	0.55; 0.26	0.39; 0.33	0.030; 0.15	0.067; 0.17
Median; range	0.53; 0.86 (0.19 to 1.05)	0.32; 1.43 (-0.14 to 1.29)	0.030; 0.73 (-0.39 to 0.35)	0.068; 0.84 (-0.28 to 0.56)
Functionally sign. effect*	19/20 (95%)	19/25 (76%)	14/96 (15%)	14/62 (23%)
CDVA				
Mean before capsulotomy	0.44	0.36	-0.01	0.14
Mean after capsulotomy	0.01	0.03	-0.01	0.00
Δ^{\dagger}				
Distribution	Normal	Normal	Non-normal	Non-normal
Mean; SD	0.43; 0.26	0.33; 0.19	0.13; 0.16	0.14; 0.16
Median; range	0.44; 1.02 (0.00 to 1.02)	0.30; 0.68 (0.02 to 0.70)	0.10; 0.82 (-0.14 to 0.68)	0.10; 0.90 (-0.10 to 0.80)
Functionally sign. effect*	16/20 (80%)	18/25 (72%)	23/96 (24%)	16/62 (26%)
Log(CS)				
Mean before capsulotomy	1.20	1.41	1.64	1.64
Mean after capsulotomy	1.74	1.72	1.71	1.75
Δ^{\dagger}				
Distribution	Normal	Normal	Non-normal	Non-normal
Mean; SD	0.53; 0.30	0.31; 0.22	0.074; 0.15	0.11; 0.13
Median; range	0.50; 0.90 (0.10 to 1.00)	0.30; 0.75 (0.00 to 0.75)	0.075; 0.95 (-0.45 to 0.50)	0.10; 0.60 (-0.15 to 0.45)
Functionally sign. effect*	18/20 (90%)	17/25 (68%)	12/96 (13%)	15/62 (24%)
VFQ-25/NL score				
Mean before capsulotomy	73.5	81.0	79.2	83.8
Mean after capsulotomy	88.6	85.9	85.0	87.7
Δ^{\dagger}				
Distribution	Normal	Normal	Non-normal	Non-normal
Mean; SD	15.1; 12.2	4.9; 4.6	4.9; 12.4	3.9; 8.3
Median; range	11.7; 40.2 (-0.14 to 40.1)	4.7; 16.9 (-2.3 to 14.6)	2.82; 83.8 (-32.2 to 51.7)	3.8; 50.3 (-29.5 to 20.8)

*Significant functional effect is defined as $\Delta \geq 0.20$, \dagger Pre capsulotomy values minus post capsulotomy values, \ddagger Post capsulotomy values minus pre capsulotomy values. PCO= Posterior Capsule Opacification, log(s)= logarithm of the straylight parameter s, SD= Standard Deviation, CDVA= Corrected Distance Visual Acuity, LogMAR= logarithm of the Minimum Angle of Resolution, Log(CS)= logarithm of Contrast Sensitivity, VFQ-25/NL= Dutch consensus translation of the 25-item Visual Function Questionnaire

regression function and $\Delta \log(s) = -0.20$). Precapsulotomy cutoff values for CDVA were also determined: the logMAR value indicating a probability of $\geq 50\%$ for functionally significant CDVA improvement is 0.21 in regenerative PCO and 0.20 in fibrotic PCO (average logMAR cutoff value of 0.21). Note that all precapsulotomy cutoff values were similar for the two PCO types.

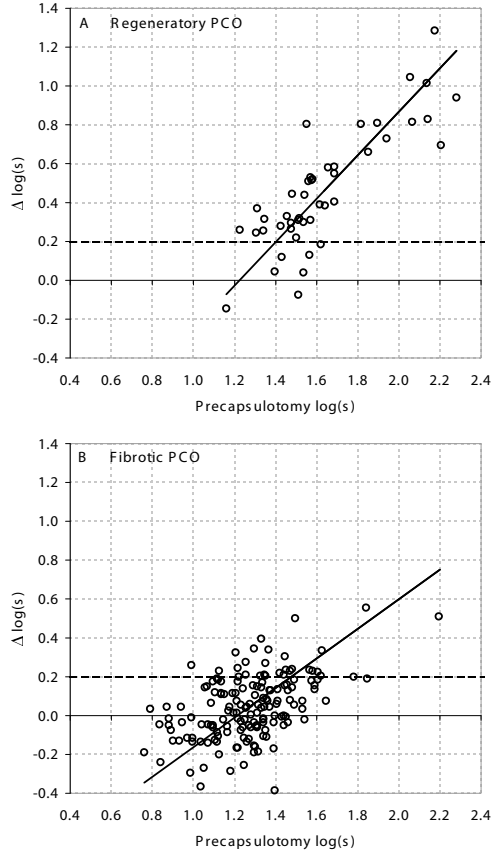


Figure 7. Straylight change (Δ logarithm of the straylight parameter s , $\Delta \log[s]$) as a function of precapsulotomy $\log(s)$, for the two regenerative categories (A) and the two fibrotic categories (B). The regression functions (diagonal, solid lines) were found by major axis regression. They were used to predict functionally significant $\log(s)$ change after capsulotomy (i.e., a treatment effect), using the $\log(s)$ value prior to capsulotomy. The horizontal, dashed $y = 0.20$ lines ($\Delta \log[s] = 0.20$), represent the lower limit of functionally significant change (defined as ≥ 0.20 log units). The intersection point of the regression function with the $y = 0.20$ line indicates the precapsulotomy $\log(s)$ value above which a treatment effect can be expected, with a probability of $\geq 50\%$. PCO= Posterior Capsule Opacification.

Posterior capsule remnants after capsulotomy

Among the pseudophakic subpopulation of 97 cases, PC remnants were present in 71 cases. It should be mentioned that those 71 cases also included very small PC remnants, i.e., remnant fractions smaller than .100. Among the 71 cases with PC remnants, were 18 cases with regenerative PCO and 53 cases with fibrotic PCO. Remnant fractions ranged from .002 to 0.280 with a median of 0.033 in regenerative PCO, and ranged from .001 to 0.758 with a median of 0.115 in fibrotic PCO. Remnant fractions were statistically significantly lower in regenerative PCO than in fibrotic PCO (Mann Whitney Test, $p = .004$). A positive correlation was found between remnant fractions and postcapsulotomy $\log(s)$

values (Spearman's ρ [97]= .26, p = .009). Remnant fractions were not related to VA, which confirms the discussion on the relation between opacification fraction and VA in the "PCO severity" subsection.

Secondary capsulotomy

Among the entire study population, 14 patients (14/240; 6%) had persistent subjective visual symptoms and substantial PC remnants in the natural pupil area. All 14 cases had fibrotic PCO. Secondary capsulotomy resulted in a reduction of remnant fraction in 8 cases (8/14; 57%). In 6 cases remnant fractions remained similar, because the positioning of the fibrotic PC remnants could not be altered by secondary capsulotomy punctures. Unfortunately, none of the secondary capsulotomies resulted in functional improvement: in the 8 cases with a reduced remnant fraction, a mean log(s) improvement of 0.02, a mean logMAR improvement of 0.06, and a mean log(CS) reduction of 0.02 was found, and in the 6 cases with an unaltered remnant fraction, a mean log(s) improvement of 0.06, a mean logMAR reduction of 0.03, and a mean log(CS) improvement of 0.04 was found.

DISCUSSION

In the present study, the effect of PCO severity and morphology on the small-angle domain of VF (VA and CS measurement) and the large-angle domain (straylight measurement) was assessed. It was demonstrated that postcapsulotomy improvement is related to PCO severity rather than PCO morphology. It can be concluded that with increasing PCO severity, straylight and CDVA impairment increase. However, the precise relation between PCO severity and these VF parameters is different: the relation between PCO severity and log(s) is linear, whereas the relation between PCO severity and logMAR is curvilinear. The former relation corresponds to the linear relation between log(s) and the fraction of the pupil area covered by capsulorhexis, found in an earlier study.¹⁸ Because of the linear relation between PCO severity and log(s), the functional effect of slight PCO can be objectified by straylight measurement. However, the functional effect can not be documented with CDVA testing, because of the curvilinear relation between PCO severity and logMAR. Meacock et al. also found that straylight is more sensitive to slight PCO than VA.³⁷ They determined the percentage of PC coverage by PCO at which a decline in VF occurred, which was 78% for VA, 46% for CS and less than 1% for straylight.³⁷ These findings illustrate that the relation between VA and straylight is limited: change of the straylight parameter is not necessarily accompanied by VA change, or vice versa.⁴ As mentioned in the Introduction, straylight (large-angle domain of VF) and VA (small-angle domain of VF) represent different aspects of VF. Straylight and VA impairment are caused by distinct optical processes. Depending on the nature of the underlying problem, straylight and VA may or may not go hand in hand: only

if an underlying problem affects both of the distinct optical processes, then straylight and VA will both be affected.

72

The main finding of the present study for ophthalmic practice is that straylight can be used as a meaningful indicator for capsulotomy. In PCO with a $\log(s)$ value ≥ 1.44 , a treatment effect (improvement ≥ 0.20 log units) can be expected from capsulotomy, with $\geq 50\%$ probability. So, the cutoff value for straylight, i.e., $\log(s) \geq 1.44$, can be used as indication criterion for capsulotomy. In PCO with a $\log(s)$ value between 1.22 and 1.44, a more modest improvement can be expected from capsulotomy.

This study found that postcapsulotomy improvement was largest in cases with substantially impaired precapsulotomy VF parameters. So, postcapsulotomy improvement of VF parameters is related to precapsulotomy values. This finding confirms a similar tendency found by Montenegro et al.¹⁴ In the present study, surprisingly low EPCO scores, assessed using retro illumination, were found in fibrotic PCO. Consequently, in these cases postcapsulotomy improvement was small. We expect that the inclusion of cases with fibrotic PCO of low severity is related to clinical evaluation of PCO severity using reflected light. In the present study, opacified PC fractions assessed with reflected light, were found to be higher than those assessed with retro illumination. This was realized earlier by Camparini et al.³⁸ As will be detailed in the next subsection, we expect reflected light examination to overestimate functional PCO severity, especially in fibrotic PCO. Overestimation of functional PCO severity may cause erroneous attribution of subjective symptoms to PCO and nonbeneficial capsulotomy referral.

Fibrotic PCO is easier to recognize,³⁸ and fine surface details are revealed better using reflected light than using retro illumination. However, reflected light examination is expected to have a less direct relation with VF: the visibility of PCO using reflected light is primarily related to the amount of light reflected, and is not related to the amount of light refracted or scattered. At the PCO surface, part of the incident light is reflected in backward direction, part is scattered in all directions, and part is transmitted (accompanied by refraction) in forward direction. The amount of light reflected is dependent on refractive index difference, among other factors. Grayscale differences in reflected light images indicate the presence of refractive index differences, rather than a functional relation with VF. As a consequence, reflected light examination may overestimate functional PCO severity, especially in fibrotic PCO. Using retro illumination, incident light is reversed as it is reflected by the fundus, and then scattered by PCO. The light is scattered in all directions, including angles wider than the opening angle of the slit-lamp camera. Light scattered over angles wider than the opening angle can not be detected by the slit-lamp camera, and the amount of incident light is no longer equal to the amount of light reflected by the fundus. As a result, at the location of

light-scattering PCO structures a reduced light intensity is recorded by the slit-lamp camera. So, light-scattering PCO structures appear as less intense, shadowy patterns in the retro illumination image. Therefore, it is expected that slit-lamp retro illumination does have a functional relation with VF, and can be used to distinguish light-scattering structures from light-transmitting (non light-scattering) structures: PCO structures appearing as shadowy patterns on retro illumination scatter light and are expected to affect VF.

Overestimation of functional PCO severity in fibrotic PCO using reflected light, may not only have caused early, often nonbeneficial capsulotomy referral in the present study, as in earlier studies. Studies on the effect of capsulotomy on CDVA and CS found limited postcapsulotomy improvement in fibrotic PCO,¹⁰ or reported that the correlation between CDVA and CS improvement and fibrosis score was close to zero.⁹ More recent studies on the effect of capsulotomy on the straylight parameter found considerable percentages of pseudophakics without functionally significant log(s) improvement (considering an improvement ≥ 0.20 log units as functionally significant): 34% (12/35)⁵ and 55% (29/53)¹⁴, as compared with 63% (151/240) in the present study. The average precapsulotomy log(s) value of 1.55 and the 34% functionally significant log(s) improvement found in our earlier study⁵ is substantially different from the average precapsulotomy log(s) value of 1.38 and the 63% functionally significant log(s) improvement found in the present study. The differences may be caused by inclusion selection, which may reflect that (1) recently, early capsulotomy referral becomes more accepted, as is early cataract extraction, and (2) current referral criteria provide clinicians with insufficient objective guidance for early, beneficial capsulotomy. They emphasize the need for a more reliable indicator for capsulotomy referral, distinguishing between early, beneficial capsulotomy and early, nonbeneficial capsulotomy.

Few regenerative PCO cases (4/45; 9%) had an opacified PC area with a fraction < 0.5 . Functionally significant improvement of log(s) was found in 2 of those cases. This may either indicate that (1) in some cases regenerative PCO with fraction < 0.5 does not cause substantial visual symptoms, or (2) in the presence of regenerative PCO with fraction < 0.5 , PCO severity was underestimated by the clinician. This reemphasizes the need for a reliable indicator for capsulotomy referral.

As mentioned previously, PCO structures appearing as shadowy patterns on retro illumination scatter light. The EPCO method for evaluation of PCO severity uses retro illumination images, and therefore gives an indication of the severity of such shadowy, light scattering PCO structures. This is confirmed by the relation between retro illumination based PCO severity (EPCO score) and straylight. Straylight is affected by PCO fraction and PCO density, whereas VA is mainly affected by PCO fraction. Because the EPCO method incorporates PCO fraction, also a relation between EPCO score and logMAR was found. However, the relation between

EPCO score and the VF parameters is subject to noise caused by the EPCO method. First, incorporation of PCO fraction and PCO density in the EPCO score, results in a comparable score assigned to posterior capsules with different PCO characteristics, e.g., a small PCO fraction of high PCO density and a large PCO fraction of low PCO density. Second, noise is caused by dividing PCO density into a discrete, 5-category grading scale instead of using a continuous quantitative scale. Because PCO density is subjectively assessed, a different density score may be assigned to areas with only small differences. Because of the noise caused by the EPCO method, we expect that the EPCO score has limited ability to predict functional impairment. Therefore, we expect the EPCO score to provide insufficient guidance for beneficial capsulotomy referral. This can be illustrated by determining its specificity. Let us assume that a functional measure of VF impairment, such as $\log(s)$, should be the guiding principle for treatment. By using $\log(s)$ as a reference standard, sensitivity and specificity of the EPCO score can be determined. Let us assume that a precapsulotomy $\log(s)$ value ≥ 1.44 (corresponding to the averaged precapsulotomy cutoff values of 1.40 and 1.48), indicating functionally significant visual impairment caused by PCO, can be used as an indicator for capsulotomy referral. A precapsulotomy $\log(s)$ value of 1.44 corresponds to an EPCO score of 2.0. Thus, EPCO scores ≥ 2.0 would indicate that capsulotomy referral is needed, and EPCO scores < 2.0 would indicate that capsulotomy referral is not needed. In 39 cases a $\log(s)$ value ≥ 1.44 was found (i.e., indication for capsulotomy), of whom 13 had an EPCO score ≥ 2 and 26 an EPCO score < 2 . So, the sensitivity of the EPCO score was 33% ($13/[13+26]$). In 59 cases a $\log(s)$ value < 1.44 was found (i.e., no indication for capsulotomy), of whom 8 had an EPCO score ≥ 2 and 51 had an EPCO score < 2 . So the specificity of the EPCO score was 86% ($51/[51+8]$). Given the assumption that $\log(s)$ can be used as a reference standard for capsulotomy referral, it should be concluded that the EPCO score is not suitable for capsulotomy referral. Only in severe PCO, with a large PCO fraction and high PCO density, the retro illumination image (EPCO score) may provide sufficient guidance for capsulotomy referral.

Apart from noise caused by EPCO method, additional noise in the relation between EPCO score and VF parameters can be expected in a nonresearch setting. This may be due to straylight by ocular structures other than PCO. It should be realized that $\log(s)$ values represent the amount of straylight in the pseudophakic eye as a whole, including the possible contribution of other ocular structures to intraocular straylight, e.g., light-scatter by the cornea and vitreous, pigmentation-dependent light transmission by the iris and sclera, and pigmentation-dependent light reflection by the fundus.^{24;39;40} In PCO cases without other co morbidity (i.e., the cases included in the present study), the amount of straylight caused by PCO will be much larger than the amount of straylight caused by other ocular structures, and the $\log(s)$ increase will be almost exclusively caused by PCO. However, in a nonresearch setting, PCO cases with other co morbidity could add noise in the relationship. In a nonresearch

setting, even more noise can be expected in the relation between EPCO score and logMAR, because VA testing can additionally be affected by suboptimal refined refraction, and by macular pathology.

The effect of PCO on straylight (large-angle domain of VF) was recently studied in-vitro.⁴¹ In-vitro and in-vivo, the proportion of fibrotic and regenerative PCO was different: in-vitro little fibrotic PCO was detected, whereas in-vivo most pseudophakics were diagnosed as having fibrotic PCO. The lower proportion of fibrotic PCO found in-vitro might be caused by differences in imaging techniques. In-vitro, a dark field microscopy set-up was used for examination of the specimen.¹⁵ Using dark field microscopy, light scattered by the specimen produces the microscope image. Although dark field microscopy is an effective technique and specimens were carefully examined, possibly low scatter by specimens with fibrotic PCO could not be recognized. This corresponds to the clinical notion that fibrotic PCO is less easy recognized using retro illumination, as compared to reflected light.³⁸ As a result, only the more severe fibrotic specimens with an important effect on straylight might be recognized in-vitro. Our in-vitro study also showed that the recognized, and probably most severe, fibrotic PCO specimens had lower log(s) values (see Figure 2C in⁴¹) than the specimens with regenerative PCO (see Figure 2D in⁴¹). In-vitro, the highest log(s) recorded was 1.40 for fibrotic PCO specimens and 2.0 for regenerative PCO specimens. This makes the in-vitro and in-vivo studies concordant: in the present in-vivo study, the highest log(s) value of 1.85 in fibrotic PCO is also lower than the highest log(s) value of 2.28 in regenerative PCO. In-vitro values obtained at visual angles of -7 and 7 degrees can be directly compared to in-vivo values measured using the C-Quant (at approximately 7 degrees).⁴¹ However, in-vivo log(s) values are higher than in-vitro log(s) values, because in-vivo values represent the amount of straylight in the eye as a whole, including light-scatter by other ocular structures, whereas in-vitro values only represent light-scatter by the posterior lens capsule-IOL complex.

The straylight parameter is not only affected by PCO severity, but is also slightly affected by age. The reported precapsulotomy cutoff values of log(s)= 1.40 and 1.48, indicating a probability of $\geq 50\%$ for functionally significant log(s) improvement after capsulotomy, are age-*independent*. A clinical guideline based on age-dependent cutoff values, distinguishing straylight increases related to normal aging of ocular structures in the pseudophakic eye from (additional) straylight increases caused by PCO, would have been important for the clinician. Theoretically, the upper limit of the 95% CI of the pseudophakic reference curve for straylight, which is 1.31 at age 50 and 1.60 at age 90, could be such an age-dependent cutoff limit. The age-*independent* precapsulotomy log(s) cutoff values are consistent with the age-dependent upper limit: the averaged cutoff value of $([1.40 + 1.48]/2)$ 1.44 corresponds to the middle of that range (Figure 3). An extended study to determine an age-dependent limit for each age decade, would require a much larger study population. Of note, Montene-

gro et al. also found a correlation between postcapsulotomy log(s) values and age (Pearson's $r(53) = .32, p = .026$).¹⁴

76

All VF parameters in the postcapsulotomy study population were worse than those found in the reference population. Corresponding findings for VA have been reported in an earlier study by Casprini et al.⁴² It should be taken into consideration that IOL repositioning after capsulotomy may potentially have affected VA and CS in the postcapsulotomy study population: IOL repositioning after capsulotomy is expected to be dependent on IOL-specific factors such as biomaterial, and may cause IOL-specific wavefront aberration differences⁴³ with a potential effect on the small angle domain of VF. Factors contributing to the significantly worse log(s) values found in the postcapsulotomy study population as compared with those found in the reference population, are yet unknown. In the present study it was found that log(s) is sensitive to structures producing low scatter (such as slight PCO). Therefore, potential light-scatter by factors such as IOL material, anterior capsule opacification (ACO),¹⁸ or PC remnants might have contributed to the log(s) differences. Their effect on log(s) is expected to be small, but cannot be completely ruled out. The differences in IOL material between the study and reference population, might have resulted in differences of potential IOL scatter. Light-scatter by IOLs can be determined isolated from light-scatter by ocular structures, by recording of light-scatter with an in-vitro technique using a goniometer set-up,^{44,45} a technique that was originally developed to record forward light-scatter by crystalline lenses.⁴⁶⁻⁴⁹ Forward light-scatter by IOLs was shown to be insignificant for two types of hydrophilic and hydrophobic acrylic IOLs.⁴⁴ The in-vitro technique was recently used to record forward light-scatter by the posterior capsule-IOL complex (e.g., hydrophobic acrylic IOLs, PMMA IOLs).^{15,41} Scatter by clear posterior capsule areas, thus including potential scatter of IOL material, was found to be low, irrespective of IOL material.^{15,41} Therefore, it seems unlikely that the log(s) differences between the postcapsulotomy study population and reference population are based on the differences in IOL material. Likewise, potential light-scatter by a factor such as ACO can not be ruled out. The cases included in the present study had a capsulorrhexis size larger than the natural pupil size under daytime light conditions. Straylight measurement was also performed under daytime light conditions. Therefore, it is unlikely that anterior capsule opacities were exposed in the pupil opening during straylight measurement. Since anterior capsule opacities outside the pupil opening are not exposed to light entering the eye, it is unlikely that they could have caused light-scatter. As a consequence, in the present study the contribution of ACO to log(s) is expected to be minor. A third factor of potential scatter, are PC remnants. Although secondary capsulotomy for PC remnants did not result in VF improvement, postcapsulotomy log(s) values and remnant fractions were correlated (Spearman's $\rho [97] = .26, p = .009$). It should be mentioned that Montenegro et al.¹⁴ found a slightly stronger correlation between postcapsulotomy log(s) values and capsule remnants analyzed using POComan software⁵⁰ (Pearson's $r(53) = .40, p = .002$).

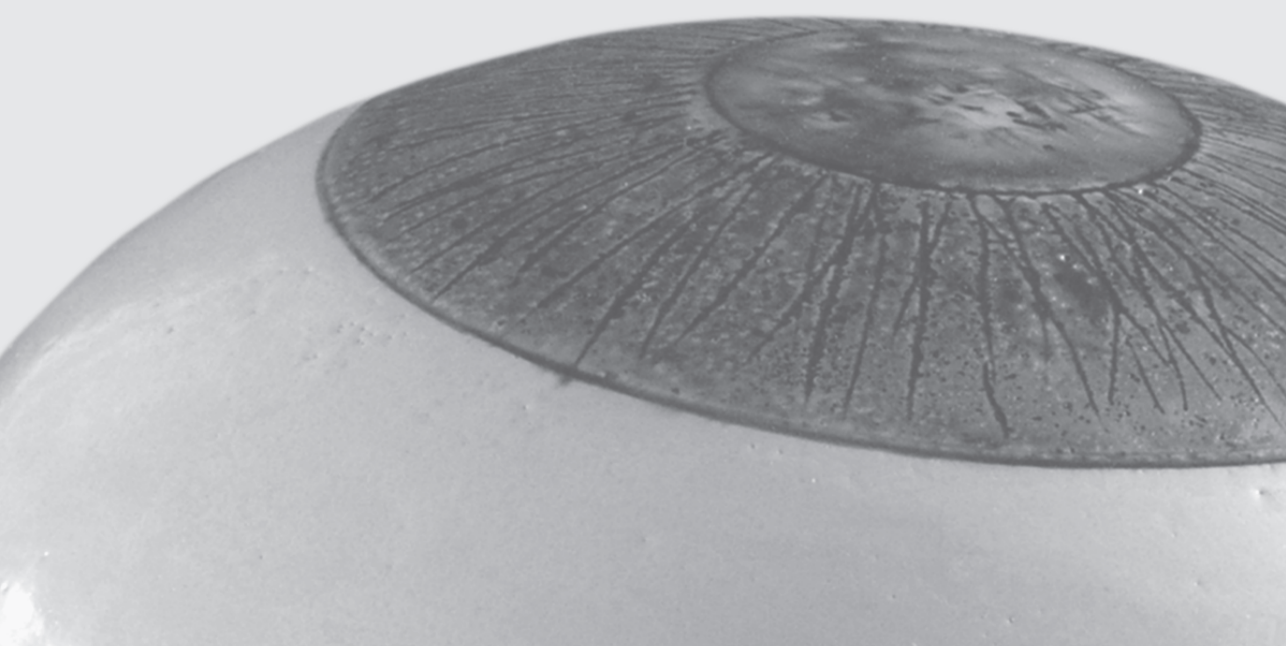
In conclusion, capsulotomy referral should be based on subjective symptoms, VF parameters, and slit-lamp retro illumination. A clinical guideline for the prediction of beneficial capsulotomy should be based on parameters relating to both aspects of VF: VA (small-angle domain of VF) and straylight (large-angle domain of VF). In cases of slight PCO, straylight is more valuable than VA, because of its susceptibility to low PCO severity scores. The log(s) cutoff value of 1.44 for functionally significant log(s) improvement and 1.22 for the absence of log(s) improvement may help the ophthalmologist in deciding whether capsulotomy is indicated. Moreover, it is concluded that PCO severity assessed with retro illumination has a functional relation with VF, whereas PCO severity assessed with reflected light is expected to have little relation to VF. Thus, the ophthalmologist should be cautious to use the reflected light image of PCO as an indication for capsulotomy.

REFERENCE LIST

1. van den Berg TJ, IJspeert JK. Straylight meter. In: Optical Society of America, ed. Technical Digest on Noninvasive Assessment of the Visual System. Washington DC: 1991:256-9.
2. van den Berg TJ, IJspeert JK. Clinical assessment of intraocular stray light. *Appl Opt* 1992;31:3694-6.
3. van den Berg TJ, Franssen L, Coppens JE. Straylight in the human eye: testing objectivity and optical character of the psychophysical measurement. *Ophthalmic Physiol Opt* 2009;29:345-50.
4. van den Berg TJ, Franssen L, Coppens JE. Ocular Media Clarity and Straylight. In: DA Dartt, ed. *Encyclopedia of the Eye*. Oxford: Academic Press, Elsevier; 2010:173-83.
5. van Bree MC, Zijlmans BL, van den Berg TJ. Effect of neodymium:YAG laser capsulotomy on retinal straylight values in patients with posterior capsule opacification. *J Cataract Refract Surg* 2008;34:1681-6.
6. Apple DJ, Solomon KD, Tetz MR, et al. Posterior capsule opacification. *Surv Ophthalmol* 1992;37:73-116.
7. Wormstone IM. Posterior capsule opacification: a cell biological perspective. *Exp Eye Res* 2002;74:337-47.
8. Wormstone IM, Wang L, Liu CS. Posterior capsule opacification. *Exp Eye Res* 2009;88:257-69.
9. Aslam TM, Patton N. Methods of assessment of patients for Nd:YAG laser capsulotomy that correlate with final visual improvement. *BMC Ophthalmol* 2004;4:13.
10. Cheng CY, Yen MY, Chen SJ, et al. Visual acuity and contrast sensitivity in different types of posterior capsule opacification. *J Cataract Refract Surg* 2001;27:1055-60.
11. Elliott DB, Bullimore MA. Assessing the reliability, discriminative ability, and validity of disability glare tests. *Invest Ophthalmol Vis Sci* 1993;34:108-19.
12. Franssen L, Coppens JE, van den Berg TJ. Compensation comparison method for assessment of retinal straylight. *Invest Ophthalmol Vis Sci* 2006;47:768-76.
13. Coppens JE, Franssen L, van Rijn LJ, van den Berg TJ. Reliability of the compensation comparison stray-light measurement method. *J Biomed Opt* 2006;11:34027.
14. Montenegro GA, Marvan P, Dexl A, et al. Posterior capsule opacification assessment and factors that influence visual quality after posterior capsulotomy. *Am J Ophthalmol* 2010;150:248-53.
15. van Bree MC, van der Meulen IJ, Franssen L, et al. Imaging of forward light-scatter by opacified posterior capsules isolated from pseudophakic donor eyes. *Invest Ophthalmol Vis Sci* 2011;52:5587-97.
16. Kohnen T. New abbreviations for visual acuity values. *J Cataract Refract Surg* 2009;35:1145.
17. van der Meulen IJ, Engelbrecht LA, van Vliet JM, et al. Straylight measurements in contact lens wear. *Cornea* 2010;29:516-22.
18. van der Meulen IJ, Engelbrecht LA, Van Riet TC, et al. Contributions of the capsulorrhexis to straylight. *Arch Ophthalmol* 2009;127:1290-5.

19. Beerthuis JJ, Franssen L, Landesz M, van den Berg TJ. Straylight values 1 month after laser in situ keratomileusis and photorefractive keratectomy. *J Cataract Refract Surg* 2007;33:779-83.
20. Lapid-Gortzak R, van der Linden JW, van der Meulen IJ, et al. Straylight measurements in laser in situ keratomileusis and laser-assisted subepithelial keratectomy for myopia. *J Cataract Refract Surg* 2010;36:465-71.
21. Rozema JJ, Coeckelbergh T, van den Berg TJ, et al. Straylight before and after LASEK in myopia: changes in retinal straylight. *Invest Ophthalmol Vis Sci* 2010;51:2800-4.
22. van Bree MC, van Verre HP, Devreese MT, et al. Straylight values after refractive surgery: screening for ocular fitness in demanding professions. *Ophthalmology* 2011;118:945-53.
23. Vignat R, Tanzer D, Brunstetter T, Schallhorn S. [Scattered light and glare sensitivity after wavefront-guided photorefractive keratectomy (WFG-PRK) and laser in situ keratomileusis (WFG-LASIK)]. *J Fr Ophtalmol* 2008;31:489-93.
24. van den Berg TJ. Analysis of intraocular straylight, especially in relation to age. *Optom Vis Sci* 1995;72:52-9.
25. van den Berg TJ, Van Rijn LJ, Michael R, et al. Straylight effects with aging and lens extraction. *Am J Ophthalmol* 2007;144:358-63.
26. The Age-Related Eye Disease Study (AREDS): design implications. AREDS report no. 1. *Control Clin Trials* 1999;20:573-600.
27. Ferris FL 3rd, Kassoff A, Bresnick GH, Bailey I. New visual acuity charts for clinical research. *Am J Ophthalmol* 1982;94:91-6.
28. Elliott DB, Bullimore MA, Bailey IL. Improving the reliability of the Pelli-Robson contrast sensitivity test. *Clin Vision Sci* 1991;6:471-5.
29. Vos JJ. Disability glare - a state of the art report. *Commission Internationale de l'Eclairage Journal* 1984;3/2:39-53.
30. van der Sterre GW, van de Graaf ES, Verezen CA, et al. National Eye Institute Visual Functioning Questionnaire-25: Dutch Consensus Translation (VFQ-25/NL). Available at <http://www.erasmusmc.nl/mage/publicaties/aanvullingen/3503529?lang=en>. Accessed January 4, 2013.
31. Mangione CM, Lee PP, Gutierrez PR, et al. Development of the 25-item National Eye Institute Visual Function Questionnaire. *Arch Ophthalmol* 2001;119:1050-8.
32. Mangione CM. National Eye Institute VFQ-25 Scoring Algorithm. August 2000. Available at http://www.nei.nih.gov/resources/visionfunction/manual_cm2000.pdf, Accessed January 4, 2013.
33. Tetz MR, Auffarth GU, Sperker M, et al. Photographic image analysis system of posterior capsule opacification. *J Cataract Refract Surg* 1997;23:1515-20.
34. Neumayer T, Findl O, Buehl W, et al. Long-term changes in the morphology of posterior capsule opacification. *J Cataract Refract Surg* 2005;31:2120-8.
35. Findl O, Buehl W, Bauer P, Sycha T. Interventions for preventing posterior capsule opacification. *Cochrane Database Syst Rev* 2010;(2):CD003738.

36. Vasavada AR, Raj SM, Shah A, et al. Comparison of posterior capsule opacification with hydrophobic acrylic and hydrophilic acrylic intraocular lenses. *J Cataract Refract Surg* 2011;37:1050-9.
37. Meacock WR, Spalton DJ, Boyce J, Marshall J. The effect of posterior capsule opacification on visual function. *Invest Ophthalmol Vis Sci* 2003;44:4665-9.
38. Camparini M, Macaluso C, Reggiani L, Maraini G. Retroillumination versus reflected-light images in the photographic assessment of posterior capsule opacification. *Invest Ophthalmol Vis Sci* 2000;41:3074-9.
39. Ijspeert JK, de Waard PW, van den Berg TJ, de Jong PT. The intraocular straylight function in 129 healthy volunteers; dependence on angle, age and pigmentation. *Vision Res* 1990;30:699-707.
40. van den Berg TJ, Ijspeert JK, de Waard PW. Dependence of intraocular straylight on pigmentation and light transmission through the ocular wall. *Vision Res* 1991;31:1361-7.
41. van Bree MC, van der Meulen IJ, Franssen L, et al. In-vitro recording of forward light scatter by human lens capsules and different types of posterior capsule opacification. *Experimental Eye Research* 2012;96:138-46.
42. Casprini F, Balestrazzi A, Tosi GM, et al. Optical aberrations in pseudophakic eyes after 2.5-mm Nd:YAG laser capsulotomy for posterior capsule opacification.
43. Rozema JJ, Koppen C, de Groot V, Tassignon MJ. Influence of neodymium:YAG laser capsulotomy on ocular wavefront aberrations in pseudophakic eyes with hydrophilic and hydrophobic intraocular lenses. *J Cataract Refract Surg* 2009;35:1906-10.
44. Nanavaty MA, Spalton DJ, Boyce JF. Influence of different acrylic intraocular lens materials on optical quality of vision in pseudophakic eyes. *J Cataract Refract Surg* 2011;37:1230-8.
45. van der Meulen IJ, Porooshani H, van den Berg TJ. Light-scattering characteristics of explanted opacified Aquasense intraocular lenses. *Br J Ophthalmol* 2009;93:830-2.
46. van den Berg TJ, Ijspeert JK. Light scattering in donor lenses. *Vision Res* 1995;35:169-77.
47. van den Berg TJ. Depth-dependent forward light scattering by donor lenses. *Invest Ophthalmol Vis Sci* 1996;37:1157-66.
48. van den Berg TJ. Light scattering by donor lenses as a function of depth and wavelength. *Invest Ophthalmol Vis Sci* 1997;38:1321-32.
49. van den Berg TJ, Spekrijse H. Light scattering model for donor lenses as a function of depth. *Vision Res* 1999;39:1437-45.
50. Bender L, Spalton DJ, Uyanonvara B, et al. POComan: new system for quantifying posterior capsule opacification. *J Cataract Refract Surg* 2004;30:2058-63.



Chapter 6

Imaging of forward light-scatter by opacified posterior capsules isolated from pseudophakic donor eyes

Maartje C.J. van Bree, Ivanka J.E. van der Meulen,
Luuk Franssen, Joris E. Coppens, Nicolaas J. Reus, Bart L.M. Zijlmans,
Thomas J.T.P. van den Berg

Investigative Ophthalmology & Visual Science 2011;52(8):5587-97



ABSTRACT

Purpose: Posterior capsule opacification (PCO) degrades visual function by reducing visual acuity, but also by increasing intra-ocular light-scatter. We used an in-vitro model to elucidate the effect of PCO-morphology on light-scatter and its functional aspect, as can be assessed with straylight measurement.

Methods: Forward PCO-scatter by opacified capsular bags was recorded with a goniometer and camera. The camera position mimicked the anatomical position of retinal photoreceptors; the camera recorded the scattered light that the photoreceptors would sense in an in-vivo situation. Scattered light was recorded at different wavelengths and scatter angles, which were divided into a near ($1^\circ < \theta \leq 7^\circ$) and far ($\theta > 7^\circ$) large-angle domain. Using scattered light, the camera produced grayscale PCO-images. The nature of the angular dependence of PCO-scatter was compared to that of scatter in the normal eye, by rescaling PCO-images relative to the normal eye's point-spread function.

Results: The scattered light images closely followed PCO-severity. The angular dependence of PCO-scatter resembled that of scatter in the normal eye, irrespective of severity and PCO-type. PCO shows the type of wavelength dependence that is normal for small particles: monotonically decreasing with increasing wavelength. At the near large-angle domain, the angular dependence of PCO-scatter and scatter in the normal eye resembled less closely.

Conclusions: Surprisingly, PCO-scatter and scatter in the normal eye have similar underlying scattering processes. However, data obtained at the near large-angle domain demonstrates that, apart from scatter, PCO may also have a refractile component, which is most pronounced in pearl-type PCO.

INTRODUCTION

It is well known that posterior capsule opacification (PCO) impairs visual function. Several studies have assessed the negative effect of PCO on visual acuity (VA) and contrast sensitivity (CS), but there is limited correspondence between VA and the degree of visual impairment experienced by the PCO-patient.¹⁻⁶ Recently, the repertoire of visual function tests was expanded by intraocular straylight measurement.⁷ Several studies have since assessed the importance of straylight in PCO.^{6,8,9} Substantial straylight elevations were found in PCO patients with good VA, which demonstrates that PCO affects VA and straylight quite independently.⁹ This finding confirms that visual function has two distinct functional domains: small-angle and large-angle,¹⁰ as will be detailed later in this section. Therefore, to assess visual function properly, different parameters relating to the functional domains must be tested. Another issue is that attempts to relate PCO severity, assessed by slit-lamp observation or image evaluation software, to VA and straylight have not been very successful.^{1-3;5;6;11-13} This may be due to the fact that functional impairment is caused by forward light-scatter, whereas slit-lamp evaluation of PCO severity is based on the amount of backward scattered light. Since backscattered light does not necessarily correspond to functional impairment, forward light-scatter should be assessed.¹⁴⁻¹⁷ We expect that both issues, (1) the independent effect of PCO on the visual function parameters VA and straylight, and (2) the lack of correspondence between PCO severity and visual function parameters, may be related to PCO morphology. Unfortunately, it is hardly possible to assess the effect of PCO morphology on visual function in-vivo.

Based on pathogenesis and cells of origin, there is a clinical differentiation between 2 morphological forms of PCO, (regenerative) pearl-type and fibrosis-type PCO.¹⁸ In addition, there are morphological differences within the pearl-type PCO, which adds to the morphological heterogeneity of PCO.¹⁹ The optical behavior of different PCO types may be diverse. Some optical characteristics may predominantly affect the small-angle domain of visual function, resulting in impaired VA, whereas others may predominantly affect the large-angle domain, resulting in an impaired straylight value. The present study focuses on straylight.

Imperfections of the eye's optical media cause aberrations and light-scatter, even in young, healthy eyes. As a result, the retinal image will not be identical to the original visual stimulus, and the quality of the retinal image suffers. A common way to address this visual degradation is to suppose that the visual stimulus is a single point of light. In the presence of optical media imperfections, the light intensity of its retinal projection will be spread out over the retina. The retinal projection will be a bright light spot in the center, surrounded by a zone of diminished light intensity (Figure 1, A-B). This light distribution on the retina is called the "point-spread function" (PSF). It comprehensively describes the eye's optical quality.

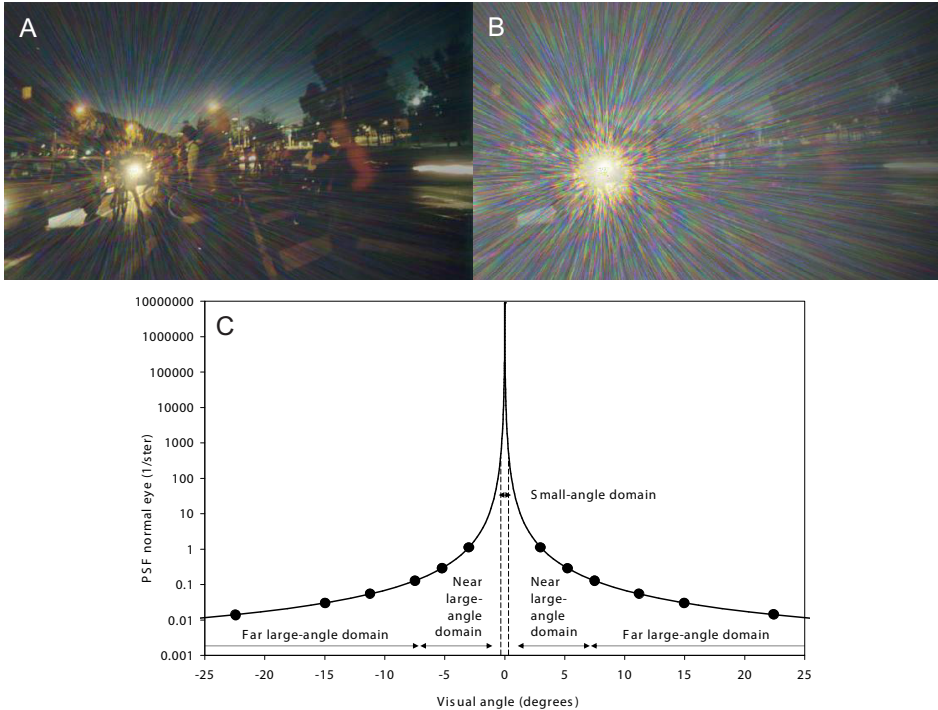


Figure 1. A retinal image of the outside world with a bright light originating from a car headlight, which is degraded by light-scatter in a normal (young, healthy) eye (A) and in an eye with media imperfections such as PCO (B). Part of the bright light is scattered in all forward directions; its retinal projection is a bright spot surrounded by a spreading of light over the entire retina. The functional effect is a veil of light, which is called straylight, projected all over the retinal image of the outside world. The Point-Spread Function (PSF) for a normal eye, according to the CIE standard (C). There are two domains of visual function, a small-angle domain and a large-angle domain (θ beyond 1°). In this study, the large-angle domain is divided into a near large-angle domain ($1^\circ < \theta \leq 7^\circ$) and a far large-angle domain ($\theta > 7^\circ$).

Figure 1C shows the PSF for a healthy, young, Caucasian eye, according to the Commission Internationale de l'Éclairage (CIE)²⁰; an International Commission on standards in vision (see <http://www.cie.co.at/>, accessed January 4, 2013). In this study, the PSF for a healthy, young, Caucasian eye will be referred to as the "normal PSF". The relative light intensity of the light point is plotted as a function of visual angle (θ). The two functional domains mentioned above are shown in Figure 1C. The small-angle domain is affected by aberrations, resulting in diminished sharpness of the retinal image and loss of contrast.¹⁰ This domain can be assessed by functional tests such as VA (VA of decimal 1.0 corresponds to $\theta \approx 0.02^\circ$) and CS (spatial frequencies of > 3.0 cycles per degree correspond to $\theta < 0.3^\circ$) and by optical approaches such as aberrometry and double-pass techniques. The large-angle domain is affected by light-scatter. Scatter affects vision predominantly because in the retinal image, light from bright areas in the visual scene spreads towards dark areas. It results in a reduced retinal

contrast, which is experienced by the subject as hazy vision and blinding. The corresponding functional impairment is called disability glare. Note that basic contrast sensitivity tests that are used in the clinical setting only assess contrast reduction caused by small-angle effects, such as aberrations. Contrast reduction caused by large-angle effects such as light-scatter, is not assessed by contrast sensitivity tests used in the clinical setting.^{10;21;22} By international consensus, disability glare is defined as straylight, because straylight was proven to predict disability glare precisely.²³ Straylight can be assessed clinically with the C-Quant (Oculus GmbH, Wetzlar, Germany).

In-vivo it is difficult to isolate the optical characteristics of PCO from the optical influence of other parts of the eye. In addition to this, capsular bags with a homogeneous coverage of a single PCO type are scarce. In the present study, the light-scattering characteristics of PCO were studied in-vitro with an optical set-up, which allows isolation of homogeneous PCO areas with a specific morphology. This optical set-up has been used previously to investigate forward light-scattering by the crystalline lens.^{24;25} A camera was used to document the light-scatter pattern, which in-vivo would have been sensed by the retinal photoreceptors. The purpose of our study was to document the scattering characteristics in different PCO types, and to elucidate the impact of PCO morphology on the large-angle domain (straylight domain, visual angles beyond 1°) of visual function.

METHODS

Human donor bulbi were used for this study. They were obtained from the Cornea Bank Amsterdam; only pseudophakic donor bulbi were selected. Information on the donor, such as ophthalmologic history, was not available. Only specimens with an intact capsule were included. As will be detailed later in this section, the specimens had to be representative of the in-vivo situation. Since the aim of this study was to document forward scattered light by PCO, there were no inclusion criteria concerning intra-ocular lens (IOL) type or dioptric power. Note that the refractive design of IOLs affects only the earlier mentioned small-angle domain. Small-sized irregularities, such as diffractive design, glistenings or Nd:YAG laser lesions of the IOL optic, could be expected to affect the large-angle domain. However, such irregularities were not present in the used specimens. IOLs potentially scatter due to less easily recognizable processes, of a more diffuse nature. It cannot be excluded that such processes played a role in specimens with clear capsules. Clear capsules always showed low level recordings. The precise level of these recordings cannot be assumed to represent faithfully the clear capsule. However, in the presence of PCO, PCO areas showed much more scatter as compared to clear areas, and PCO-scatter dominated over IOL processes.

After the Cornea Bank Amsterdam had removed the corneoscleral disk for transplantation purposes, we isolated the specimens, which were capsular bags enclosing an IOL, from the bulbi. As capsular bags are fragile and easily damaged during preparation, many specimens had to be discarded. During the study, damage of the capsular bags was reduced by immersion of the bulbus in a fixative prior to preparation and by improvement of the preparation technique. Initially, an immersion medium of phosphate-buffered saline (PBS) only was used, because it was unclear whether a fixative would affect the optics of the capsular bag tissue. It is important to assure tissue stability of unfixated specimens during the recording process. Therefore, at the end of the entire recording procedure the first recording was repeated and served as a quality control.²⁴ During the study, the effect of a 1% paraformaldehyde/PBS fixative on the appearance of opacified capsular bags was studied. Immediately after immersion and also after 2, 4, 6, 8 and 24 hours, the specimen's appearance was carefully monitored using the darkfield microscopy set-up shown in Figure 2.²⁶ After it was found that there were no discernible changes, the 1% paraformaldehyde/PBS solution was used to fixate the bulbi.

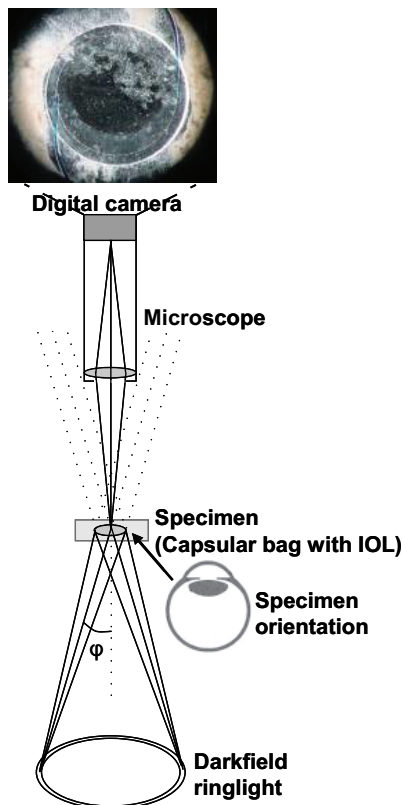


Figure 2. Darkfield microscopy set-up (side view, not to scale) used to examine and photograph the specimens. A digital camera was mounted on the microscope. The specimens were placed under the microscope with its posterior side down and illuminated by a darkfield ring light.

To isolate the capsular bag, the donor bulbus was put in an eye holder and positioned under a microscope. The initial preparation technique included removal of the iris, and cutting of the zonular fibers over 360 degrees (deg), at a position close to the ciliary body. The capsular bag was carefully lifted out using a spoon-shaped surgical spatula, and at the same time vitreous adhesions were removed. Later, we used a different preparation technique, which resembles the Miyake-Apple technique.^{27,28} After removal of the iris, a continuous 360-deg pars plana incision was made parallel to the limbus. This yielded a specimen of a capsular bag with IOL, attached by zonula fibers to a scleral rim approximately 2 mm wide. The specimen was carefully lifted out to avoid vitreous traction, and vitreous adhesions to the posterior capsule were removed. The specimen was then transferred to a Petri dish and was examined for free iris pigment and residual vitreous. Any pigment present was removed by rinsing the specimen in several Petri dishes with fresh PBS. After residual vitreous had been removed, the specimen was put in a clean Petri dish.

Because it was important that the specimens corresponded closely to in-vivo capsular bags, all specimens obtained were carefully examined by experienced ophthalmologists (I.J.E.M. and B.L.M.Z.). For this purpose, the specimen was put under a microscope (Stemi SV 11 stereomicroscope, Zeiss, New York, USA) (Figure 2). This set-up also included slit-lamp illumination (not shown), corresponding to the observation technique used by ophthalmologists when examining capsular bags in-vivo. To ensure that the in-vitro microscope view corresponded to the in-vivo ophthalmologist view, the specimen was placed with the posterior side down. It was illuminated from an angle of 30 deg using a darkfield ring light (Schott AG, Mainz, Germany) fed by a cold light source (KL 1500 LCD, Schott AG, Mainz, Germany). In order to prevent small surface imperfections of the Petri dish producing artefacts in the photomicrograph, the specimen was raised slightly by placing it on a small rubber ring (outer diameter 15 mm, inner diameter 10 mm, thickness 2.5 mm). Color photomicrographs of the specimens were made using a digital camera (DSC-S75, Sony Electronics Inc., California, USA), mounted on the microscope. The white balance of the camera was carefully set using the illumination light reflected off a white standard (Spectralon® Diffuse Reflectance Standard SRS-99-010, Labsphere Inc., North Sutton, USA). Camera settings, such as shutter speed and focus distance were fixed.

To image the light scattered by the specimen it was transferred to a goniometer set-up, which was previously used for studies on the crystalline lens.^{24,25} A top view representation of the set-up is shown in Figure 3. As a rule, the intensity of scattered light in human eyes is low. Therefore, it is essential to carefully control the amount of light scattered by sources other than the specimen, such as dust particles. A Hellma cell (700.000-OG, height 50 mm × width 50 mm × depth 10 mm; Hellma GmbH, Müllheim, Germany) was meticulously cleaned with a Hellmanex® cleaning concentrate diluted in distilled water (concentration

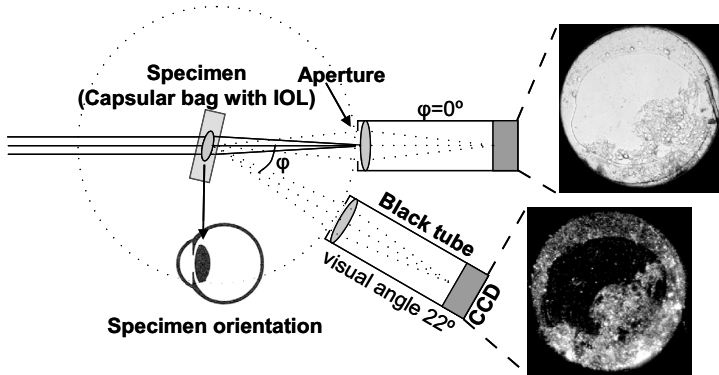


Figure 3. Goniometer set-up (top view, not to scale) used to obtain grayscale images of PCO. The posterior part of the specimen was oriented towards the camera. The camera served as the in-vitro counterpart of the in-vivo retinal photoreceptors and recorded scattered light. The scattered light was used to produce grayscale images of PCO.

1%; Hellma GmbH, Müllheim, Germany). Next, the cell was filled with PBS and placed in the goniometer set-up. A light-scatter baseline was measured. The maximum accepted value was $\log[s] = -1$, corresponding to approximately 1% of the average amount of straylight in healthy, young eyes.²⁵ The definition of “ $\log[s]$ ” is described elsewhere.^{25;29} The specimen was immersed in the PBS-filled cell. To remove the effects of surface reflections of the cell from the measurement, it was rotated by 13 deg from the $\theta = 0$ deg position (Figure 3). As may be expected, this had virtually no effect on the recordings of the specimen itself. To ensure that the amount of light scattered by the PBS-filled cell had not altered during the process of image acquisition, after each experiment the specimen was carefully removed and the light-scatter baseline measurement was repeated.²⁴

In the goniometer set-up, light was emitted by a halogen light source and passed through an infrared blocking filter and a narrowband interference filter. Narrowband interference filters transmit a narrow range of selected wavelengths. Three narrowband (Full Width at Half Height [FWHH] 10 nm) interference filters were used: red (peak wavelength of 661 nm), green-yellow (peak wavelength of 561 nm) and blue (peak wavelength of 440 nm) (Optics Balzers AG, Balzers, Liechtenstein). The 561 nm data are given unless otherwise noted. A circular area of the specimen with a diameter of 4 mm, which corresponds to an average photopic/mesopic pupil diameter, was illuminated. The posterior part of the specimen was oriented towards the camera. So, the incident light first reached the anterior capsule and then the posterior capsule, as it does in-vivo. The part of the incident light that is scattered in the forward direction by the specimen, was collected by a charge-coupled device (CCD) camera.³⁰ The camera represents the in-vitro counterpart of the in-vivo retinal photoreceptors, which detect the light scattered towards the retina. The images obtained were grayscale images of scattered light. The amount of light collected by the camera is limited by the

aperture diameter. In the set-up an aperture diameter of 3 mm was used and the distance from aperture to the specimen was 14 cm, this resulted in an aperture of 1.2 deg diameter.

If the camera is positioned at $\theta = 0$ deg (Figure 3), the light transmitted directly (non-scattered light) is collected. This can be compared with a clinical retrograde slit-lamp image, although the direction of the light is reversed (because the fundus is used as a reflector). In a retrograde image, the differences in light intensity can result from differences in the amount of light scattered. At opacified areas, some of the incident light is scattered, so only a reduced amount of light will be detected at $\theta = 0$ deg. As a consequence, opacified areas will appear as less intense, shadowy patterns in the retrograde image.

The specimen scattered the incident light in different forward directions. The scattered light was recorded by rotating the camera in the horizontal plane around the specimen and acquiring images at fixed scatter angles ($\theta_{\text{in air}} = -30, -20, -15, -10, -7, -4, +4, +7, +10, +15, +20$ and $+30$ deg). In-vivo the scattered light projects towards the retina through the vitreous body, a medium with a refractive index of 1.336.³¹ The recording angles were corrected for this refractive index, resulting in visual angles of $\theta = -22, -15, -11, -7, -5, -3, +3, +5, +7, +11, +15, +22$ deg, as indicated by the black dots in Figure 1C. All these visual angles are beyond 1.0° and therefore concern the large-angle domain only. The visual angles $\theta = -7, -5, -3, +3, +5, +7$ deg are nearer to the small-angle domain than the angles $\theta = -22, -15, -11, +11, +15, +22$ deg. In this study the angles $\theta = -7, -5, -3, +3, +5, +7$ deg are indicated as the "near large-angle domain", and the angles $\theta = -22, -15, -11, +11, +15, +22$ deg are indicated as the "far large-angle domain" (Figure 1C). The visual angles can be used to compare in-vitro and in-vivo light scattering characteristics.²⁵ For each specimen, all images obtained were combined in an image-set.

For each scatter angle θ , the corresponding PSF value was calculated by dividing the amount of light collected at angle θ (I_θ) by the total amount of light passing through the specimen (I_{total}), or $\text{PSF}(\theta) = I_\theta / I_{\text{total}}$ (1/steradian).²⁵ I_{total} was measured by positioning the camera at $\theta = 0$ deg (Figure 3), and using a wide aperture of 10 deg diameter. As the light intensity collected at $\theta = 0$ deg is high, there is a risk that the image will be saturated. To reduce the intensity by a factor of approximately 10^3 , a calibrated neutral density filter was inserted in front of the infrared blocking filter.²⁵

In the normal PSF, the intensity diminishes as a function of θ , approximately as $1/\theta^2$ (Stiles-Holladay approximation for $\theta > 1$ deg).²⁰ Because of the steeply declining scatter intensity, much light is collected at the smallest angles of this domain and the amount collected diminishes substantially with increasing angle. For example, at $\theta = 5$ deg ($1/\theta^2 = 1/25$) the light intensity would be about a factor 20 times higher than the light intensity at $\theta = 22$ deg

($1/\theta^2 = 1/484$). Without rescaling, the grayscale images collected at large angles would be very dark. To obtain images of similar brightness, the light intensities of the images obtained were rescaled using the normal PSF.²⁰ So, at each angle the recorded PCO-intensities were divided by the corresponding PSF-intensity (black dots in Figure 1C). If, after this rescaling, intensity differences exist between the images of an image-set, these differences indicate how PCO-scatter differs from that of the healthy, young eye (normal PSF). Areas of relatively bright intensity indicate more light-scatter than the normal PSF, whereas dark areas indicate less light-scatter than the normal PSF.

The angular and the wavelength dependence of scattered light can be used to assess the size of small scattering particles.¹⁵ In this study, the type of wavelength dependence of PCO-scatter is assessed using the three different peak wavelengths mentioned earlier in this section. The intensity of scattered light depends on particle size. Scattering by particles much smaller than the light wavelength has strong wavelength dependence and weak or no angular dependence, especially for the angular range investigated in this study. Larger particles have weaker or no wavelength dependence and strong angular dependence. In the earlier mentioned in-vitro studies on the human crystalline lens, the wavelength and angular dependence found was of intermediate strength, corresponding to particles of the same order of magnitude as wavelength.^{24;25} It should be noted that the wavelength dependence of retinal straylight has long been controversial. Although early in-vivo studies found no significant wavelength dependence,^{32;33} later in-vitro and in-vivo studies did demonstrate wavelength dependence.^{15;34;35} The weak effect found in the early in-vivo studies was clarified as the result of opposing wavelength dependencies and relatively imprecise measurement techniques.^{15;34;35}

RESULTS

In total, 59 specimens with capsule were obtained. As mentioned earlier, it was important that the specimens closely corresponded to in-vivo capsular bags, according to the assessment of experienced ophthalmologists (I.J.E.M. and B.L.M.Z.). This assessment identified 25 representative PCO specimens. Figure 4 shows photomicrographs of 8 of these specimens. The 8 specimens represent the morphologic variation that was found among the included 25 specimens. Specimen no. 8 in Figure 4 shows a nearly clear posterior capsule. The posterior capsule of specimen no. 3 is covered by a mild, diffuse PCO. The posterior capsule of specimen no. 6 has areas of mild, diffuse PCO and relatively clear areas. It also shows posterior capsule folds. Specimen no. 1 shows fibrosis-type PCO, whereas specimens no. 2, 4, 5 and 7 show pearl-type (regenerative) PCO. According to the ophthalmologists, the PCO severity in specimens no. 2, 4, and 7 would have justified Nd:YAG laser posterior capsulotomy.

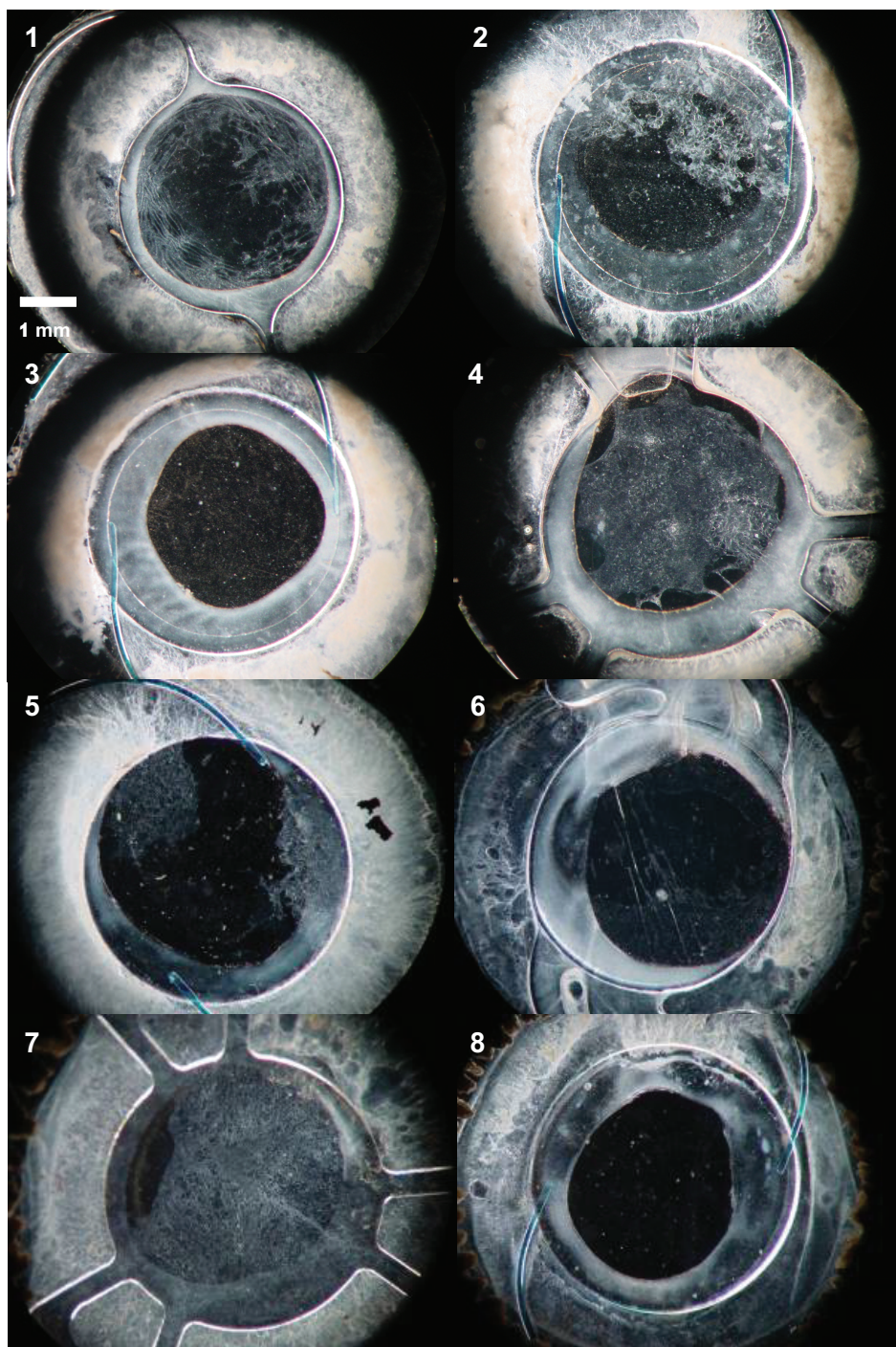


Figure 4. Photomicrographs of eight representative specimens, obtained with the darkfield microscopy set-up shown in Figure 2.

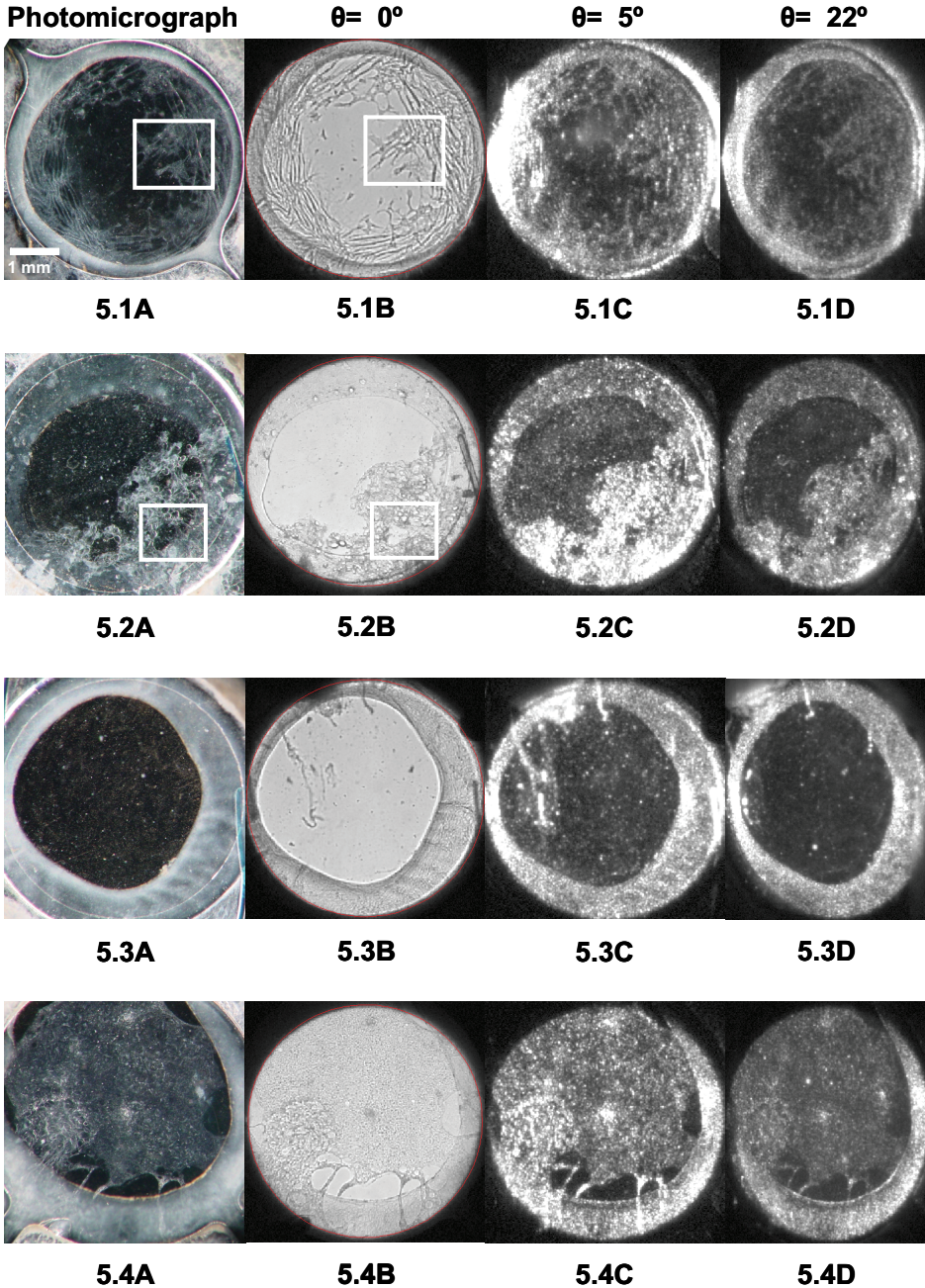


Figure 5. A comparison between photomicrographs obtained with the darkfield microscopy set-up (Figure 2) and grayscale images obtained with the goniometer set-up (Figure 3) at $\theta = 5$ deg and $\theta = 22$ deg in 4 different specimens. In each row, the photomicrograph and the "retrograde" image ($\theta = 0$ deg) complement each other.

Specimens no. 2 and 7 show mild fibrosis of the anterior capsule and specimens no. 3, 4 and 6 show severe fibrosis of the anterior capsule.

Figure 5 shows a comparison between images obtained in capsular bags no. 1-4 shown in Figure 4. The first column shows the photomicrographs obtained with darkfield microscopy, the other columns show images obtained with the goniometer. The second column shows the "retrograde" images ($\theta=0$ deg), the third column the scattered light images captured at the near large-angle domain ($\theta=5$ deg) and the fourth column shows the scattered light images captured at the far large-angle domain ($\theta=22$ deg). For proper comparison with the images from the goniometer, the photomicrographs were inverted, rotated, and size adjusted. Note that the photomicrographs show an image that is the complement of the "retrograde" image. As mentioned in the methods section, the photomicrographs were obtained using the technique of darkfield microscopy. This technique collects scattered light only, which is why light-scattering parts of the capsule show up brightly against a dark background. On the contrary, a "retrograde" image shows only directly transmitted light. Since in light-scattering areas some light is scattered and therefore lost from direct transmission, the light intensity of scattering areas is reduced and they show up as "shadow-like" areas. For example, image 5.3A shows the enhanced light intensity of the anterior capsule and image 5.3B shows its complement, a "shadow-like" area of diminished light intensity. Similarly, the Elschnig pearl edges in image 5.2A have an enhanced light intensity, as opposed to the corresponding edges in image 5.2B, which have a diminished light intensity. See also the detailed images in Figure 6.

Figures 7 and 8 show the angular dependence of PCO-scatter. They are complete image-series of scattered light obtained in specimens no. 1 and 2 shown in Figure 4. There seems to be

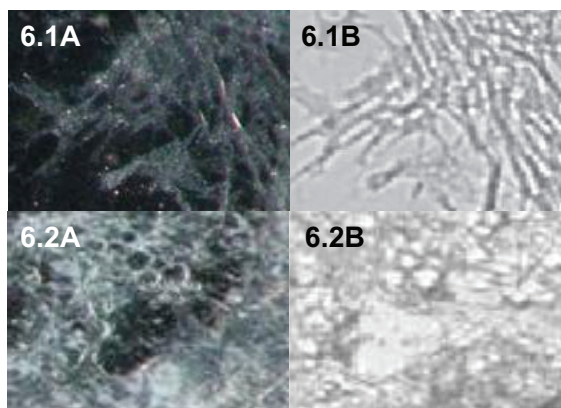


Figure 6. A comparison between detailed photomicrographs and complementary grayscale images ($\theta=0$ deg) obtained in specimen no. 1 and 2 (Figure 4).

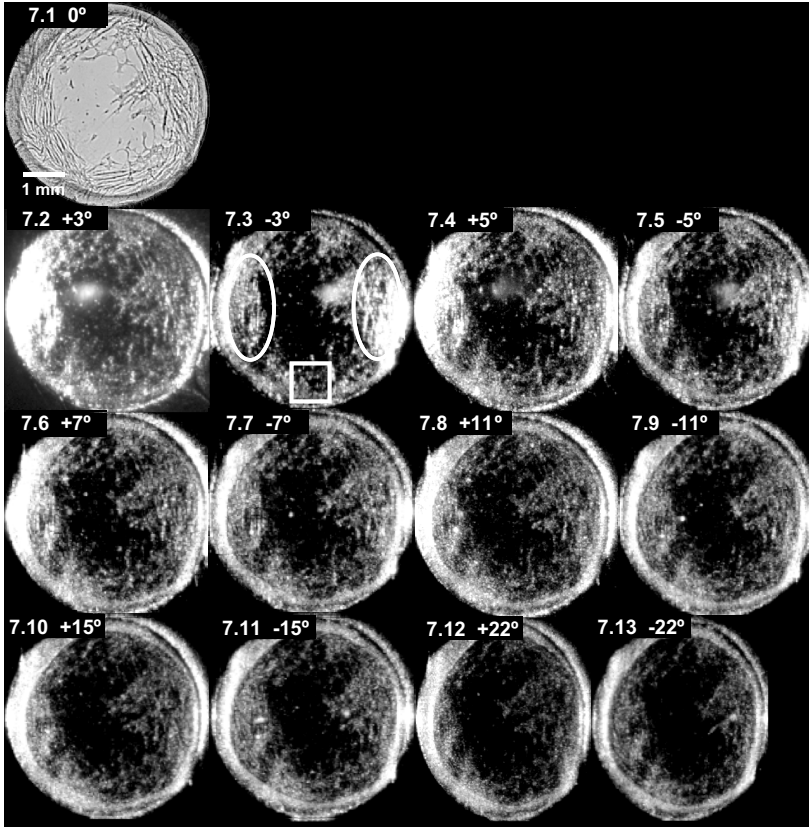


Figure 7. The angular dependence of scattered light images obtained in specimen no. 1 (Figure 4) with the goniometer set-up (Figure 3). The overall light intensity is higher in images obtained at the near large-angle domain ($1^\circ < \theta \leq 7^\circ$) than in those obtained at the far large-angle domain ($\theta > 7^\circ$). Note that images collected at the far large-angle domain (e.g. $\theta = -22$ deg, $\theta = +22$ deg) are somewhat elliptical, due to the oblique angle of observation.

little difference between positive and negative angles, so scattering seems to be symmetrical to opposite sites. As mentioned in the methods section, intensity differences between the images of the image-sets shown in Figures 7 and 8 can be used to assess the nature of the angular dependence of PCO-scatter. The intensity differences within the image-sets are small. Put differently, the straylight part of the PCO-PSF has more or less the same course as the straylight part (large-angle domain) of the normal PSF. Figure 9 shows quantitative data on the angular dependence of PCO-scatter. Figure 9A shows the average difference in shape between the PCO-PSF obtained from the complete set of representative specimens, and the normal PSF as a function of visual angle (short-dashed curve, right vertical axis). Note that if the slope of the short-dashed curve would have been zero, it would indicate an exact correspondence between angular dependence of the PCO-PSF and the normal PSF. The error bars represent standard deviations over all representative specimens. From these bars it is

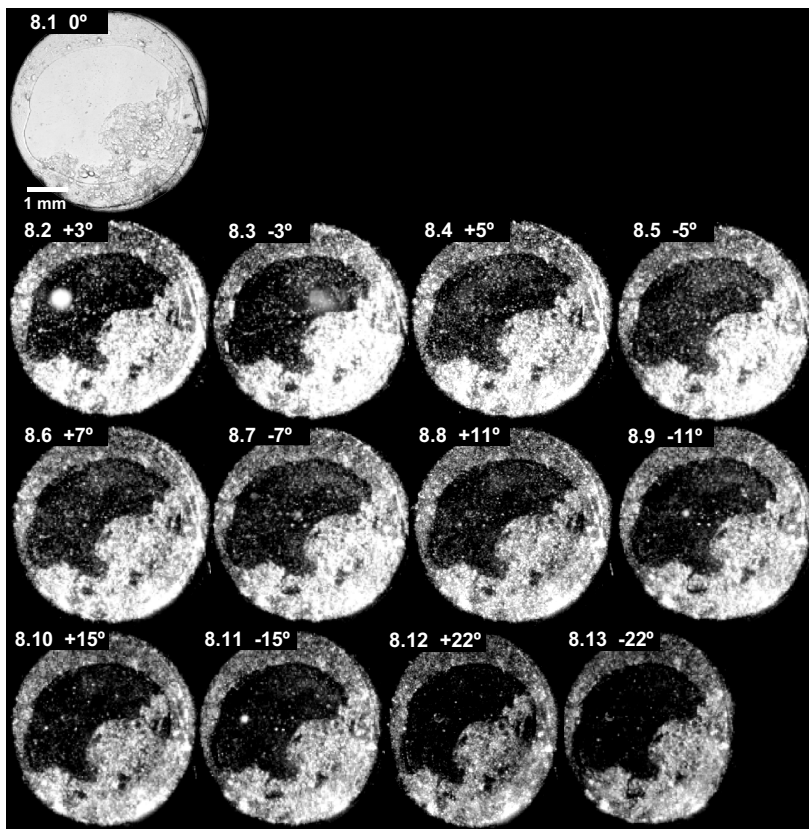


Figure 8. The angular dependence of scattered light images obtained in specimen no. 2 (Figure 4) with the goniometer set-up (Figure 3). The PCO area shows an increased overall light intensity, especially at the near large-angle domain ($1^\circ < \theta \leq 7^\circ$). Again, the images collected at the far large-angle domain are somewhat elliptical.

clear quantitatively that the difference in angular dependence among all specimens is small. Figure 9A also shows the same average result, but on an absolute PSF scale (solid line, left vertical axis). The long-dashed curve represents the normal PSF (corresponding to Figure 1) The two curves show a close correspondence.

However, close scrutiny of Figures 7 and 8 reveals slight intensity differences. The overall light intensity in the images captured at the near large-angle domain is higher than in the images captured at the far large-angle domain, e.g., the brightness differences between images 7.2 and 7.13 of the set in Figure 7. The brightness differences between images 8.2 and 8.13 of the set in Figure 8 are most pronounced. The intensity differences also show up in Figure 9. The slope of the short-dashed curve in Figure 9A is slightly steeper than that of the normal PSF. Also note the on average steeper slope of the three dashed curves corresponding to the

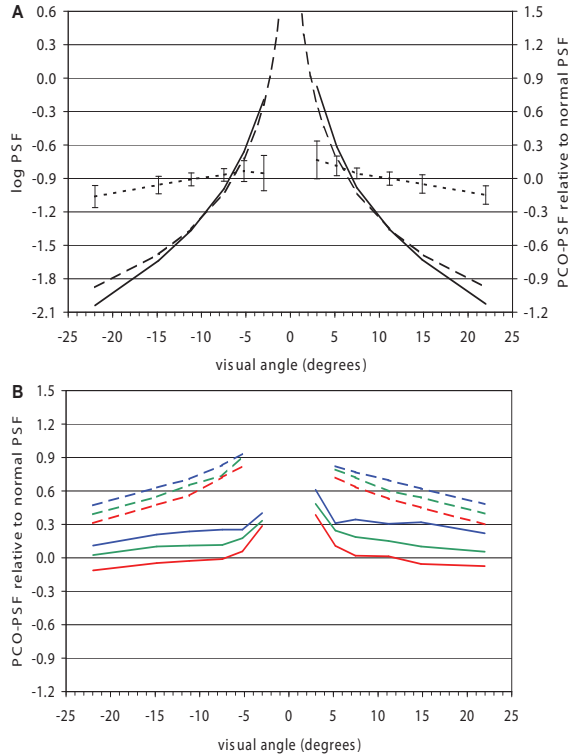


Figure 9. Quantitative data on the angular (A) and wavelength dependence (B) of PCO-scatter. Figure 9A: The short-dashed curve (right vertical axis) shows the average difference in shape between the PCO-PSF, obtained from the complete set of representative specimens, and the normal PSF as a function of visual angle. The error bars represent standard deviations over all representative specimens. The same average result is also shown on an absolute PSF-scale (solid line, left vertical axis). The long-dashed curve represents the normal PSF. Figure 9B: PCO-PSF values obtained with a blue light filter (440nm, blue curves), a green-yellow light filter (561nm, green curves) and a red light filter (661nm, red curves) as a function of visual angle. PCO-PSF values obtained in fibrosis-type PCO (specimen no. 1 in Figure 4) are given as solid curves and those obtained in pearl-type PCO (specimen no. 2 in Figure 4) are given as long-dashed curves. For clarity, the long-dashed curves are displaced 0.30 upward along the vertical axis.

pearl-type specimen in Figure 9B, as compared with the slope of the three solid curves corresponding to the fibrosis-type specimen. Another finding is that the light intensity observed in pearl-type PCO (Figure 8) is enhanced as compared to fibrosis-type PCO (Figure 7).

Figure 7 also shows that the fibrosis-type specimen has fiber structures with different orientations; a predominantly vertical orientation at the 3 and 9 o'clock positions, indicated by the ellipses, and a predominantly horizontal orientation at the 6 o'clock position, indicated by the square. Closer scrutiny reveals that the vertically oriented fiber structures have a markedly brighter appearance than those oriented horizontally. Because of their convex surface, the fiber structures are expected to have a rod-like behavior. It was realized before that structures

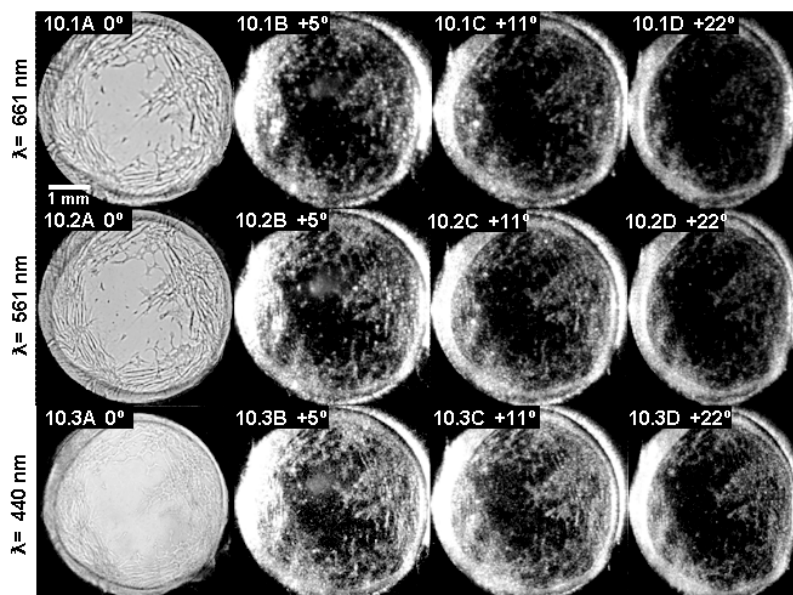


Figure 10. The wavelength dependence of scattered light images obtained in specimen no. 1 (Figure 4) with the goniometer set-up (Figure 3). The images obtained with a blue light filter (440 nm, third row) are brighter than those obtained with the green-yellow (561 nm, second row) or the red light filter (661 nm, first row).

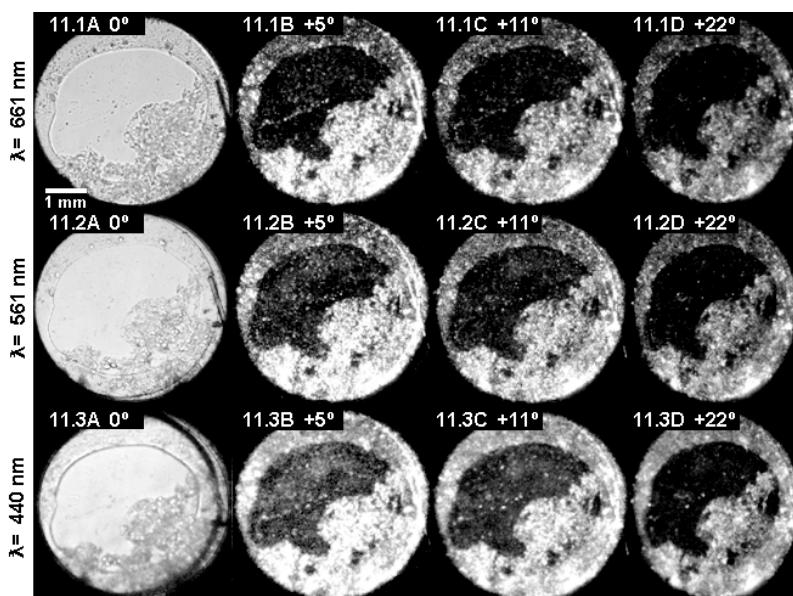


Figure 11. The wavelength dependence of scattered light images obtained in specimen no. 2 (Figure 4) with the goniometer set-up (Figure 3). The pearl area is only slightly brighter when the blue light filter (440 nm, third row) is used, as compared with the green-yellow (561 nm, second row) or the red light filter (661 nm, first row).

with a rod-like shape, such as posterior capsule folds, behave optically like rods.^{18;36} This is called the “Maddox-rod phenomenon”.^{18;37} We expect that other structures with a convex surface, such as the fiber structures in fibrosis-type PCO, will behave similarly. In these structures, incident light is focused as a line perpendicular to the axis of the fiber structure. So, vertically oriented fiber structures focus incident light as a horizontal line, which is recorded by the optical set-up of this study. Because light deflected in other planes is not recorded by this set-up, only the vertically oriented fiber structures have a brighter appearance. These brightness differences between the two orientations are most distinct at the near large-angle domain (Figure 7).

Figures 10 and 11 show the wavelength dependence of the scattered light images obtained in specimens no. 1 and 2 in Figure 4, using the three different wavelengths (661 nm, 561 nm and 440 nm). In both specimens, the scattered light images obtained with the three wavelengths appear quite similar. Closer inspection reveals some brightness differences between the images in a set recorded at identical angles but using different wavelengths, for example differences between images 10.1B, 10.2B and 10.3B of the set in Figure 10. The images at wavelengths of 561 nm and 661 nm are less bright than those at 440 nm. As described in the Methods section, all data were normalized with respect to the direct beam. This was done for each wavelength independently. So, with decreasing wavelength the *fraction* of the light that is scattered increases. This is in correspondence with the color photomicrographs in Figure 4 showing a blue hue. Close scrutiny of the image-sets of Figures 10 and 11 reveals that the wavelength dependence in pearl-type PCO is weaker than that of fibrosis-type PCO. Note the minimal brightness differences of the pearly area in images 11.1B, 11.2B and 11.3B, as compared with those of the fibrosis area in images 10.1B, 10.2B and 10.3B. Figure 9B shows quantitative data on wavelength dependence of light scattered by pearl-type PCO and fibrosis-type PCO. Note the narrowly spaced dashed curves in blue, green and red obtained in pearl-type PCO, as compared to the more widely spaced solid curves obtained in fibrosis-type PCO (Figure 9B).

The mildly opacified anterior capsule (images 11.1B, 11.2B and 11.3B) shows a slightly stronger wavelength dependence as compared with the pearl- and fibrosis-type areas.

DISCUSSION

In this study, the scattering characteristics that are important in PCO were documented. The nature of the angular dependence of light scattered by different PCO-types was assessed by comparing it to that of a normal eye. In addition, the wavelength dependence of light scattered by different PCO-types was visualized.

We found that the angular dependence of PCO-scatter is similar to that of scatter in the normal eye. In-vitro crystalline lens studies already found that the angular dependence of light scattered by the crystalline lens is similar to that of scatter in the normal eye,^{24,25} which corresponds to the finding of an early study that in the normal aging eye, the crystalline lens is the dominant straylight source.²³ We must conclude that the angular dependence of PCO-scatter and lenticular scatter is similar to that of scatter in the normal eye. This is surprising, because PCO has a different morphology by comparison with lenticular opacification. It should be noted that, despite of the similar angular dependence, in PCO the scatter intensity can be much higher than in the normal eye. The morphological heterogeneity of PCO showed up in details; it was found that the angular dependence of light scattered by pearl-type PCO is stronger than light scattered by fibrosis-type PCO. As a consequence, pearl-type and fibrosis-type PCO may have a different functional effect on visual quality, as will be described further in this section.

Close inspection of the image-series in Figures 7 and 8 did reveal an exception to the similarity in angular dependence of PCO-scatter and scatter in the normal eye: at the near large-angle domain ($1^\circ < \theta \leq 7^\circ$), the angular dependence of PCO-scatter is slightly stronger, which implies the presence of additional light-spreading pattern caused by a refractile component. The Maddox-rod phenomenon in fibrosis-type PCO, which was described in the results section, appears to cause such additional light-spreading pattern. On the basis of physics theory it can be expected that because of its morphological appearance, pearl-type (regenerative) PCO might also produce an additional light-spreading pattern. Although we did find that PCO-scatter has some wavelength dependence, especially in pearl-type PCO it is weak. This marginal wavelength dependence implies the presence of a refractile component in the light-spreading pattern caused by pearl-PCO.

The angular and wavelength dependence found in this study, suggest that PCO-scatter is dominated by small particles. This also applies to the scattering particles of opacified anterior capsules. The size of these particles is in the order of wavelength of visible light (400 nm to 700 nm). However, apart from scatter PCO has a refractile component caused by structures much larger than wavelength, such as rods and pearls. These refractile structures affect the near large-angle domain. This effect might be an extrapolation from the small-angle domain. Depending on the ratio between small particles and refractile structures in PCO, PCO may mainly affect the small-angle or the large-angle domain, which may elucidate the quite independent effect of PCO on the visual function parameters VA and straylight. The ratio in pearl-type PCO may be in favor of refractile structures, whereas in fibrosis-type PCO it may be in favor of small particles. As a consequence, pearl-type PCO may affect VA to a larger extent than straylight, whereas fibrosis-type PCO may affect straylight to a larger extent than VA.

In this study, the CCD camera served as the in-vitro counterpart of the in-vivo photoreceptors. So, the camera recorded the scattered light that the photoreceptors would sense in an in-vivo situation. Regarding this analogy, two remarks must be made. The first is that the visual scene 'perceived' by the camera differs from the visual scene that would have been perceived by a PCO-patient. The visual scene captured by the CCD camera was the specimen (Figures 7, 8, 10 and 11), whereas that perceived by a PCO-patient is a scene of the outer world (e.g., Figure 1A-B). Second, the cone photoreceptors would not detect the exact same amount of light as captured on the images, because of the Stiles-Crawford effect. The Stiles-Crawford effect refers to the directional sensitivity of photoreceptors, particularly those in the central fovea; foveal cones are less sensitive to rays of light passing through the pupil margin. The amount of light captured on the images in this study most closely corresponds to the amount of light detected by peripheral photoreceptors. So, the effect of PCO on retinal image formation detected by the photoreceptors may depend on PCO localization. Moreover, PCO located behind the peripheral margin of the pupil has little effect on both retinal image formation and light-scatter. On the contrary, centrally located PCO deteriorates retinal image formation and also increases light-scatter.

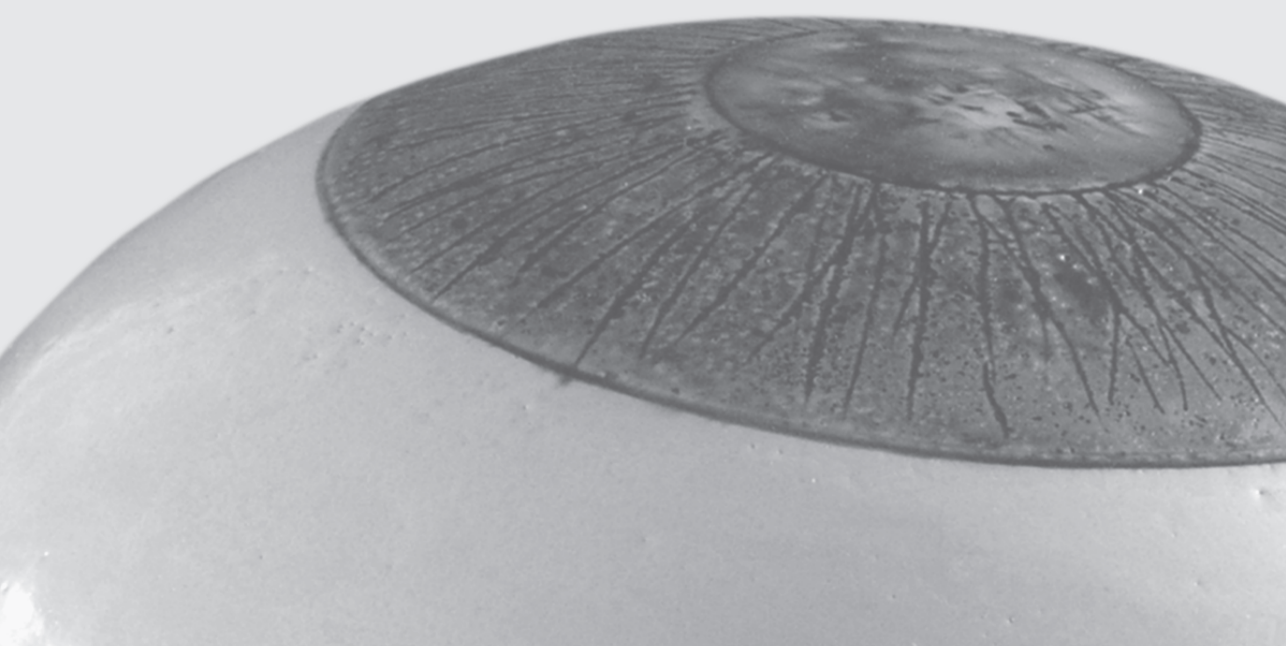
In summary, although PCO shows an increased intensity of scatter, the light-scattering characteristics of PCO are very similar to those of the normal eye. This indicates the presence of small particles in PCO. However, PCO and especially pearl-type PCO, has an additional light-spreading pattern caused by refractile components with weaker wavelength dependence, which is typical for refractile structures. We expect that the size ratio between small particles and refractile structures in PCO determines its effect on the two domains of visual function and their corresponding functional impairments. Fibrosis-type PCO may predominantly consist of small particles, which mainly affect the large-angle domain. Functionally, fibrosis may have a more important effect on straylight than on VA. In pearl-type PCO refractile structures may be relatively more important, affecting the small-angle domain. Functionally, pearls may have a more important effect on VA than on straylight.

REFERENCE LIST

1. Aslam TM, Aspinall P, Dhillon B. Posterior capsule morphology determinants of visual function. *Graefes Arch Clin Exp Ophthalmol* 2003;241:208-12.
2. Buehl W, Sacu S, Findl O. Association between intensity of posterior capsule opacification and visual acuity. *J Cataract Refract Surg* 2005;31:543-7.
3. Buehl W, Sacu S, Findl O. Association between intensity of posterior capsule opacification and contrast sensitivity. *Am J Ophthalmol* 2005;140:927-30.
4. Cheng CY, Yen MY, Chen SJ, et al. Visual acuity and contrast sensitivity in different types of posterior capsule opacification. *J Cataract Refract Surg* 2001;27:1055-60.
5. Meacock WR, Spalton DJ, Boyce J, Marshall J. The effect of posterior capsule opacification on visual function. *Invest Ophthalmol Vis Sci* 2003;44:4665-9.
6. Montenegro GA, Marvan P, Dexl A, et al. Posterior capsule opacification assessment and factors that influence visual quality after posterior capsulotomy. *Am J Ophthalmol* 2010;150:248-53.
7. Franssen L, Coppens JE, van den Berg TJ. Compensation comparison method for assessment of retinal straylight. *Invest Ophthalmol Vis Sci* 2006;47:768-76.
8. Tan JC, Spalton DJ, Arden GB. Comparison of methods to assess visual impairment from glare and light scattering with posterior capsule opacification. *J Cataract Refract Surg* 1998;24:1626-31.
9. van Bree MC, Zijlmans BL, van den Berg TJ. Effect of neodymium:YAG laser capsulotomy on retinal straylight values in patients with posterior capsule opacification. *J Cataract Refract Surg* 2008;34:1681-6.
10. van den Berg TJ, Franssen L, Coppens JE. Straylight in the human eye: testing objectivity and optical character of the psychophysical measurement. *Ophthalmic Physiol Opt* 2009;29:345-50.
11. Aslam TM, Patton N. Methods of assessment of patients for Nd:YAG laser capsulotomy that correlate with final visual improvement. *BMC Ophthalmol* 2004;4:13.
12. Buehl W, Findl O, Menapace R, et al. Reproducibility of standardized retroillumination photography for quantification of posterior capsule opacification. *J Cataract Refract Surg* 2002;28:265-70.
13. Camparini M, Macaluso C, Reggiani L, Maraini G. Retroillumination versus reflected-light images in the photographic assessment of posterior capsule opacification. *Invest Ophthalmol Vis Sci* 2000;41:3074-9.
14. Patel SV, McLaren JW, Hodge DO, Bourne WM. The effect of corneal light scatter on vision after penetrating keratoplasty. *Am J Ophthalmol* 2008;146:913-9.
15. van den Berg TJ. Light scattering by donor lenses as a function of depth and wavelength. *Invest Ophthalmol Vis Sci* 1997;38:1321-32.
16. van den Berg TJ, Spekrijse H. Light scattering model for donor lenses as a function of depth. *Vision Res* 1999;39:1437-45.

17. van den Berg TJ, Van Rijn LJ, Michael R, et al. Straylight effects with aging and lens extraction. *Am J Ophthalmol* 2007;144:358-63.
18. Apple DJ, Solomon KD, Tetz MR, et al. Posterior capsule opacification. *Surv Ophthalmol* 1992;37:73-116.
19. Neumayer T, Findl O, Buehl W, et al. Long-term changes in the morphology of posterior capsule opacification. *J Cataract Refract Surg* 2005;31:2120-8.
20. Vos JJ, van den Berg TJ. Report on disability glare. CIE collection 1999;135:1-9.
21. van den Berg TJ, Franssen L, Coppens JE. Ocular media clarity and straylight. In: DA Dartt, ed. *Encyclopedia of the Eye*. Vol. 3. Oxford: Elsevier; 2010:173-83.
22. van den Berg TJ. On the relation between glare and straylight. *Doc Ophthalmol* 1991;78:177-81.
23. Vos JJ. Disability glare - a state of the art report. *Commission Internationale de l'Eclairage Journal* 1984;3/2:39-53.
24. van den Berg TJ, IJspeert J. Light scattering in donor lenses. *Vision Res* 1995;35:169-77.
25. van den Berg TJ. Depth-dependent forward light scattering by donor lenses. *Invest Ophthalmol Vis Sci* 1996;37:1157-66.
26. Kruijt B, van den Berg TJ. Effects of tissue fixation on light scatter by PCO. *Curr Eye Res* 2012;37:159-61.
27. Apple DJ, Lim ES, Morgan RC, et al. Preparation and study of human eyes obtained postmortem with the Miyake posterior photographic technique. *Ophthalmology* 1990;97:810-6.
28. Miyake K, Miyake C. Intraoperative posterior chamber lens haptic fixation in the human cadaver eye. *Ophthalmic Surg* 1985;16:230-6.
29. van den Berg TJ. Analysis of intraocular straylight, especially in relation to age. *Optom Vis Sci* 1995;72:52-9.
30. de Wit GC, Coppens JE. Stray light of spectacle lenses compared with stray light in the eye. *Optom Vis Sci* 2003;80:395-400.
31. Wyszecki G, Stiles WS. Chapter 2: The Eye. In: *Color Science: concepts and methods, quantitative data and formulae*. New York: John Wiley & Sons, Wiley-Interscience; 1982:108-12.
32. Whitaker D, Steen R, Elliott DB. Light scatter in the normal young, elderly, and cataractous eye demonstrates little wavelength dependency. *Optom Vis Sci* 1993;70:963-8.
33. Wooten BR, Geri GA. Psychophysical determination of intraocular light scatter as a function of wavelength. *Vision Res* 1987;27:1291-8.
34. Coppens JE, Franssen L, van den Berg TJ. Wavelength dependence of intraocular straylight. *Exp Eye Res* 2006;82:688-92.
35. van den Berg TJ, IJspeert JK, de Waard PW. Dependence of intraocular straylight on pigmentation and light transmission through the ocular wall. *Vision Res* 1991;31:1361-7.

36. Holladay JT, Bishop JE, Lewis JW. Diagnosis and treatment of mysterious light streaks seen by patients following extracapsular cataract extraction. *J Am Intraocul Implant Soc* 1985;11:21-3.
37. Eggers H. The Maddox-rod phenomenon. *AMA Arch Ophthalmol* 1959;61:246-7.



Chapter 7

In vitro recording of forward light-scatter by human lens capsules and different types of posterior capsule opacification

Maartje C.J. van Bree, Ivanka J.E. van der Meulen, Luuk Franssen,
Joris E. Coppens, Bart L.M. Zijlmans, Thomas J.T.P. van den Berg

Experimental Eye Research 2012;96(1):138-46.



ABSTRACT

Purpose: The purpose of the present study was to elucidate the effect of posterior capsule opacification (PCO) on the straylight domain of visual function. PCO is heterogeneous with regard to morphology and severity; both aspects contribute to its functional effect.

Methods: The isolated impact of capsule areas with specific morphology and severity on straylight was studied in-vitro by recording forward light-scatter. Forward light-scatter by four different capsule types, *i.e.*, anterior capsule (AC), clear posterior capsule (PC), fibrotic and regenerative PCO, was recorded at several visual angles with a goniometer, using different wavelengths. Angular (θ^a) and wavelength dependencies (λ^b) were studied by determining exponents a and b .

Results: Recorded straylight values of isolated capsule areas varied between 10× below to 10× above the value normal for the human eye, depending on the capsule's condition (clear to opacified). The angular dependence of light scattered by clear PCs was weaker, whereas in the other capsule types it was stronger than in the normal eye. On average, the wavelength dependence of light scattered by different capsule types was similar, but the variation was considerable. At the smallest visual angles, increased angular and decreased wavelength dependence was found, especially in fibrotic and regenerative PCO.

Conclusions: It was concluded that the range of straylight values found in-vitro in lens capsules properly corresponded to that found previously in in-vivo pseudophakics. Surprisingly, the wavelength dependence of PCO indicated that small-particle light-scattering is important in PCO. Refractile effects were more important at small visual angles, as indicated by the combined stronger angular and weaker wavelength dependence.

INTRODUCTION

Transparency of optical media, such as the crystalline lens and its surrounding lens capsule, is important for optimal visual function (VF). Cataract formation reduces the transparency of the crystalline lens. Cataract formation is largely age-related, and therefore affects visual function of a substantial part of the world population. Although a cataractous lens can be replaced by a transparent, artificial intra-ocular lens (IOL), the outcome of cataract surgery is frequently complicated by opacification of the lens capsule. Posterior capsule opacification (PCO) causes VF impairment similar to that caused by cataract. Therefore, PCO is a major hindrance to long-term VF restoration. The present study contributes to a better understanding of the impact of PCO on visual function.

PCO results from a wound-healing response caused by mechanical trauma during cataract surgery. Unfortunately, it is impossible to extract all lens cells. Wound-healing promotes residual lens epithelial cells (LECs) to proliferate, (trans)differentiate, and to deposit extracellular matrix, via autocrine and paracrine cell signaling.^{1,2} Migration of the cells into the space between IOL and posterior lens capsule causes opacification, and is called PCO. Clinically, two morphologically different PCO-types can be distinguished: PCO with a pearl appearance and PCO with a fibrotic appearance. Pearl-type PCO, or regenerative PCO, is thought to be caused by proliferation and swelling of LECs.³ Fibrosis-type PCO is thought to be caused by LEC transdifferentiation.^{1,2}

As mentioned in the first paragraph of this section, PCO causes VF impairment: it deteriorates VF by reducing visual acuity and increasing intra-ocular straylight.^{4,5} The impact of PCO on visual acuity does not necessarily correspond to its impact on straylight.^{4,5} The distinct impact of PCO on visual acuity and straylight is expected to be related to the degree and localization of posterior capsule (PC) coverage by PCO. Moreover, which parameter of visual function is predominantly affected depends on the optical characteristics of PCO. Optical characteristics can be assumed to depend primarily on the characteristic size of PCO-irregularities: irregularities much larger than the wavelength of light refract light, and smaller sized particles scatter light. Refractile irregularities may predominantly affect the small-angle domain of visual function and reduce visual acuity, whereas scattering particles may predominantly affect the large-angle domain of visual function (visual angles beyond 1.0°) and increase straylight.^{5,6}

In the present study, forward light-scatter by PCO was recorded in-vitro with a goniometer set-up. The set-up records scatter intensities at the large-angle domain of visual function. The in-vitro setting allows studying light-scattering by a specific ocular structure, separately from light-scattering by other ocular structures. The concept for in-vitro forward light-scatter recordings with a goniometer set-up has been developed by Van den Berg et al. to study

forward light-scatter by human crystalline lenses.^{7,8} Recently, the goniometer set-up was used to study light-scatter by PCO as it would appear functionally, i.e. light-scatter was recorded for a 4 mm circular central zone of the IOL-posterior capsule complex.⁵ PCO is heterogeneous and therefore most 4 mm central zones included clear PC areas and opacified PC areas of different type and severity. Central zone scatter characteristics result from composite scatter characteristics of all heterogeneous areas. As will be detailed in the Results section, scatter intensities can be translated into straylight values: the quantity defining the in-vivo visual function result. Straylight is expressed as the logarithm of the straylight parameter "s", or $\log(s)$. For example, if the central zone is filled for 10% with PCO of $\log(s) = 2.0$, and for 90% with PCO of $\log(s) = 1.0$, the straylight value experienced by the patient is $\log(0.1 * 10^2 + 0.9 * 10^1) = 1.28$.

For a better understanding of the light-scattering characteristics of heterogeneous PCO areas, in which the contributions of different PCO types and severities are mixed, the light-scattering characteristics of isolated areas with a specific PCO type and severity need to be investigated. In the present study, the goniometer set-up was used to study light-scatter by isolated, homogeneous capsule areas. The studied capsule areas were either clear or opacified, and opacified capsule areas had different severity and morphology.

METHODS

The techniques for specimen preparation and scattered light registration used in this study are largely identical to those previously described in detail.⁵ Therefore, the two following subsections only provide a summary.

Specimen preparation and selection

Pseudophakic donor bulbi were obtained from the Cornea Bank Amsterdam. Specimens were capsular bags (lens capsules) with an IOL. Initially, capsular bags were unfixated. After it had been concluded that a 1% paraformaldehyde fixative had no effect on the optical properties of capsular bags, bulbi were immersed in fixative (>24 hours) prior to preparation.⁹ Specimens were isolated using either of the two preparation techniques previously described.⁵ Isolated specimens were examined and selected by experienced ophthalmologists (I.J.E.M. and B.L.M.Z.), using a darkfield set-up with a darkfield ring light for retro illumination and slit illumination for reflected light examination. The purpose of darkfield examination was two-fold: (1) to ascertain close correspondence to in-vivo capsular bags, and (2) to identify small-sized IOL irregularities such as IOL glistenings or deposits. However, in none of the used specimens, IOL irregularities were observed.⁵ Whereas small-sized IOL irregularities and potential IOL-scatter might affect the large-angle domain, refractive IOL design only affects

the small-angle domain. Therefore there were no inclusion criteria concerning IOL type or dioptric power.

Goniometer registration of scattered light

Light scattered by the specimens was recorded with a goniometer and a charge-coupled device camera. The specimen's posterior part was oriented towards the camera. Light emitted by a halogen light source passed an infrared blocking filter and a narrowband interference filter with a peak wavelength of either 661 nm, 561 nm or 440 nm. The incident light passed the specimen in the same direction as in an in-vivo situation. The specimen scattered part of the incident light in different forward directions towards the camera, which served as the in-vitro counterpart of the in-vivo photoreceptors.⁵ The camera rotated in the horizontal plane around the specimen, and collected forward light-scatter at fixed angles corresponding to visual angles of $\theta = -22, -15, -11, -7, -5, -3, +3, +5, +7, +11, +15$ and $+22$ degrees (deg). It should be noted that the visual angles apply to the specimen's center. So, if the studied capsule area had a left-right decentration from the specimen's center, the actual visual angles were slightly different from those specified above, and were not corrected. All visual angles were >1 deg, and therefore represent the large-angle domain of the point-spread function (PSF).⁶

For each specimen 13 goniometer registrations per wavelength were obtained: 12 grayscale images corresponding to the 12 visual angles, and one grayscale image collected at the $\theta = 0$ deg position. Images collected at the $\theta = 0$ deg position can be compared with clinical retrograde slit-lamp images, although the light direction is reversed. At the $\theta = 0$ deg position, non-scattered, directly transmitted light is recorded. In the presence of opacified areas some of the incident light will be scattered. Consequently, the amount of recorded transmitted light is reduced and opacified areas appear as less intense, shadowy patterns (Figure 1A).

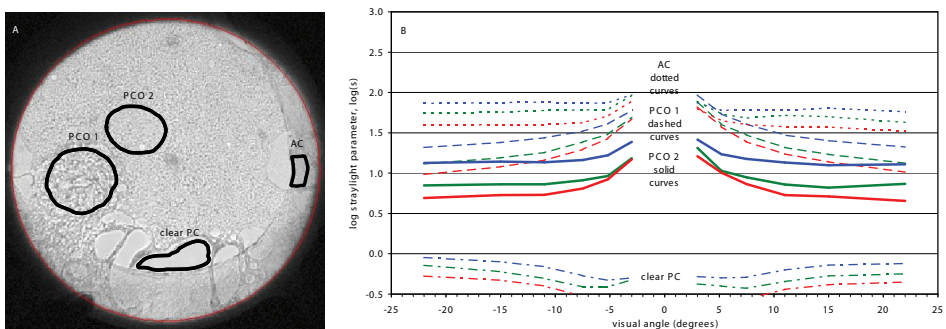


Figure 1. Image of a representative regenerative PCO specimen captured at the $\theta = 0$ degrees position, using the goniometer set-up. Selected lens capsule areas are indicated: an anterior capsule (AC) area, two posterior capsule opacification (PCO) areas of different severity, and a clear posterior capsule (PC) area (A). Their scatter characteristics were recorded using a blue light filter (440 nm, blue curves), a green-yellow light filter (561 nm, green curves) and a red light filter (660 nm, red curves) (B).

Straylight parameter

The goniometer set-up was calibrated according to the PSF-definition of the Commission Internationale de l'Éclairage (CIE) (see <http://www.cie.co.at/>). The CIE norm of the PSF of a healthy, young eye was used as a reference.¹⁰ Scatter intensities are expressed as absolute PSF-values in terms of the straylight parameter “ s ”, according to $s = \theta^2 \times \text{PSF}(\theta)$.⁷ The logarithm of s , or $\log(s)$, was used. By using $\log(s)$ as a unit, the in-vitro values recorded in the present study can directly be compared to in-vivo values measured using the C-Quant instrument (Oculus GmbH, Wetzlar, Germany). Theoretical details concerning the comparison of in-vivo and in-vitro $\log(s)$ values are given elsewhere.⁸

Selection of isolated capsule areas

To represent the heterogeneous nature of human capsular bags, isolated capsule areas with different morphology and severity were selected. Selected capsule areas were divided into 4 categories; (A) anterior capsule (AC) areas, (B) relatively clear PC areas, (C) areas of fibrotic PCO, and (D) areas of regenerative PCO. Because AC and PC areas overlap, light scattered by AC areas could not be isolated from light scattered by PC areas. Therefore, only AC areas overlapping relatively clear PC areas were eligible. Both clear and fibrotic AC areas were selected. Using Matlab software (MathWorks, Inc., Natick, Massachusetts; version 7.11.0.584), selected capsule areas were specified as regions of interest. Examples of selected capsule areas are shown in Figure 1A. As explained earlier in the Methods section, for each region of interest $\log(s)$ values were recorded at all visual angles and wavelengths (Figure 1B).

Optical characteristics

The nature of the angular and wavelength dependence can be used to assess the particle-size dominating light-scattering in different parts of the lens capsule. Particles much smaller than the wavelength of light typically show a weak angular and a strong wavelength dependence, whereas particles larger than the wavelength of light typically show a strong angular and a weak wavelength dependence.

The angular dependence of intraocular straylight can be described as θ^a , with approximate exponent $a \approx -2$ (Figure 2, dashed curves).^{7;8;11-14} It was found that $a \approx -2$ in young, healthy eyes and in aging, cataractous eyes.^{8;11-14} In this study, the angular dependence of light scattered by the different lens capsule types was assessed by determining exponent a .

The wavelength dependence of scattered light can be described as λ^b . Light scattered by very small particles is called Rayleigh scatter, and has a strong wavelength dependence with exponent $b = -4$. Light scattered by particles much larger than the wavelength of light typically has no wavelength dependence, with exponent $b = 0$. The wavelength dependence of

light scattered by particles of intermediate size can be described as λ^b , with $-4 < \text{exponent } b < 0$. In the present study, the wavelength dependence of light scattered by different lens capsule types was assessed by determining exponent b .

Detailed knowledge of optical characteristics such as angular and wavelength dependence, can be obtained by calculating exponents a and b . The exponents are important if one aims to derive effective particle size with physical-optical theory.^{15,16} However, in the present study, exponents a and b were used to elucidate the impact of different capsule types on the straylight part of visual function.

RESULTS

As previously described, 25 representative PCO specimens were identified by experienced ophthalmologists.⁵ Eleven AC areas, 10 clear PC areas, 7 areas of fibrotic PCO and 13 areas of regenerative PCO were selected in the present study. Examples of isolated capsule areas are shown in Figure 1. The remainder of this Results section describes findings for the four different capsule types, concerning (1) scatter intensity (first subsection and Figure 2), (2) angular dependence (second subsection and Figures 3-4), and (3) wavelength dependence (third subsection and Figures 5-6).

Intensity of light-scatter by different capsule types

The variation in scatter intensity found in different capsule types is illustrated by Figure 2. It shows the 561 nm scatter characteristics of all selected (A) AC areas, (B) clear PC areas, (C) areas of fibrotic PCO, and (D) areas of regenerative PCO. The $\log(s)$ parameter is shown as a function of visual angle. The thin, solid curves represent individual isolated capsule areas, and the thick, solid curves are average curves for each of the four different capsule types. The thick dashed curve represents the PSF for a healthy and young eye (expressed in terms of the straylight parameter), and can be used as a reference. As mentioned in the Methods section, there is a close correspondence of in-vivo and in-vitro $\log(s)$ values, both theoretically and practically.⁶ The clinical C-Quant instrument measures straylight at approximately 7 deg. Therefore, we will focus on averaged $\log(s)$ values obtained at $\theta = -7$ and $+7$ deg: those values can be directly compared to in-vivo straylight values obtained in the clinic. The scatter intensity found in AC at $\theta = -7$ and $+7$ deg ranges from $\log(s) = 0.0$ to $\log(s) = 2.1$, with an average of $\log(s) = 1.2$ (Figure 2A). The scatter intensity found in clear PC areas is relatively low and ranges from $\log(s) = 0.1$ to $\log(s) = 1.1$, with an average of $\log(s) = 0.6$ (Figure 2B). The scatter intensity in fibrotic PCO areas ranges from $\log(s) = 0.7$ to $\log(s) = 1.4$, with average $\log(s) = 1.2$ (Figure 2C). The scatter intensity in the regenerative PCO areas ranges from $\log(s) \approx 0.6$ to $\log(s) \approx 2.0$, with an average $\log(s) = 1.2$ (Figure 2D).

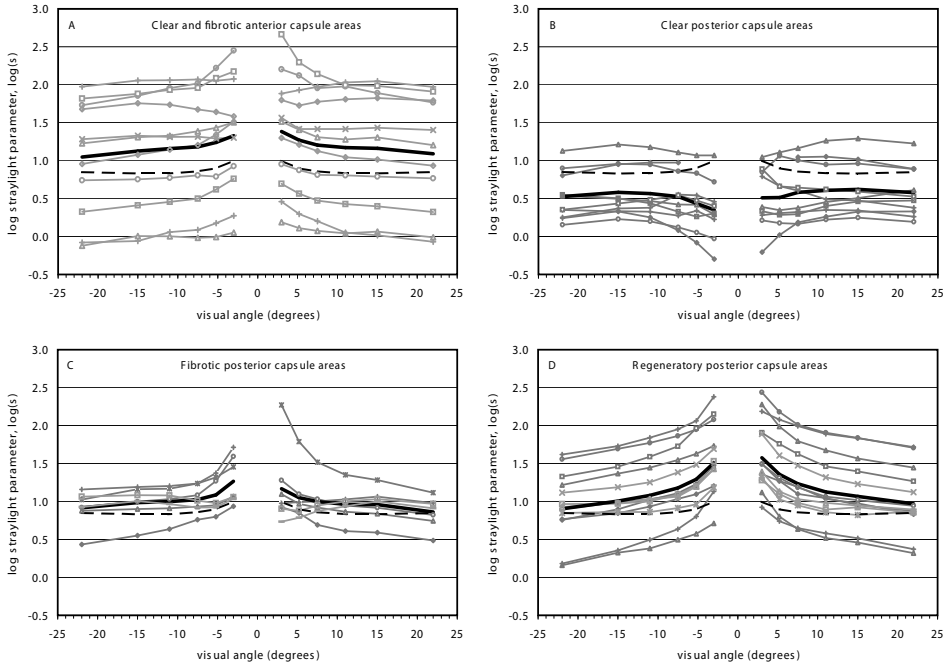


Figure 2. Scatter characteristics of clear and fibrotic anterior capsule areas ($n= 11$) (A), clear posterior capsule areas ($n= 10$) (B), fibrotic PCO areas ($n= 7$) (C) and regeneratory PCO areas ($n= 13$) (D), recorded using a green-yellow light filter (561 nm). Recorded scatter intensities, expressed as $\log(s)$, are shown as a function of visual angle (thin, solid curves). The thick, solid curves represent the average curves for each of the different capsule types. The thick, dashed curves represent a healthy, young eye and can be used as a reference.

Figure 2 shows that in most areas, similar scatter intensities were recorded at positive and negative visual angles. However, in some capsule areas slightly asymmetrical scatter intensities were recorded. These were observed if the selected capsule area was left-right decentrated in relation to the specimen's center. As described in the Methods section, such decentration causes a small error in actual visual angle, resulting in slightly asymmetrical scatter intensities. Finally, in fibrotic PCO areas of similar severity, different scatter intensities were recorded; the scatter intensity is much stronger in some areas as compared to other areas (Figure 2C). As will be detailed in the following subsection, differences in angular dependence were also found in these areas.

Angular dependence of light-scatter by different capsule types

The shapes of curves obtained from distinct capsule areas were compared; most curves of PCO areas (Figures 2C and D) are steeper than those of AC (Figure 2A) and clear PC areas (Figure 2B). In other words, the angular dependence of light scattered by PCO areas is on average stronger than that scattered by AC and clear PC areas. The shape of the average curves was also compared with that of the reference curve. The shape of the AC and

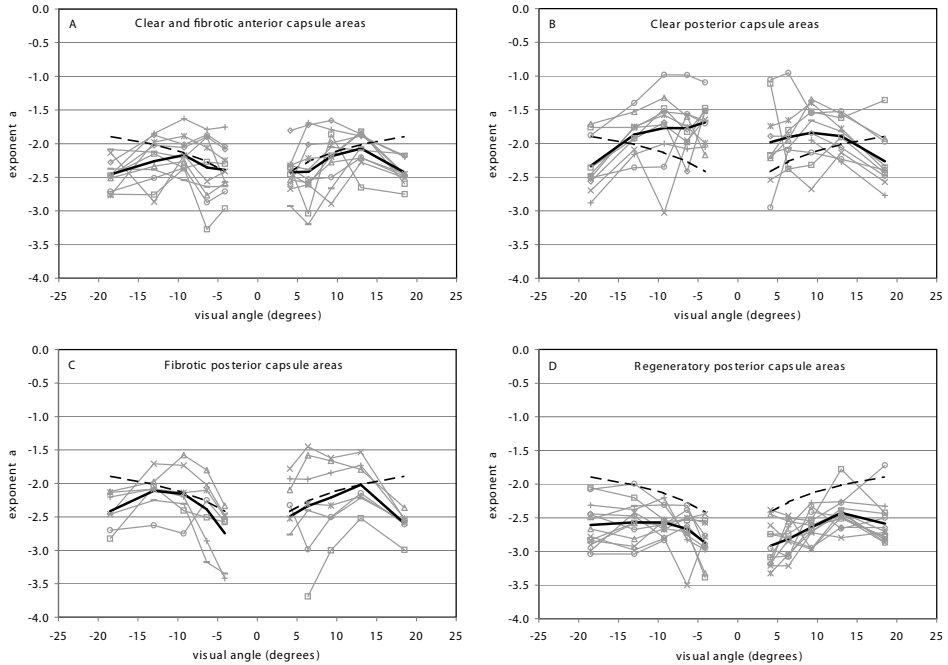


Figure 3. The angular dependence of scattered light is described by θ^a . The thin, solid curves show exponent a as a function of visual angle for each anterior capsule area ($n=11$) (A), each clear posterior capsule area ($n=10$) (B), each fibrotic PCO area ($n=7$) (C) and each regenerative PCO area ($n=13$) (D) ($\lambda=561$ nm). The thick, solid curves represent the average exponent a for the four different capsule types. The thick, dashed curves represent the strength of the angular dependence in a healthy, young eye.

fibrotic PCO curves was similar to that of the reference curve. In other words, the angular dependence of light scattered by AC and fibrotic PCO areas is similar to the average angular dependence of approximately $\theta^{2.2}$ found in healthy, young eyes (Figures 2A and C).^{7,8} The angular dependence of clear PC areas is weaker than in a healthy, young eye (Figure 2B), whereas in regenerative PCO it is stronger than in a healthy, young eye (Figure 2D).

By calculating the slope, or exponent a , of the $\log(s)$ curves shown in Figure 2, shape differences between $\log(s)$ curves and shape differences between the $\log(s)$ curves and the reference curve for a healthy, young eye can be assessed in detail. The slope (exponent a) of each line segment connecting successive visual angles (Figure 2; thin, solid curves) was calculated and plotted as a function of visual angle for all (A) AC areas, (B) clear PC areas, (C) fibrotic PCO areas and (D) regenerative PCO areas (Figure 3; thin, solid curves). The average exponent a for each of the four different capsule types is shown by thick, solid curves. The reference exponent for a healthy, young eye is shown by thick, dashed curves, and can be used as a reference. Remember from the 'Optical characteristics' subsection of the Methods, that the reference exponent is approximately -2 . Its precise value depends on visual angle: it

varies over the angular range from -1.9 to -2.4 , and approaches -2.2 at 7 deg. Figures 3A and C show that the average exponent a of the AC and fibrotic PCO areas is slightly stronger than the reference exponent, especially at the largest angles of the angular range; it is on average -2.3 for both the AC and the fibrotic PCO areas. Figure 3B shows that the average exponent a of clear PCO areas is slightly weaker than the reference exponent at visual angles $-22 > \theta > -15$ deg and $22 < \theta < 15$ deg, whereas it is stronger at the other visual angles; the average exponent a is -1.9 . Figure 3D shows that the average exponent $a = -2.7$ for the regenerative PCO areas is stronger than the reference exponent at all visual angles, especially at the largest angles of the angular range.

As mentioned in the "intensity of light-scatter" subsection, light scattered by fibrotic PCO areas could vary in intensity. In addition, the angular dependence of light scattered by these areas could vary. This is illustrated by the fibrotic specimen in Figure 4A. In Figure 4A, PCO areas are represented by shadowy patterns. The intensity of the shadowy patterns of PCO

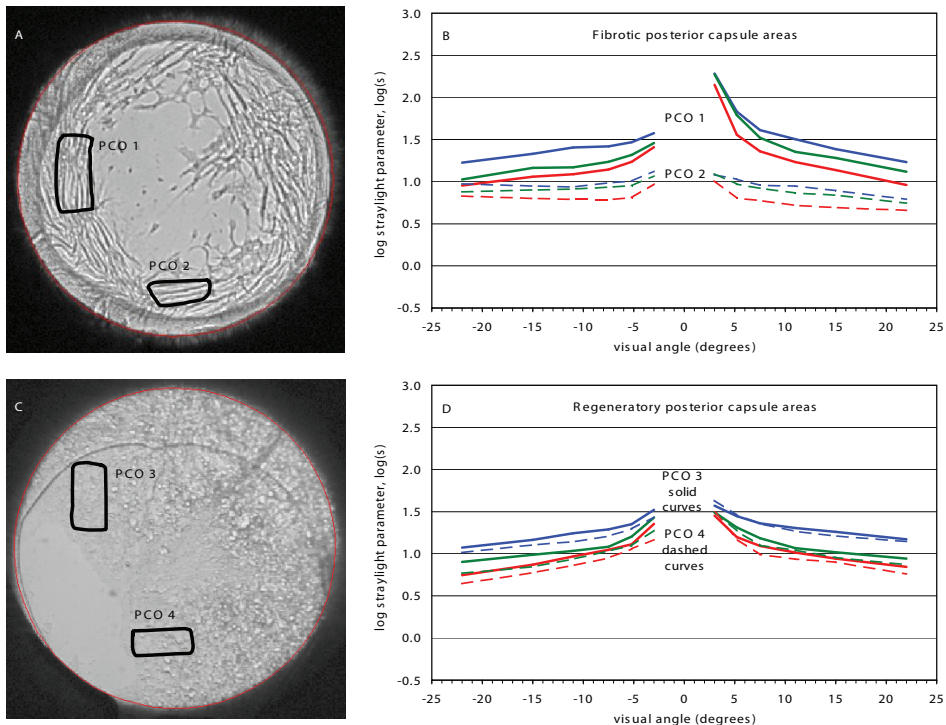


Figure 4. Images of specimens with fibrotic PCO (A) and regenerative PCO (C), captured at the $\theta = 0$ degrees position using the goniometer set-up. Figure 4A shows two selected fibrotic PCO areas with horizontally (PCO 2) and vertically (PCO 1) oriented fiber structures. Figure 4B shows the increased scatter intensity and angular dependence in PCO area 1 as compared to those in PCO area 2. Figure 4C shows two selected regenerative PCO areas without a distinct fiber structure. Their similar scatter intensity and angular dependence are shown in Figure 4D.

areas 1 and 2 is similar (Figure 4A), which suggests similar PCO severity. However, their scatter intensities and angular dependence is different: the curves of PCO area 2 are rather flat, whereas those of PCO area 1 have steeper slopes (Figure 4B). PCO areas 1 and 2 have fiber structures of different orientations. As described in a previous study,⁵ fiber structures with a convex surface, such as those shown in Figure 4A, are expected to behave optically as rod structures. The optical behaviour of structures with a rod-like shape is called the "Maddox-rod phenomenon" and refers to the phenomenon that in rod structures incident light is deflected as a line perpendicular to the rod's axis.^{3,17} So, horizontally oriented fibers deflect incident light as a vertical line, and vertically oriented fibers deflect it as a horizontal line. The optical set-up used in this study records light spreading in the horizontal plane. So, in the presence of vertically oriented fibers strong light spreading is recorded, whereas in the presence of horizontally oriented fibers weaker light spreading is recorded. In PCO area 2 the fiber structures are oriented horizontally, whereas in area 1 they are oriented vertically (Figure 4A); this translates to weaker scatter intensities recorded in area 2 than in area 1 (Figure 4B). Furthermore, the angular dependence of light spreading by area 2 is weaker than that by area 1 (Figure 4B). For comparison, two regenerative PCO areas of similar severity, PCO areas 3 and 4, are shown in Figure 4C. None of the areas has a fiber structure, and a similar scatter intensity and angular dependence is found in both areas (Figure 4D). The curves of PCO areas 1-4 have two characteristics in common at the smallest angles in the angular range, (1) an increasing slope, indicating increasing angular dependence, and (2) a narrowing in the spacing of the blue, green and red curves, indicating decreasing wavelength dependence (Figures 4B and D).

Wavelength dependence of light-scatter by different capsule types

Figures 5 and 6 focus on wavelength dependencies. The solid blue, green and red curves in Figure 5 show average scatter characteristics of all selected (A) AC areas, (B) clear PC areas, (C) areas of fibrotic PCO, and (D) areas of regenerative PCO, recorded with 440 nm, 561 nm and 661 nm. Again, the black, dashed curves represent a healthy, young eye, to be used as a reference. Figure 5 shows that for each capsule type, the corresponding blue, green and red curves have a similar shape. To put it differently, for the three wavelengths the angular dependence is similar. Furthermore, Figure 5 shows that for all capsule types, the lowest log(s) values were recorded at 661 nm and the highest at 440 nm, i.e. scatter intensity increases with decreasing wavelength. The strength of the wavelength dependence is indicated by the spacing of the blue, green and red curves. In case scattered light has no wavelength dependence, the blue, green and red curves would show no spacing, whereas in case of strong wavelength dependence the curves would be widely spaced. Figure 5 shows a similar spacing of the solid blue, green and red curves for the different capsule types. However, especially in the fibrotic PCO and regenerative PCO areas, the spacing between the blue, green and red curves decreases at the smallest angles of the angular range.

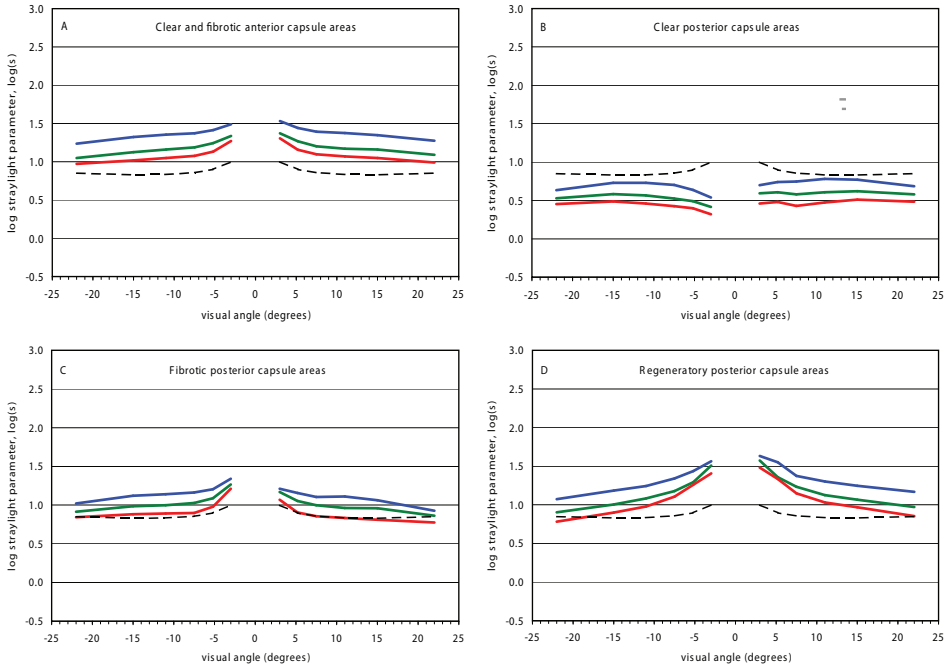


Figure 5. Average scatter characteristics of anterior capsule areas ($n= 11$) (A), clear posterior capsule areas ($n= 10$) (B), fibrotic PCO areas ($n= 7$) (C) and regenerative PCO areas ($n= 13$) (D), obtained with a blue light filter (440 nm, blue curves), a green-yellow light filter (561 nm, green curves) and a red light filter (660 nm, red curves). The dashed, black curves are reference curves for a healthy, young eye.

Differences in wavelength dependence can be assessed in detail by determining exponent b . As mentioned in the previous paragraph, at a particular visual angle different scatter intensities were recorded at 661, 561 and 440 nm, with the lowest $\log(s)$ values at 661 nm and the highest $\log(s)$ values at 440 nm (Figure 5). For each angle, exponent b was derived from the scatter intensities recorded at 661, 561 and 440 nm. In Figure 6, exponent b is plotted as a function of visual angle for all (A) AC areas, (B) clear PC areas, (C) fibrotic PCO areas and (D) regenerative PCO areas (thin, solid curves). The average exponent b (see the ‘Optical characteristics’ subsection of the Methods) for each of the four different capsule types is shown by thick, solid curves. The average exponent b is around -1.5 , but there is quite some variation, possibly caused by the fact that derivatives (slopes) are sensitive to noise in the recordings. The narrowing in the spacing between the blue, green and red curves at the smallest angles of the angular range in AC, fibrotic PCO and regenerative PCO areas that was mentioned in the “angular dependence” subsection, indicates a decrease in wavelength dependence, which is confirmed by Figures 5A, C and D. On average, the value of exponent b is less negative at the smallest angles as compared with its value at larger angles, which illustrates the decreasing wavelength dependence more clearly (Figures 6A, C and D).

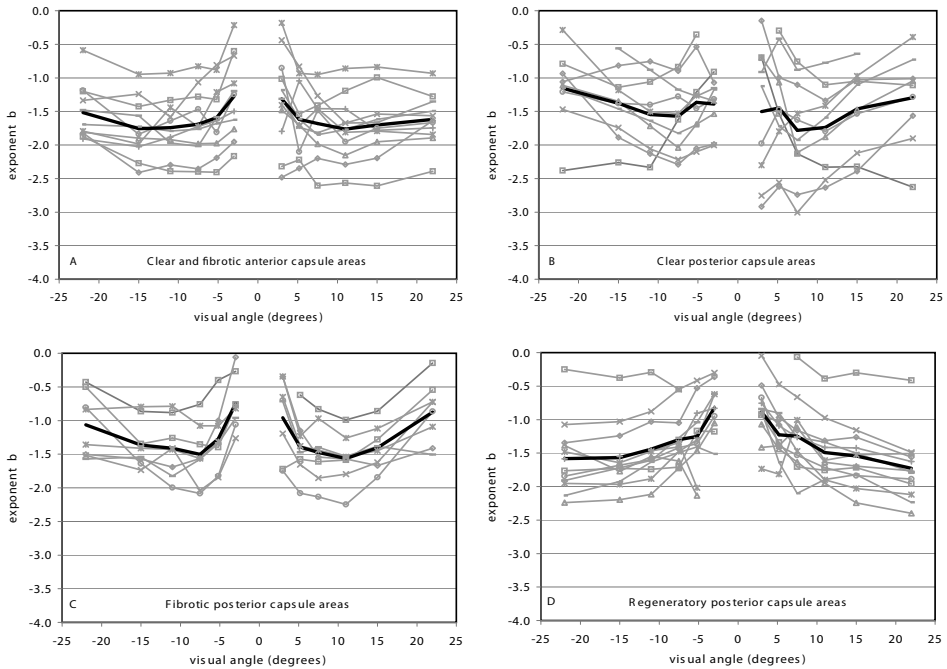


Figure 6. The wavelength dependence of scattered light is described by λ^b . The thin, solid curves show exponent b as a function of visual angle for each anterior capsule area ($n= 11$) (A), each clear posterior capsule area ($n= 10$) (B), each fibrotic PCO area ($n= 7$) (C) and each regenerative PCO area ($n= 13$) (D) ($\lambda= 561$ nm). The thick, solid curves represent the average exponent b for the four different capsule types.

DISCUSSION

In the present study we determined light-scattering by isolated capsule areas. Light-scattering is expressed in terms of PSF. Because the straylight parameter ($\log[s]$) was used as an unit, the present in-vitro findings and in-vivo findings previously obtained with the C-Quant instrument can be compared in absolute sense. This will be elaborated in the following subsection.

In-vivo population studies in healthy, young eyes found a reference value of $\log(s)= 0.9$.¹⁸⁻²¹ An in-vivo population study in pseudophakics with clear and opacified posterior capsules, found $\log(s)$ values ranging from $\log(s)= 0.6$ to 2.0 with an average of 1.3 .²⁰ In pseudophakics with PCO and an indication for neodymium:YAG laser capsulotomy, $\log(s)$ values ranging from $\log(s)= 1.1$ to 2.4 , with an average of 1.6 were found.⁴ The in-vivo upper limits in pseudophakics of $\log(s)= 2.0$ and 2.4 , approximately correspond to the highest value of $\log(s)= 2.0$ found in a PCO area in the present in-vitro study. The $\log(s)$ value of 2.0 found in an isolated area of severe PCO, corresponds to a 12.6 -fold increase (corresponding to 1.1 log units) in straylight, as compared to the reference value of 0.9 in healthy, young eyes.

In-vitro, a lower limit of $\log(s)= 0.1$ was found in clear capsules, which does not correspond to the in-vivo lower limit of $\log(s)= 0.6$ found in a population of pseudophakics including clear capsules.²⁰ The underlying reason is that in-vitro $\log(s)$ values represent only the amount of straylight caused by the lens capsule-IOL complex, whereas in-vivo $\log(s)$ values represent the amount of straylight in the pseudophakic eye as a whole, including the contribution of other ocular structures to intraocular straylight, e.g., light-scatter by the cornea and vitreous, pigmentation-dependent light transmission by the iris and sclera, and pigmentation-dependent light reflection by the fundus.^{12,13,22} It has been estimated that 2/3 of the total amount of straylight in a healthy and young eye, i.e. corresponding to $\log(s)= 0.7$, is caused by all these ocular structures together, the crystalline lens excepted.¹⁴

As described in the Introduction, the straylight value experienced by the patient results from the combined contribution of clear and opacified capsule areas of different severity. In the previous in-vitro study, $\log(s)$ values were recorded over a 4 mm circular central zone. The 4 mm $\log(s)$ values found in the previous in-vitro study ranged from $\log(s)= 0.1$ to 1.6 with an average of 1.0.⁵ Comparing the already mentioned in-vivo upper limits of $\log(s)= 2.0$ and 2.4 in pseudophakics^{4,20} to the upper limit of $\log(s)= 1.6$ found in the previous in-vitro study,⁵ it appears that the latter is much lower. However, one should realize that the value of 2.4 concerned pseudophakic patients with PCO and an indication for neodymium:YAG capsulotomy, whereas the in-vitro study concerned random pseudophakic eyes.

It should be noted that in the present study a wide range of scatter intensities was observed in areas that were marked as clear PC. As described in the Methods section, capsules were examined by experienced ophthalmologists, using a darkfield microscopy set-up that included slit-lamp examination with reflected light and retro illumination.²³ Despite the careful examination, some PC areas that were marked as clear might have had minimal, sub-clinical opacification. As described in the Methods section, it can also not be ruled out that in some truly clear PC areas, diffuse scatter processes induced by IOLs might have caused a small amount of scatter. Because of these two issues, (1) possible sub-clinical opacification and (2) potential scatter by IOLs, the precise level of scatter-intensities obtained in areas marked as clear PC may not faithfully represent the clear capsule.

The four different capsule types selected in the present study showed distinct scatter characteristics, especially concerning angular dependence. The distinct angular dependence of the capsule types was characterised by $\log(s)$ curves with a distinct shape (Figure 2), and therefore a different exponent a (different slope) (Figure 3). The angular dependence of clear PC areas was weaker than in a healthy, normal eye, whereas in AC, fibrotic PCO and regenerative PCO areas it was stronger than in a healthy, young eye (Figure 3). Apart from different capsule types, areas of different severity were included. The results indicate that

severity differences are characterised by differences in scatter intensity, resulting in vertical displacement of $\log(s)$ curves (Figure 2). In summary, differences in angular dependence result in $\log(s)$ curves with a distinct shape, and differences in scatter intensity result in vertical displacement of the curves (Figure 2).

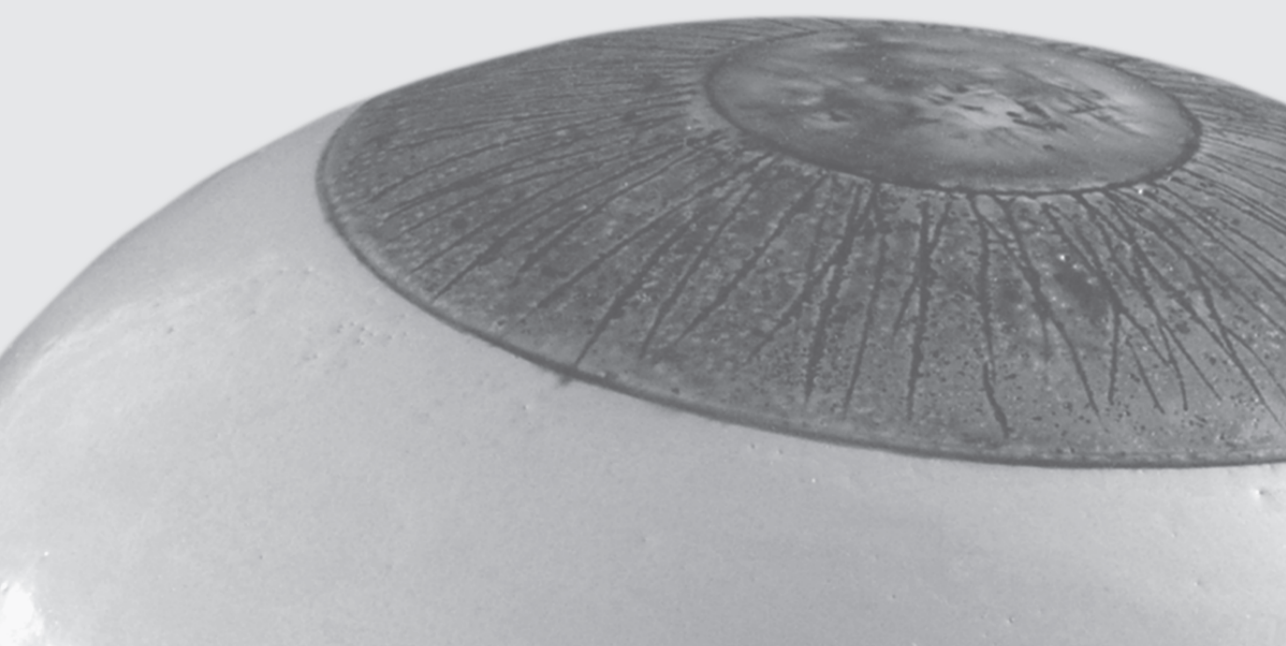
Besides determining the scatter intensity and angular dependence of light scattered by isolated capsule areas, the present study also assessed wavelength dependence. Detailed assessment of wavelength dependence showed that exponent b was approximately -1.5 in all capsule types, but with considerable variation. Especially in the fibrotic PCO and regenerative PCO areas, exponent b was less negative at the smallest angles, which indicates that the wavelength dependence decreases with decreasing angle. As described in the “angular dependence” subsection, a combined increased angular dependence and decreased wavelength dependence at the smallest angles of the angular range, was found in especially fibrotic (Figures 5C and 6C) and regenerative PCO areas (Figures 5D and 6D). According to optical light-scattering theory,^{15,16} the combination of these optical characteristics implies the presence of light spreading caused by refractile PCO-structures. As mentioned in the Introduction, light refraction is caused by structures much larger than the wavelength of light. Rod-like fibers present in fibrotic PCO and pearl-like structures present in regenerative PCO, could be such refractile structures. An example of light-spreading by refractile PCO structures is the Maddox-rod phenomenon described in the “angular dependence” subsection.

We expected the light-scattering characteristics of PCO to be drastically different from those of the crystalline lens, due to differences in morphological appearance. In the large-angle domain, light-scattering in the crystalline lens is dominated by particles of about 1 micrometer in size.^{15,16} However, cells that constitute PCO are much larger. So, the angular and wavelength dependencies found in the present study surprised us. Especially the wavelength dependence found in PCO clearly indicates that, based on physical-optical light-scattering theory,^{15,16} small particle light-scattering is also important in PCO. However, apart from small particle scattering, the current data also indicate that refractile effects become more important at smaller visual angles, as witnessed by the combination of stronger angular and weaker wavelength dependence.

REFERENCE LIST

1. Wormstone IM. Posterior capsule opacification: a cell biological perspective. *Exp Eye Res* 2002; 74:337-47.
2. Wormstone IM, Wang L, Liu CS. Posterior capsule opacification. *Exp Eye Res* 2009;88:257-69.
3. Apple DJ, Solomon KD, Tetz MR, et al. Posterior capsule opacification. *Surv Ophthalmol* 1992;37: 73-116.
4. van Bree MC, Zijlmans BL, van den Berg TJ. Effect of neodymium:YAG laser capsulotomy on retinal straylight values in patients with posterior capsule opacification. *J Cataract Refract Surg* 2008;34:1681-6.
5. van Bree MC, van der Meulen IJ, Franssen L, et al. Imaging of forward light-scatter by opacified posterior capsules isolated from pseudophakic donor eyes. *Invest Ophthalmol Vis Sci* 2011;52: 5587-97.
6. van den Berg TJ, Franssen L, Coppens JE. Straylight in the human eye: testing objectivity and optical character of the psychophysical measurement. *Ophthalmic Physiol Opt* 2009;29:345-50.
7. van den Berg TJ, IJspeert JK. Light scattering in donor lenses. *Vision Res* 1995;35:169-77.
8. van den Berg TJ. Depth-dependent forward light scattering by donor lenses. *Invest Ophthalmol Vis Sci* 1996;37:1157-66.
9. Kruijt B, van den Berg TJ. Effects of tissue fixation on light scatter by PCO. *Current Eye Research* 2012;37:159-61
10. Vos JJ, van den Berg TJ. Report on disability glare. CIE collection 1999;135:1-9.
11. de Waard PW, IJspeert JK, van den Berg TJ, de Jong PT. Intraocular light scattering in age-related cataracts. *Invest Ophthalmol Vis Sci* 1992;33:618-25.
12. IJspeert JK, de Waard PW, van den Berg TJ, de Jong PT. The intraocular straylight function in 129 healthy volunteers; dependence on angle, age and pigmentation. *Vision Res* 1990;30:699-707.
13. van den Berg TJ. Analysis of intraocular straylight, especially in relation to age. *Optom Vis Sci* 1995;72:52-9.
14. Vos JJ. Disability glare - a state of the art report. *Commission Internationale de l'Eclairage Journal* 1984;3/2:39-53.
15. van den Berg TJ. Light scattering by donor lenses as a function of depth and wavelength. *Invest Ophthalmol Vis Sci* 1997;38:1321-32.
16. van den Berg TJ, Spekrijse H. Light scattering model for donor lenses as a function of depth. *Vision Res* 1999;39:1437-45.
17. Eggers H. The Maddox-rod phenomenon. *AMA Arch Ophthalmol* 1959;61:246-7.
18. Rozema JJ, van den Berg TJ, Tassignon MJ. Retinal straylight as a function of age and ocular biometry in healthy eyes. *Invest Ophthalmol Vis Sci* 2010;51:2795-9.

19. van Bree MC, van Verre HP, Devreese MT, et al. Straylight values after refractive surgery: screening for ocular fitness in demanding professions. *Ophthalmology* 2011;118:945-53.
20. van den Berg TJ, Van Rijn LJ, Michael R, et al. Straylight effects with aging and lens extraction. *Am J Ophthalmol* 2007;144:358-63.
21. van der Meulen IJ, Engelbrecht LA, van Vliet JM, et al. Straylight measurements in contact lens wear. *Cornea* 2010;29:516-22.
22. van den Berg TJ, IJspeert JK, de Waard PW. Dependence of intraocular straylight on pigmentation and light transmission through the ocular wall. *Vision Res* 1991;31:1361-7.
23. Camparini M, Macaluso C, Reggiani L, Maraini G. Retroillumination versus reflected-light images in the photographic assessment of posterior capsule opacification. *Invest Ophthalmol Vis Sci* 2000;41:3074-9.



Chapter 8

Straylight values after refractive surgery: screening for ocular fitness in demanding professions

Maartje C.J. van Bree, Hedwig P. van Verre, Marina T. Devreese,
Frans Larminier, Thomas J.T.P. van den Berg

Ophthalmology 2011;118(5):945-53.



ABSTRACT

Purpose: To study straylight testing as a screening method for ocular fitness after refractive surgery in demanding professions and to determine the distribution of elevations in straylight as a result of refractive surgery in a nonresearch setting in contrast to earlier reports in research settings.

Methods: Data were collected as part of routine testing at The Queen Astrid Military Hospital (Belgium), an independent military institution responsible for medical fitness examinations. Intraocular straylight was measured using the commercially available C-Quant instrument (Oculus Optikgeräte GmbH, Wetzlar, Germany), using the psychophysical compensation comparison (CC) method. For the refractive surgery population 373 eyes in 198 subjects with a history of refractive surgery were selected. For the reference population 402 eyes in 214 young individuals without a history of refractive surgery were selected. Fellow eyes were compared to evaluate methodological aspects. The prevalence of impaired straylight values was evaluated for two age-independent cutoff criteria, a 2.0-fold and 3.2-fold increase, and an age-dependent cutoff criterion corresponding to an increase of 0.20 log units. Methodological aspects such as repeatability, systematic differences, and distance to impaired scores were assessed.

Results: The CC method exhibited good repeatability, and the chance of impaired scores due to variability in measurement was very small. The prevalence of impaired straylight values was minimal in the reference population. In the refractive population, 9% (33/373) of values were above the factor 2.0 criterion, 2% (7/373) were above the factor 3.2 criterion, and 12% (45/373) were 0.20 log units above the age reference.

Conclusions: Straylight testing is a viable screening method for ocular fitness after refractive surgery. Significant postoperative straylight elevations are more frequent in refractive surgery patients from the general population than in refractive surgery patients from high-quality research centers.

INTRODUCTION

Although overall patient satisfaction after refractive surgery is high, subjective symptoms, such as night vision disturbances and glare sensitivity, have been reported relatively frequently.¹⁻⁹ The effect of glare sensitivity resulting in visual impairment is called disability glare.¹⁰ Disability glare is a general phenomenon and is understood to be the effect of light-scatter in the eye. International agreement has defined disability glare as straylight.^{10,11} Straylight exerts its effect by reducing retinal sensitivity, which is even more relevant in conditions with retinal dysfunction, such as retinitis pigmentosa.^{12,13} Straylight can affect retinal sensitivity to a larger extent than the classical parameters of visual function: visual acuity and contrast sensitivity.¹⁴ The first studies of straylight in refractive surgery populations, including an early version of the straylight meter (direct compensation [DC] method),¹⁵⁻¹⁷ obtained different results. Some studies found strong deterioration, some found only slight deterioration, and yet others found no deterioration.^{2,18-24} Because of early positive results with regard to safety, efficacy, and quality of vision, photorefractive keratectomy (PRK) and laser-assisted in situ keratomileusis (LASIK) were accepted in some military organizations.^{22,25} With the introduction of the C-Quant instrument (Oculus Optikgeräte GmbH, Wetzlar, Germany) using the compensation comparison (CC) method, straylight measurement has become more reliable and applicable in a routine setting.^{26,27} The CC method is a recently developed psychophysical technique including a reliability check.²⁷ A validation study comparing the CC method with optical laboratory techniques showed virtually identical results.²⁸ An independent group verified the reliability.²⁶

Several research teams have used the C-Quant instrument in their own refractive surgery populations. The results have been surprisingly good; none of the teams found significant deterioration overall.^{2,29-31} However, all of the teams reported incidental cases of elevated straylight, with corresponding symptoms and clinical findings.^{2,29-31} Because these studies referred to patients at their own refractive surgery centers, one may wonder whether the results can be extrapolated.

In particular, one may wonder about the effects in a population of applicants for demanding professions (e.g., military, pilots) who have to meet strict requirements for visual function, and for whom dependence on glasses or contact lenses can be considered a hazard. Poor distance vision is the most common reason for medical disqualification,²⁵ and refractive surgery may be beneficial for applicants. However, the approval of refractive surgery in demanding professions is controversial because of exposure to difficult visual conditions (e.g., military operations at night) for which glare problems can be significant. In most guidelines for demanding professions, night vision and glare sensitivity are required to be normal. However,

specifications concerning the method of glare measurement and cutoff criteria for the test are lacking.

In the present study, the possible introduction of intraocular straylight as an ocular fitness criterion in demanding professions was evaluated. For such an introduction, a normal reference set is crucial. Whether reference data available in the literature correspond to findings in a testing center must be studied. Thus, to establish a reference population, straylight was studied in a group of young and healthy individuals visiting a testing center for approval of military function. To reduce potential confounding effects, eyes with uncorrected distance visual acuity (UDVA) of ≤ 0.00 log minimum angle of resolution (logMAR) (decimal ≥ 1.0) were selected.³² In addition, straylight was studied in eyes with a history of refractive surgery, with the refractive surgery being unrelated to the testing center. The present study could be used to judge the prevalence of impaired straylight values after refractive surgery in a nonresearch setting. Prevalence is important if straylight testing is introduced in testing centers. Thus, a choice must be made for the limit value in assessing impairment. A 2.0-fold increase in intraocular straylight compared to a young and healthy eye was used as the most strict limit value; a 2.0-fold increase in straylight was considered to correspond to the normal effect of aging in otherwise healthy eyes reaching 65 years.^{11,33,34} In the military, physical fitness is customarily assumed to be insufficient above 65 years of age for the most demanding tasks. In the present study, a 3.2-fold increase in straylight (normal at 79 years of age) was used as the limit value for less demanding professions. The 3.2 limit corresponds to an increase of 0.50 log units above the reference level for young and healthy eyes and is associated with self-reported driving difficulties, especially at night (European GLARE study; available at <http://www.glare.eu>, accessed January 4, 2013).^{14,35-37}

For the possible introduction of a new test for ocular fitness in demanding professions, several methodological requirements must be considered. A detailed overview of the requirements have been given by others, including criterion validity, face validity, construct validity, repeatability, discriminative ability, added value, applicability, and resistance to fraud.³⁶ Most of these criteria were met by an early version of the straylight meter that used the DC method.¹⁵⁻¹⁷ However, the DC method has some limitations concerning applicability and resistance to fraud.³⁶ The CC method was introduced to overcome these limitations.^{38,39} The CC method implemented in a laboratory-type instrument was used in the European GLARE study, the study from which data were used to establish a reference database for healthy eyes for the commercial C-Quant instrument.³⁴ Whether this reference database fits with the findings from the reference group in the present study was assessed in addition to evaluating the results with respect to methodological aspects and the prevalence of impairment.

METHODS

Data were collected as part of routine testing at The Queen Astrid Military Hospital (Brussels, Belgium), an independent military institution responsible for medical examinations imposed by the Belgian Governmental Department of Defense. The ocular fitness of military applicants is evaluated in an entrance examination. The primary purpose of the entrance examination is to establish whether the legal ocular fitness requirements are met. The secondary purpose is to determine a medical profile for admission to military functions. Military personnel with demanding functions have to continue to meet strict ophthalmologic requirements during the course of their career. The preservation of ocular fitness is evaluated during periodical re-examinations, annually in the most demanding professions.⁴⁰⁻⁴⁴

We used a reference population consisting of 214 young subjects with healthy eyes (average age 21 years, range 15-47 years). Only eyes with a UDVA of ≤ 0.00 logMAR were included.³² In 188 subjects, both eyes had a UDVA of ≤ 0.00 logMAR; 26 subjects had only one eye with a UDVA of ≤ 0.00 logMAR for a total of 402 eyes in the reference population. The refractive surgery population consisted of 373 eyes with a history of refractive surgery in 198 subjects (average age 35 years, range 19-56 years). LASIK had been performed on 162 eyes, radial keratotomy (RK) on 107 eyes, and PRK on 92 eyes. For 12 eyes, the exact refractive laser procedure was unknown. At the time of inclusion, 175 subjects had undergone treatment on both eyes and 23 had undergone treatment on 1 eye. Straylight was tested in all treated eyes. The UDVA ranged from 0.52 to 0.00 logMAR, and the mean UDVA was 0.03 logMAR.³² The postoperative period was not recorded but was required to be more than 6 months. Both study populations were recruited during the medical entrance examinations and reexaminations at Queen Astrid Military Hospital. Exclusion criteria included a history of ocular pathology and opacification of the ocular media that was not a consequence of refractive surgery. Because of the non-invasive study design, the institutional review board/ethics committee provided a waiver of consent. The study adhered to the guidelines of the Declaration of Helsinki.

Visual acuity was measured monocularly with natural pupil at 5m in a darkened examination room, using the CSO CP 3137 chart projector (optotypes, Sloan's letters with a linear progression; contrast, 100%; Pro-Vision Instruments, Bousval, Belgium), and recorded in decimal notation corresponding to the row in which the subject could correctly identify all optotypes. The decimal score was translated into logMAR for data processing and reporting. Abbreviations were used for visual acuity values, according to the format proposed by Kohnen.³²

Intraocular straylight was measured using the commercially available C-Quant instrument utilizing the CC method and expressed as the logarithm of the straylight parameter s , $\log(s)$. In young and healthy eyes, the European GLARE study obtained an average $\log(s)$ value of 0.87. As mentioned earlier, the reference set from this study was used as reference for the commercial C-Quant instrument. Because the reference value is important for job selection, whether small differences in the average $\log(s)$ values of young, healthy eyes in each testing center exist must be considered. First, differences may be related to the use of the prototype instrument versus the C-Quant instrument. Second, differences may be related to population differences. Third, small calibration differences might occur between instruments. Therefore, each testing center should establish its own reference population of young, healthy eyes. If this task is not feasible for practical reasons, reference values obtained from population studies using the actual C-Quant instrument should be used. Recently, two such population studies obtained reference $\log(s)$ values of 0.931 and 0.938.^{45,46} The present study obtained a reference $\log(s)$ value of 0.959. Starting from the reference value, intraocular straylight increases with age according to $\log(1+(\text{age}/65)^4)$.^{33,34} Therefore, the average $\log(s)$ value in healthy eyes increases by 0.30 log units at age 65, which corresponds to a 2.0-fold increase in straylight. The quality of each individual measurement is assessed in the C-Quant using two reliability parameters, the expected standard deviation (ESD) and the quality parameter (Q). The ESD is the most important parameter as it is predictive of the repeated-measures standard deviation (RM SD) of the straylight value $\log(s)$.²⁷ In the present study, individual straylight measurements were accepted when ESD was ≤ 0.08 and Q was ≥ 0.50 , excluding poor quality measurements. All testing was done with natural pupil diameter.

Data treatment and statistical analyses were performed with Excel 2003 (Microsoft Corp., Redmond, WA) and SPSS 15.0 (SPSS Inc., Chicago, IL). Significance was set at $p \leq 0.05$.

RESULTS

Figures 1 and 2 show $\log(s)$ values as a function of age for the reference and refractive surgery populations, respectively. The horizontal dashed line at $\log(s) = 0.959$ represents the average straylight value in a young, healthy eye, which was used as an age-independent straylight reference level. The factor 2.0 reference level (horizontal dashed line at $\log(s) = 1.26$) represents a doubling of the amount of straylight compared with the reference level. The factor 3.2 reference level (horizontal dashed line at $\log(s) = 1.46$) represents a straylight increase of 0.50 log units compared with the reference level.

The 95% confidence interval (CI) depicted in Figures 1 and 2 was derived from the standard deviation (SD) in the reference population, which was 0.14; corresponding to a 95% width

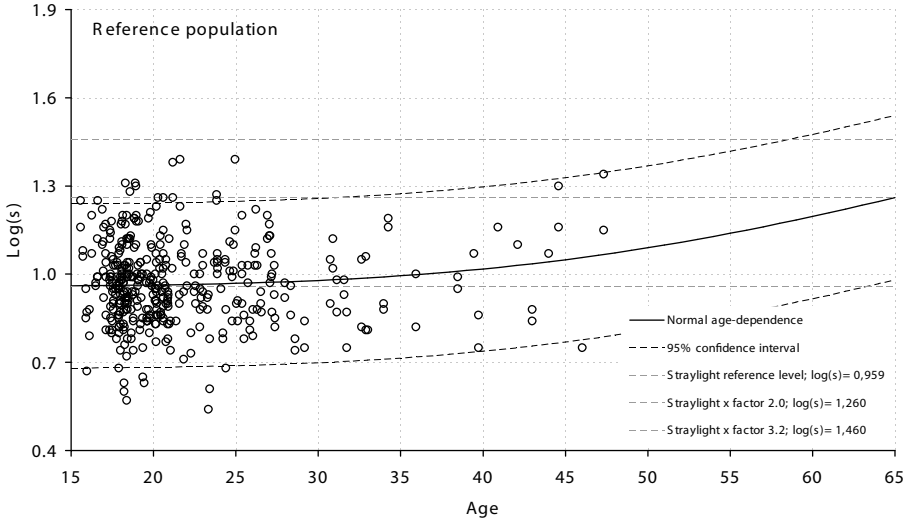


Figure 1. Straylight values ($\log(s)$) as a function of age for the reference population. The curved solid line represents the normal age-dependence of straylight. The curved dashed lines give the 95% confidence interval (CI) based on the spread with respect to the solid line. The horizontal dashed lines represent age-independent straylight reference levels of $\log(s) = 0.959$, $\log(s) = 1.260$, and $\log(s) = 1.460$.



Figure 2. Straylight values ($\log(s)$) as a function of age for the refractive surgery population. The curved solid line represents the normal age-dependence of straylight. The curved dashed lines give the 95% confidence interval (CI) based on the spread with respect to the solid line. The horizontal dashed lines represent age-independent straylight reference levels of $\log(s) = 0.959$, $\log(s) = 1.260$, and $\log(s) = 1.460$.

of 0.28 log units ($1.96 \times SD$). The width of a 95% CI reflects both measurement accuracy and physiological variation in the population. The European glare study showed an overall SD in the healthy population of 0.10 log units, corresponding to a 95% CI width of 0.20 log units.

Table 1. Prevalence of impaired straylight values above age-independent and age-dependent cutoff limits

Study populations	Eyes	Log(s) > reference level + 0.30 (straylight x factor 2)	Log(s) > reference level + 0.50 (straylight x factor 3.2)	> Upper limit 95% CI
Reference population	402	10/402 (2%)	0/402 (0%)	14/402 (3%)
Refractive surgery population	373	33/373 (9%)	7/373 (2%)	26/373 (7%)
Subpopulations	LASIK	162	10/162 (6%)	2/162 (2%)
	RK	107	13/107 (12%)	3/107 (3%)
	PRK	92	10/92 (11%)	2/92 (2%)
	LASIK/PRK (unknown)	12	0/12 (0%)	0/12 (0%)

CI= confidence interval, LASIK= laser in situ keratomileusis, PRK= photorefractive keratectomy, RK= radial keratotomy, log(s)= logarithm of the straylight parameter *s*

In that study, each eye was tested twice and the results averaged. In the present study, each eye was tested only once, so it can be understood that the spread is somewhat greater. The refractive surgery population had a SD of 0.16 log units.

Table 1 shows the number of eyes with straylight values above the cutoff limits for impairment (> factor 2.0 level; > factor 3.2 level). In the reference population, 2% of values were above the factor 2 level and none were above the factor 3.2 level. In the refractive surgery population, 9% of values were above the factor 2.0 level and 2% were above the factor 3.2 level. Figures 3 and 4 show how these elevations corresponded between fellow eyes. The second eye measurements are plotted vertically versus those of the first eye horizontally for both the reference population (376 eyes of 188 subjects) and refractive surgery population

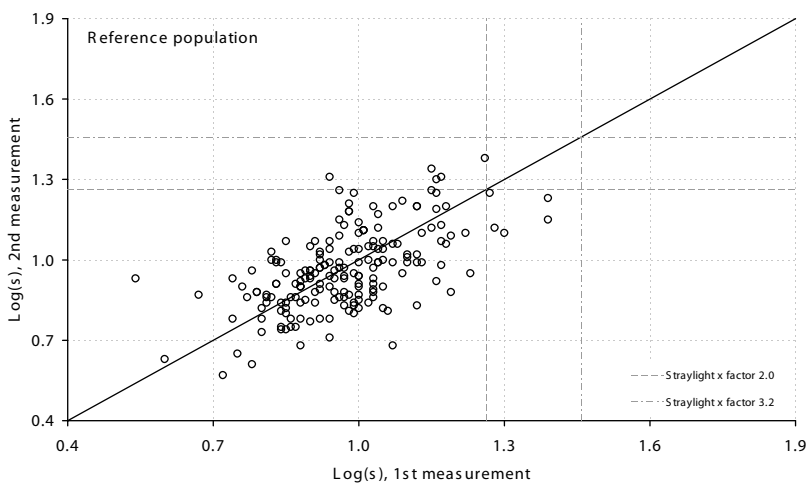


Figure 3. Correspondence of the straylight values (log[s]) between fellow eyes in the reference population. The dashed lines represent the factor 2.0 limit, and the dotted dashed lines represent the factor 3.2 limit.

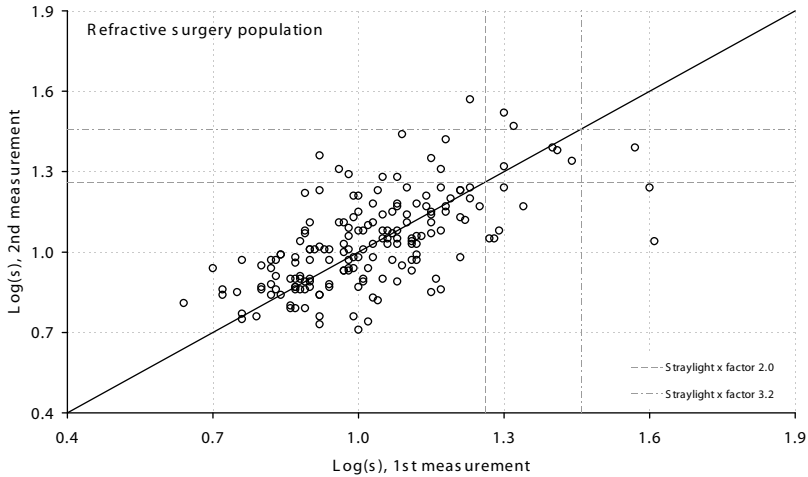


Figure 4. Correspondence of the straylight values ($\log[s]$) between fellow eyes in the refractive surgery population. The dashed lines represent the factor 2.0 limit, and the dotted dashed lines the factor 3.2 limit.

(350 eyes of 175 subjects). The vertical and horizontal dashed lines represent the factor 2.0 and factor 3.2 limits. Straylight values positioned to the right of the vertical reference level or above the horizontal reference level represent eyes with 2.0 \times or 3.2 \times the amount of straylight compared to the reference value $\log(s)=0.959$. When averages over fellow eyes were considered, 0% of subjects in the reference population (with both eyes tested) had values above the factor 2.0 level. In the refractive surgery population, 4% (7/175) had values above the factor 2.0 level and none were above the factor 3.2 level.

Figures 3 and 4 suggest the absence of systematic differences (e.g., no learning effect) between the first and second measurements. The mean differences between the first and second measurements were 0.007 and 0.011 log units for the reference and refractive populations, respectively, but both values were not statistically different from zero. Figures 5 and 6 show Bland-Altman plots, which can be used to assess a potential relationship between the $\log(s)$ differences of an individual and its mean and to assess variability over the range of measurement.^{47,48} Changes in the magnitude of the straylight parameter were not accompanied by changes in the differences.

As mentioned previously, each eye was tested only once in the present study. For this reason the RM SD of the present populations could not be calculated. However, the comparison of fellow eye measurements was used for an upper limit estimation of the RM SD. The differences between the first and second measurements in all subjects were determined and the SD was calculated and divided by $\sqrt{2}$. This calculation resulted in an upper limit estimation of 0.09 log units in the reference population and 0.10 log units in the refractive surgery

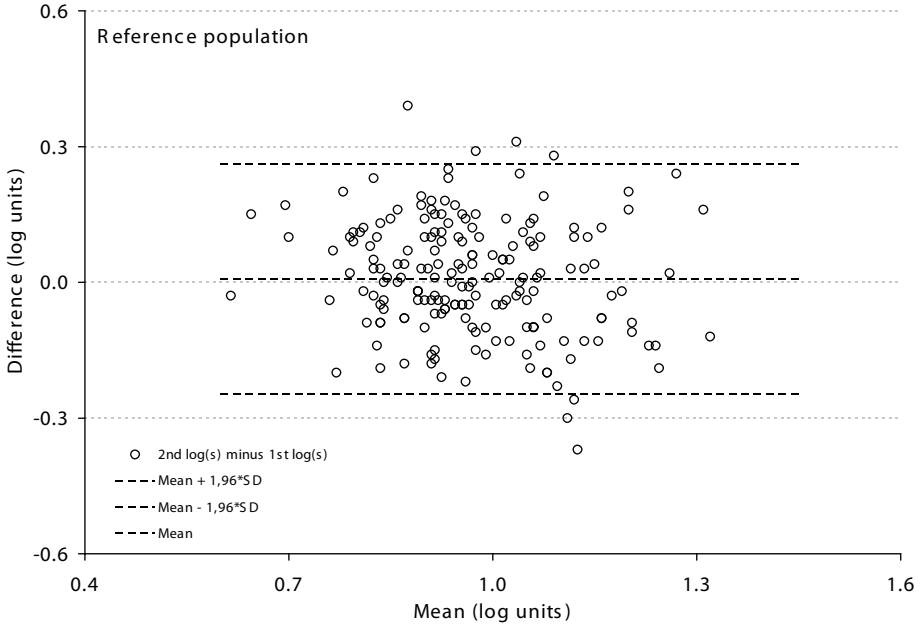


Figure 5. Bland-Altman plot for the straylight values in the reference population. The second straylight value minus the first straylight value is plotted against the mean.

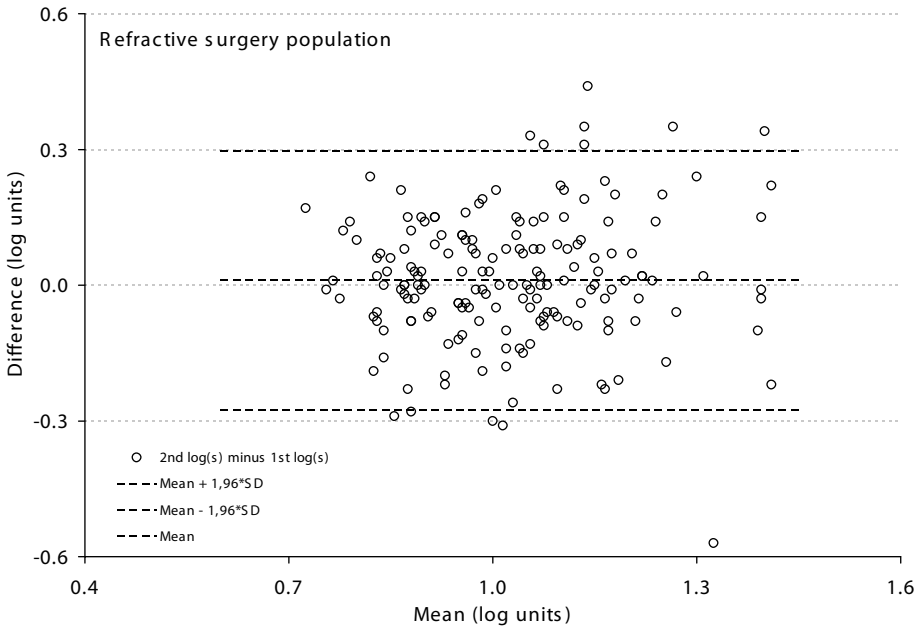


Figure 6. Bland-Altman plot for the straylight values in the refractive surgery population. The second straylight value minus the first straylight value is plotted against the mean.

Table 2. Repeatability coefficient, range of data, repeatability and distance to impaired scores

Population	Repeatability coefficient	Range	Repeatability (ratio RC/R)	Straylight x factor 2.0 limit Distance to impaired values (units RC)	Straylight x factor 3.2 limit Distance to impaired values (units RC)
Reference	0.20	0.85	0.23	1.52	2.53
Refractive surgery	0.20	0.97	0.20	1.52	2.53

RC= repeatability coefficient, R= range of data

population. Because of possible physiological differences between fellow eyes, the upper limit estimation of the RM SD is expected to be slightly higher than the true RM SD, especially for the refractive surgery population as structural differences between fellow eyes may be induced by the treatment itself or by differences in postoperative recovery. Assessment of the true repeatability of the CC method in the European GLARE study resulted in an RM SD estimation of 0.07 log units. The 1-sided F-test for analysis of variance showed that the SD values in the present populations, 0.09 and 0.10, are significantly different from 0.07 ($p < .0005$). This finding indicates that, in both populations, physiological differences exist between fellow eyes.

Table 2 shows the repeatability coefficient (RC), range (R) of data, repeatability (ratio RC/R), and distance to impaired scores for each population. The RC was calculated as the 0.07 log units (the true RM SD) multiplied by $2\sqrt{2}$.⁴⁷ The R was calculated as the difference between the obtained maximum and minimum log(s) value in the corresponding population. The repeatability was 0.23 in the reference population and 0.20 in the refractive surgery population. The 5th and 6th columns of Table 2 give the distance to impaired values, indicating the chance of an impaired test result in a perfect eye due to measurement variability. The distance to impaired values was calculated by dividing the increase in the log(s) value corresponding to a 2.0-fold and 3.2-fold increase in straylight (0.30 and 0.50 log units, respectively) by the RC. The distances to impaired values were 1.52 and 2.53 RC units, respectively.

Unreliable straylight measurements were detected by the reliability parameters Q and ESD (Figures 7 and 8). As mentioned earlier, ESD is considered to be the most efficient parameter, estimating RM SD.²⁷ In both study populations, the average ESD was 0.06 log units.

DISCUSSION

Visual perception is not the same as visual acuity. Some of the most common problems after refractive surgery are night vision disturbances and glare sensitivity, especially during nighttime driving.¹⁻⁹ These problems have been recognized in clinical practice since the

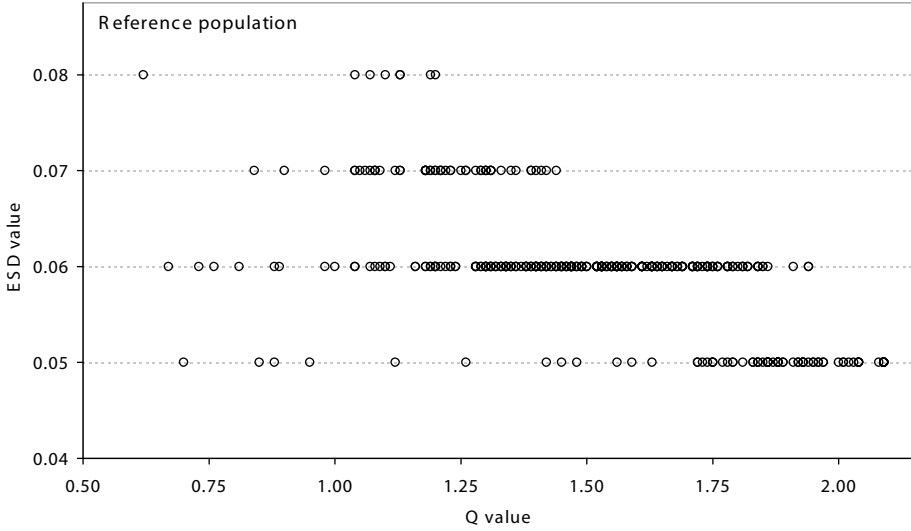


Figure 7. Reliability parameters expected standard deviation (ESD) and quality (Q) in the reference population.

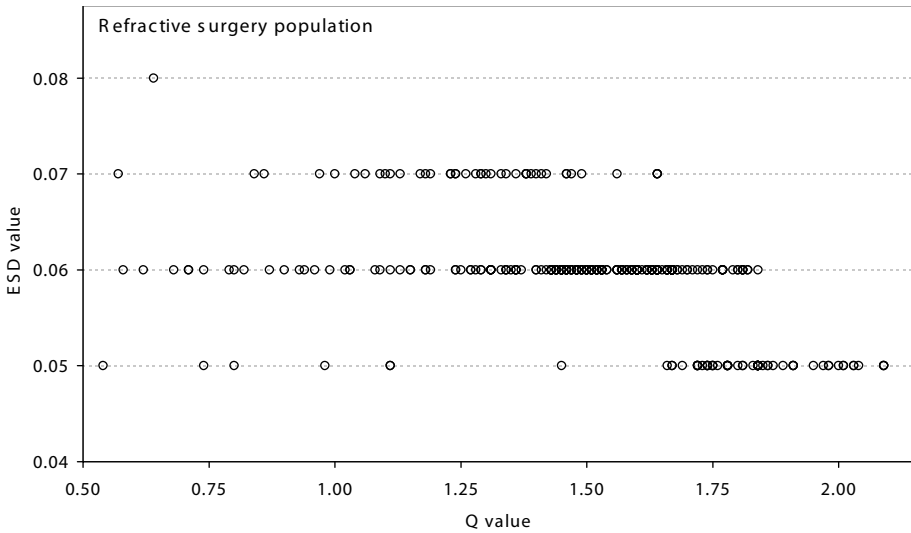


Figure 8. Reliability parameters expected standard deviation (ESD) and quality (Q) in the refractive surgery population.

beginning of refractive surgery. Forward scatter is at the root of glare. The normal cornea is not an important source of forward scatter. The corneal wound healing response after refractive surgery may result in clinically significant corneal haze due to changes in corneal cellularity (e.g., density and phenotype) or structure (e.g., disorganized extracellular matrix components).^{49,50} These changes can be a potential source of increased forward scatter.

Glare testing is clinically important to explain subjective symptoms after refractive surgery. Increased glare values are hypothesized to slow down the velocity of task execution in the presence of counter light, which can be critical in demanding situations. In this study, glare testing was used to evaluate the prevalence of impaired straylight values in a population of civil pilots and military personnel to evaluate the possible introduction of straylight testing as a screening method for ocular fitness in demanding professions. Relevant aspects, such as methodological requirements and potential cutoff criteria for the distinction between fitness qualification and disqualification, were addressed.

The methodological aspects studied were repeatability, systematic differences, and distance to impaired scores. The RM SD could not be calculated for the study populations; thus, straylight measurements in fellow eyes were used to obtain an upper limit estimation of the RM SD. As expected, these upper limit estimations were slightly higher compared to the true RM SD (0.07) obtained in the European GLARE study. Average values for the psychometrically established ESD were 0.06 in both groups. Therefore, the RM SD of both study populations is likely close to the earlier established value of 0.07. The results also suggest that true physiological differences exist between fellow eyes. This finding may not be surprising for the refractive surgery population, but it would be interesting for further study in the reference population.

Systematic differences between the first and second measurements, as well as the variability of differences over the range of measurement, were examined. Results showed that no effects exist for experience with the testing method or straylight level. This finding corresponds to earlier reports that the CC method is fraud-proof and reliable.^{26,27} The distances to impaired values indicate that the chance of impaired scores due to measurement variability is small for the factor 2.0 level and negligible for the factor 3.2 level, corresponding to the results in the reference population of 2% above the factor 2.0 level and 0% above the factor 3.2 level.

In the present study, the factor 2.0 level was used as a cutoff limit between normal and impaired log(s) values in demanding professions, and the factor 3.2 level for less demanding tasks. If the average value between both eyes is used for decision making, 4% (7/175) of the refractive subjects (both eyes measured) did not meet the factor 2.0 criterion, and all subjects did meet the factor 3.2 criterion. The factor 2.0 and 3.2 levels are age-independent and represent increases compared to a young and healthy eye.

The age-independent cutoff results may be less important for the clinician compared with the testing center. The clinician may be more interested in a change with respect to the preoperative situation (i.e., the treatment effect). If preoperative data are not available, the deviation from normal *for the respective age* can be used. The 95% CI in Figures 1 and 2

represents the age-dependent reference level of ± 0.28 (corresponding to $1.96 \times SD$ in the reference population; see also Table 1). The upper limit of the 95% CI can be used to distinguish between straylight increases related to normal aging and (additional) increases related to ocular pathology. Figure 2 shows 7 $\log(s)$ values above the factor 2.0 level but below the upper limit of the 95% CI. In these eyes, the increase in straylight could be induced by refractive surgery, represent normal aging, or be a combination of these factors.

The results obtained in the present study must be compared to data on refractive surgery cases in the literature.^{2,29-31} These data were obtained in patient populations at the respective research centers. In the present study, the refractive population was treated elsewhere in several clinical centers unrelated to the testing center, enabling a more general estimation of the prevalence of impaired straylight values after refractive surgery. In most earlier studies, a straylight increase of ≥ 0.20 log units after treatment was considered, which constitutes a significant functional change.^{2,29,30} The prevalence of increased straylight values after refractive surgery in the present study was compared to the prevalence found in 4 recent studies using the CC method (Table 3).^{2,29-31} As mentioned earlier, the results of recent studies have been surprisingly good. On average, straylight values after refractive surgery are not elevated. Only incidental cases of impaired straylight values have been observed. The prevalence of increased straylight values above the factor 2 level is highest in the present study compared to previous studies (Table 3). Thus, the prevalence of impaired straylight values may be different in subjects treated in research versus nonresearch settings.

Some practical considerations must be discussed if straylight testing is introduced in testing centers. First, a limit value needs to be defined for the assessment of impaired function. In the present study, a factor 2.0 level was used as cutoff limit between normal and impaired $\log(s)$ values in demanding professions because a 2.0-fold increase in straylight corresponds to the normal effect of aging in otherwise healthy eyes reaching 65 years and, in the military,

Table 3. Prevalence of impaired straylight values in the present study versus 4 recent studies using the compensation comparison method

Study	Refractive technique	Eyes	Average age	Post-operative period	Log(s) > ref. + 0.30 (straylight x factor 2.0)	Log(s) > ref. + 0.50 (straylight x factor 3.2)	Log(s) > 0.20 log units above age reference
Present study	LASIK, PRK, RK	373	35	6 months	33/373 (9%)	7/373 (2%)	45/373 (12%)
Beerthuisen ²	LASIK, PRK	24	-	1 month	0/24 (0%)	0/24 (0%)	3/24 (13%)
Lapid-Gortzak ²⁹	LASIK, LASEK	239	39	3 months	17/239 (7%)	3/239 (1%)	17/239 (7%)
Rozema ³⁰	LASEK	86	35	6 months	5/86 (6%)	0/86 (0%)	9/86 (10%)
Vignal ³¹	LASIK, PRK	52	32	12 months	3/52 (6%)	0/52 (0%)	4/52 (8%)

LASIK= laser in situ keratomileusis, LASEK= laser sub-epithelial keratomileusis, PRK= photorefractive keratectomy, RK= radial keratotomy, $\log(s)$ = logarithm of the straylight parameter s

it is assumed that in those aged older than 65 years of age, physical fitness is insufficient for the most demanding tasks. If this criterion is applied to the average log(s) value of both eyes, none of the present reference population and 4% of the refractive population would be disqualified.

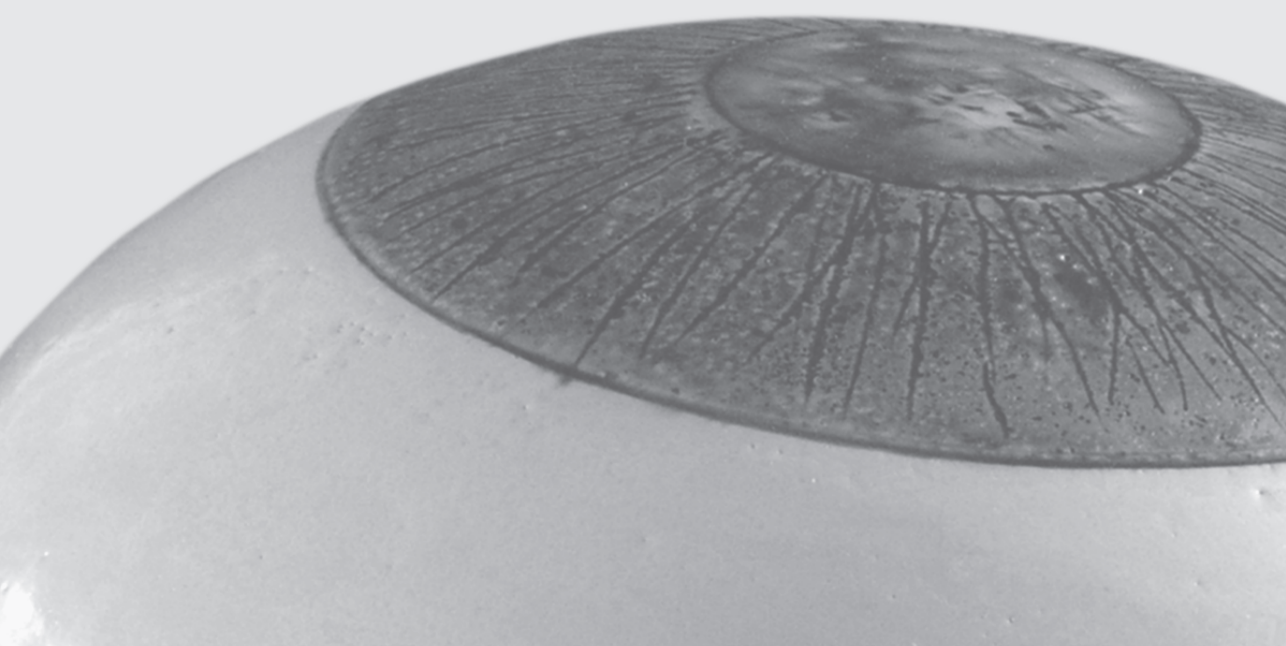
In conclusion, although patient satisfaction after refractive surgery is high in the general population, glare problems have been reported relatively frequently.^{1,2,4,6,7} Because glare can affect the velocity of execution of visually guided tasks, glare sensitivity is required to be normal for the most demanding professions. The present investigation studied straylight testing as a screening method for ocular fitness in demanding professions. Patients from the general population who have undergone refractive surgery had significant elevations more frequently than patients from high-quality research center populations. A 2.0-fold elevation on average for both eyes is suggested for use as a cutoff criterion for the most demanding professions. The application of this criterion in the present refractive population would result in a 4% disqualification rate.

REFERENCE LIST

1. Bailey MD, Mitchell GL, Dhaliwal DK, et al. Patient satisfaction and visual symptoms after laser in situ keratomileusis. *Ophthalmology* 2003;110:1371-8.
2. Beerthuizen JJ, Franssen L, Landesz M, van den Berg TJ. Straylight values 1 month after laser in situ keratomileusis and photorefractive keratectomy. *J Cataract Refract Surg* 2007;33:779-83.
3. Brunette I, Gresset J, Boivin JF, et al. Functional outcome and satisfaction after photorefractive keratectomy. Part 2: survey of 690 patients. *Ophthalmology* 2000;107:1790-6.
4. Fan-Paul NI, Li J, Miller JS, Florakis GJ. Night vision disturbances after corneal refractive surgery. *Surv Ophthalmol* 2002;47:533-46.
5. Hammond MD, Madigan WP Jr, Bower KS. Refractive surgery in the United States Army, 2000-2003. *Ophthalmology* 2005;112:184-90.
6. Krueger RR, Thornton IL, Xu M, et al. Rainbow glare as an optical side effect of IntraLASIK. *Ophthalmology* 2008;115:1187-95.
7. Pop M, Payette Y. Risk factors for night vision complaints after LASIK for myopia. *Ophthalmology* 2004;111:3-10.
8. Rajan MS, Jaycock PD, O'Brart B, et al. A long-term study of photorefractive keratectomy; 12-year follow-up. *Ophthalmology* 2004;111:1813-24.
9. Schallhorn SC, Tanzer DJ, Kaupp SE, et al. Comparison of night driving performance after wavefront-guided and conventional LASIK for moderate myopia. *Ophthalmology* 2009;116:702-9.
10. van den Berg TJ. On the relation between glare and straylight. *Doc Ophthalmol* 1991;78:177-81.
11. Vos JJ. Disability glare - a state of the art report. *Commission Internationale de l'Eclairage Journal* 1984;3/2:39-53.
12. Grover S, Alexander KR, Choi DM, Fishman GA. Intraocular light scatter in patients with choroideremia. *Ophthalmology* 1998;105:1641-5.
13. Grover S, Alexander KR, Fishman GA, Ryan J. Comparison of intraocular light scatter in carriers of choroideremia and X-linked retinitis pigmentosa. *Ophthalmology* 2002;109:159-63.
14. van den Berg TJ, van Rijn LJ, Kaper-Bongers R, et al. Disability glare in the aging eye. Assessment and impact on driving. *J Optom* 2009;2:112-8.
15. IJspeert JK, van den Berg TJ. Design of a portable Straylight Meter. *Conf Proc IEEE Eng Med Bio Soc* 1992;14:1592-4.
16. van den Berg TJ, IJspeert JK. Straylight Meter. In: *Optical Society of America, American Academy of Optometry. Noninvasive Assessment of the Visual System. Washington, D.C.: Optical Society of America; 1991:256-259. Technical Digest series. v. 1.*
17. van den Berg TJ IJspeert JK. Clinical assessment of intraocular straylight. *Appl Optics* 1992;31:3694-6.

18. Applegate RA, Trick LR, Meade DL, Hartstein J. Radial keratotomy increases the effects of disability glare: initial results. *Ann Ophthalmol* 1987;19:293-7.
19. Butuner Z, Elliott DB, Gimbel HV, Slimmon S. Visual function one year after excimer laser photorefractive keratectomy. *J Refract Corneal Surg* 1994;10:625-30.
20. Harrison JM, Tennant TB, Gwin MC, et al. Forward light scatter at one month after photorefractive keratectomy. *J Refract Surg* 1995;11:83-8.
21. Patel SV, Maguire LJ, McLaren JW, et al. Femtosecond laser versus mechanical microkeratome for LASIK: a randomized controlled study. *Ophthalmology* 2007;114:1482-90.
22. Schallhorn SC, Blanton CL, Kaupp SE, et al. Preliminary results of photorefractive keratectomy in active-duty United States Navy personnel. *Ophthalmology* 1996;103:5-22.
23. Veraart HG, van den Berg TJ, Ijspeert JK, Cardózo OL. Stray light in radial keratotomy and the influence of pupil size and straylight angle. *Am J Ophthalmol* 1992;114:424-8.
24. Veraart HG, van den Berg TJ, Hennekes R, Adank AM. Stray light in photorefractive keratectomy for myopia. *Bull Soc belge Ophtalmol* 1993;249:57-62.
25. Stanley PF. Laser refractive surgery in the United States Navy. *Curr Opin Ophthalmol* 2008;19:321-4.
26. Cerviño A, Montes-Mico R, Hosking SL. Performance of the compensation comparison method for retinal straylight measurement: effect of patient's age on repeatability. *Br J Ophthalmol* 2008;92:788-91.
27. Coppens JE, Franssen L, van Rijn LJ, van den Berg TJ. Reliability of the compensation comparison stray-light measurement method. *J Biomed Opt* 2006;11:34027.
28. van den Berg TJ, Franssen L, Coppens JE. Straylight in the human eye: testing objectivity and optical character of the psychophysical measurement. *Ophthalmic Physiol Opt* 2009;29:345-50.
29. Lapid-Gortzak R, van der Linden JW, van der Meulen JJ, et al. Straylight in hyperopic LASIK and LASEK. *Journal of Cataract and Refractive Surgery* 2010;In press.
30. Rozema JJ, Coeckelbergh T, van den Berg TJ, et al. Straylight before and after LASEK in myopia: changes in retinal straylight. *Invest Ophthalmol Vis Sci* 2010;51:2800-4.
31. Vignal R, Tanzer D, Brunstetter T. [Scattered light and glare sensitivity after wavefront-guided photorefractive keratectomy (WFG-PRK) and laser in situ keratomileusis (WFG-LASIK)]. *J Fr Ophthalmol* 2008;31:489-93.
32. Kohnen T. New abbreviations for visual acuity values. *J Cataract Refract Surg* 2009;35:1145.
33. van den Berg TJ. Analysis of intraocular straylight, especially in relation to age. *Optom Vis Sci* 1995;72:52-9.
34. van den Berg TJ, van Rijn LJ, Michael R, et al. Straylight effects with aging and lens extraction. *Am J Ophthalmol* 2007;144:358-63.
35. Relevance of glare sensitivity and impairment of visual function among European drivers 2005: 41. EU project: SUB-B27020B-E3-GLARE-2002-S07. 18091. Available at: http://www.glare.be/Rapport2004_33_wo_articles.pdf. Accessed January 4, 2013.

36. Assessment of vision function of driving-license holders. 2003:17-52. EU project: I-TREN E3 2007/SI282826. Available at: http://www.glare.be/EU_report2002%20.pdf. Accessed January 4, 2013.
37. van Rijn LJ, Nischler C, Gamer D, et al. Measurement of stray light and glare: comparison of Nyk-totest, Mesotest, stray light meter, and computer implemented stray light meter. *Br J Ophthalmol* 2005;89:345-51.
38. Franssen L, Coppens JE, van den Berg TJ. Compensation comparison method for assessment of retinal straylight. *Invest Ophthalmol Vis Sci* 2006;47:768-76.
39. van den Berg TJ, Coppens JE, inventors; Konink NL Akademie van Wetens, applicant. Method and device for measuring retinal stray light. European patent EP 1659929. May 31, 2006.
40. Royal Decree of medical fitness as a paratrooper and commando [in Dutch] [legislation]. Ministry of Defence. Bulletin of Acts and Decrees-Belgian Official Paper. *Belgisch Staatsblad*. April 27, 1999: 13864-71. Available at: <http://www.ejustice.just.fgov.be/cgi/welcome.pl>. Accessed January 4, 2013.
41. Royal Decree establishing the medical eligibility criteria for service as military [in Dutch] [legislation]. Ministry of Defence. Bulletin of Acts and Decrees-Belgian Official Paper. *Belgisch Staatsblad*. April 11, 2003:18394-461. Available at: <http://www.ejustice.just.fgov.be/cgi/welcome.pl>. Accessed January 4, 2013.
42. Royal Decree concerning medical fitness of military air traffic controllers [in Dutch] [legislation]. Ministry of Defence. Bulletin of Acts and Decrees-Belgian Official Paper. *Belgisch Staatsblad*. April 30, 2004:35931-41. Available at: <http://www.ejustice.just.fgov.be/cgi/welcome.pl>. Accessed January 4, 2013.
43. Royal Decree on the suitability for air service [in Dutch][legislation]. Ministry of Defence. Bulletin of Acts and Decrees-Belgian Official Paper. *Belgisch Staatsblad*. September 17, 2005:51387-93. Available at: <http://www.ejustice.just.fgov.be/cgi/welcome.pl>. Accessed January 4, 2013.
44. Royal Decree amending various provisions concerning the status of military. Ministry of Defence. Bulletin of Acts and Decrees-Belgian Official Paper. *Belgisch Staatsblad*. September 24, 2008: 49580-82. Available at: <http://www.ejustice.just.fgov.be/cgi/welcome.pl>. Accessed January 4, 2013.
45. Rozema JJ, van den Berg TJ, Tassignon MJ. Retinal Straylight as a Function of Age and Ocular Biometry in Healthy Eyes. *Invest Ophthalmol Vis Sci* 2010;51:2795-9.
46. van der Meulen IJ, Engelbrecht LA, van Vliet JM, et al. Straylight measurements in contact lens wear. *Cornea* 2010;29:516-22.
47. Bland JM, Altman DG. Statistical methods for assessing agreement between two methods of clinical measurement. *Lancet* 1986;1:307-10.
48. Bland JM, Altman DG. Measuring agreement in method comparison studies. *Stat Methods Med Res* 1999;8:135-60.
49. Dupps WJ Jr, Wilson SE. Biomechanics and wound healing in the cornea. *Exp Eye Res* 2006;83: 709-20.
50. Netto MV, Mohan RR, Ambrosio R Jr, et al. Wound healing in the cornea; a review of refractive surgery complications and new prospects for therapy. *Cornea* 2005;24:509-22.



Summary



The aim of this thesis is to evaluate whether the straylight parameter may be suited as an additional VF indicator in ophthalmic practice. VF has distinct functional domains: a small angle domain affected by aberrations causing blur, that can be assessed by VA and CS tests, and a large angle domain affected by light-scatter that can be assessed by straylight measurement. Ocular conditions, such as PCO, may affect the different VF domains to a different extent. Therefore, all VF parameters representing different functional domains should be tested. In this thesis, the relevance of straylight measurement for proper and objective VF assessment and clinical decision-making was evaluated: the straylight parameter was used to predict functionally beneficial treatment, and was used as a visual quality standard for ocular fitness.

In this thesis, PCO specimens obtained from human donor eyes were used. Images of real-world scenes were captured through the PCO specimens. The images illustrate how these particular PCO patients may have perceived those scenes. The images in **Chapter 3** demonstrate the importance of straylight for VF, by showing how straylight acts as a veil of light covering the entire scene, affecting perception of the scene. Furthermore, they demonstrate that despite the VA of the donors seems to have been unimpaired, VF seems to have been impaired by straylight. It emphasises that straylight and VA represent different aspects of visual quality.

The rather independent behaviour of straylight and VA was re-emphasised in **Chapter 4**, in which straylight by PCO was studied in-vivo, in cases with good and poor CDVA. Chapter 4 describes that half of the PCO cases with good VA had increased straylight values. So, in PCO cases with good VA there was no significant correlation between straylight and VA. Only in PCO cases with poor VA, a significant correlation between straylight and VA was found.

In **Chapter 5**, the effect of PCO severity and morphology on different aspects of VF, the small angle (VA testing [reported as the logarithm of the Minimum Angle of Resolution, logMAR] and CS testing) and the large angle domain (straylight testing [reported as the logarithm of the straylight parameter s , $\log(s)$]), was evaluated. Postcapsulotomy VF improvement was found to be related to PCO severity, rather than PCO morphology. VA and straylight impairment increase with increasing PCO severity. The relation between PCO severity and logMAR was curvilinear, whereas the relation between PCO severity and $\log(s)$ was linear. The linear relation between PCO severity and $\log(s)$ illustrates that the functional effect of slight PCO can already be documented by straylight measurement, whereas it can not be documented with VA testing. Therefore, straylight is more sensitive to slight PCO than VA. Furthermore, it was found that postcapsulotomy VF improvement is related to precapsulotomy VF values: postcapsulotomy improvement was largest in cases with substantially impaired precapsulotomy VF. The precapsulotomy $\log(s)$ value with a $\geq 50\%$ probability for a functionally significant treatment effect was 1.44. The precapsulotomy $\log(s)$ value with a $\geq 50\%$ probability for

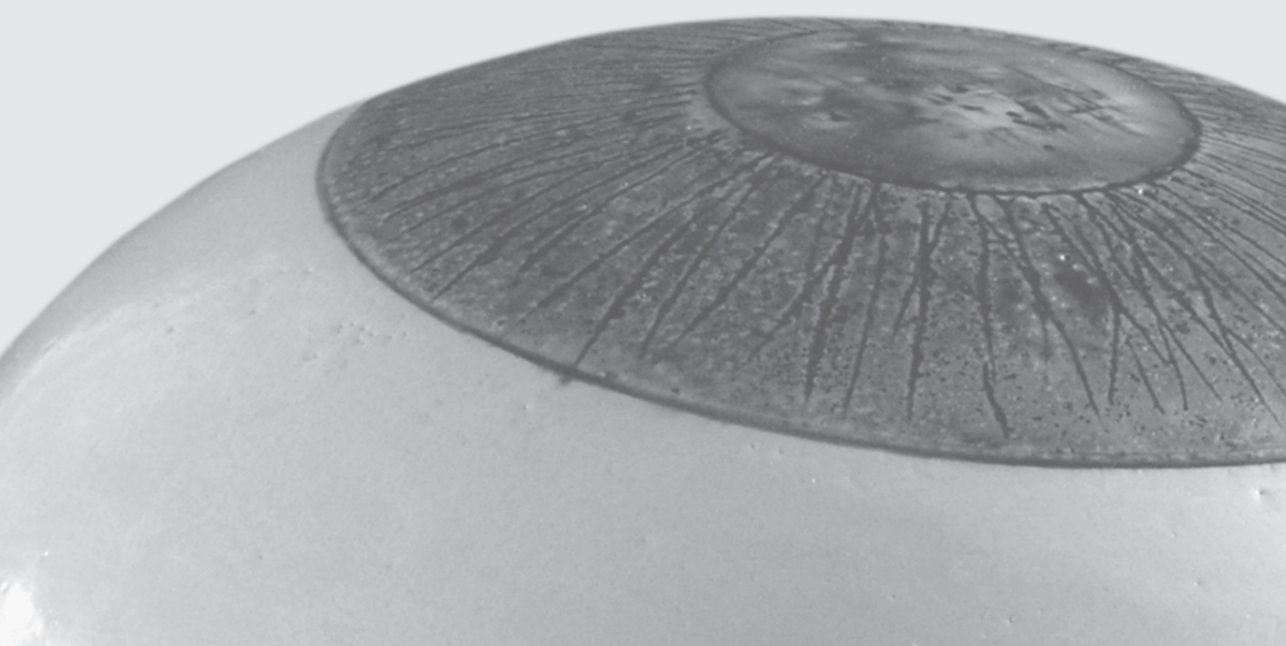
absent log(s) improvement was 1.22. These precapsulotomy log(s) values could be used as a clinical guide in deciding whether capsulotomy might be indicated. It can be concluded that straylight is a valuable, additional indicator for appropriate posterior capsulotomy referral.

In **Chapter 6**, light-scatter by PCO specimens obtained from human donor eyes was documented in-vitro. The specimens were of the fibrotic and regenerative type. The found angular and wavelength dependence of light scattered by PCO, indicate that the light scattering effect of small-sized PCO particles prevails over the effects of larger sized particles. However, the scatter characteristics not only indicate the presence of small, scattering particles, but also the presence of larger particles, such as rod-like structures in fibrotic PCO and pearl-like structures in regenerative PCO, that refract light. It was found that the ratio between small, scattering PCO structures and larger, refractile PCO structures is different for the two PCO types: in fibrotic PCO the ratio was in favour of small, scattering PCO structures, whereas in regenerative PCO the ratio was in favour of larger, refractile PCO structures. As a consequence, it was concluded that fibrotic PCO may affect straylight (large-angle domain) to a larger extent than VA (small-angle domain). The opposite may be the case in regenerative PCO: regenerative PCO may affect VA to a larger extent than straylight.

In **Chapter 7**, the intensity and optical characteristics of light-scatter by isolated lens capsule areas were recorded and compared to those in a young, healthy eye. Scatter intensities found in isolated capsule areas ranged from a factor 10 below (clear capsule areas) to a factor 10 above (PCO areas) the normal value for a young, healthy eye. The range of the in-vitro straylight values (scatter intensities) corresponded to in-vivo straylight values in pseudophakics. The angular dependence of light scattered by clear PC areas was weaker than that in the normal eye, whereas it was stronger in the other capsule areas. The wavelength dependence of scattered light was similar in all capsule areas. The wavelength dependence indicates that light-scatter by small particles is important in PCO. However, in PCO areas, a combined increased angular dependence and decreased wavelength dependence was found at small visual angles, which implies the presence of refractile PCO structures much larger than the wavelength of light. So, apart from the small, scattering particles that are important in PCO, it was also concluded that larger, refractile PCO structures become increasingly important at small visual angles.

In **Chapter 8**, straylight testing as an additional screening method for ocular fitness after refractive surgery, was studied in applicants for demanding professions. Potential cutoff limits for the distinction between fitness qualification and disqualification were addressed: a strict limit of $\log(s) \geq 1.26$ (average of fellow eyes), to be used in the most demanding professions, and a less strict limit of $\log(s) \geq 1.46$ (average of fellow eyes), to be used in less demanding professions. The strict limit corresponds to a 2-fold straylight increase, and the less strict limit

corresponds to a 3.2-fold straylight increase, as compared to a young, healthy eye (reference value: $\log(s) = 0.959$). Application of the factor 2 limit in the present population of applicants with a history of refractive surgery and an uncorrected distance VA ≤ 0.00 (logMAR), would result in a 4% disqualification rate. Methodological requirements of straylight measurement were addressed: repeatability was good, systematic differences were absent and the chance of impaired scores due to variability in measurement was small.



Summary in Dutch – Samenvatting



Het doel van dit proefschrift is het evalueren van de geschiktheid van de strooilicht parameter als additionele indicator voor visuele functie (VF) in de oogheekkundige praktijk. VF kent verschillende functionele domeinen: een kleine hoek domein dat beïnvloed wordt door aberraties en wazig zicht veroorzaakt, en een grote hoek domein dat beïnvloed wordt door lichtverstrooiing en onder andere verblindingsklachten veroorzaakt. Het kleine hoek domein kan beoordeeld worden met gezichtsscherpte en contrast gevoeligheids testen; het grote hoek domein kan beoordeeld worden met strooilichtmetingen. Oogaandoeningen zoals nastaar, kunnen de parameters die de verschillende VF domeinen representeren in verschillende mate beïnvloeden. Daarom zouden alle VF parameters die de verschillende functionele domeinen representeren getest moeten worden. In dit proefschrift is het belang van strooilichtmeting voor gedegen en objectieve VF beoordeling en klinische besluitvorming geëvalueerd: de strooilicht parameter is gebruikt om te voorspellen of behandeling functioneel effectief is, en daarnaast is de strooilicht parameter gebruikt als visuele kwaliteitsstandaard voor de oogheekkundige gezondheidstoestand.

In dit proefschrift werden nastaar preparaten afkomstig van menselijke donor ogen gebruikt. Door de nastaar preparaten heen werden opnamen gemaakt van de “werkelijke buitenwereld”. Deze opnamen werden gebruikt om te illustreren hoe de buitenwereld door de betreffende PCO patiënten zou kunnen zijn waargenomen. De opnamen in **Hoofdstuk 3** laten het belang van strooilicht voor VF zien: ze tonen hoe strooilicht als een lichtsluier het gehele visuele tafereel bedekt, wat de waarneming ervan sterk beïnvloedt. Daarnaast laten ze zien dat hoewel de donoren een goede gezichtsscherpte gehad lijken te hebben, de VF door strooilicht aangetast lijkt te zijn geweest. Dit benadrukt dat strooilicht en gezichtsscherpte verschillende aspecten van de VF vertegenwoordigen.

Het nogal onafhankelijke gedrag van strooilicht en gezichtsscherpte werd nog eens benadrukt in **Hoofdstuk 4**, waarin strooilicht door nastaar in patiënten met goede, danwel slechte gezichtsscherpte, werd bestudeerd. In Hoofdstuk 4 wordt beschreven dat de helft van de nastaar patiënten met een goede gezichtsscherpte een verhoogde strooilicht waarde heeft. Bij nastaar patiënten met een goede gezichtsscherpte werd er dan ook geen significant verband gevonden tussen strooilicht en gezichtsscherpte. Alleen in nastaar patiënten met een slechte gezichtsscherpte werd er een significant verband gevonden tussen strooilicht en gezichtsscherpte.

In **Hoofdstuk 5**, werd het effect van nastaar ernst en morfologie op verschillende aspecten van VF, namelijk het kleine hoek (gezichtsscherpte [gerapporteerd als de logaritme van de “Minimum Angle of Resolution”, logMAR] en contrastgevoeligheid tests) en grote hoek (strooilichtmeting [gerapporteerd als de logaritme van de strooilicht parameter s , $\log(s)$]) domein, geëvalueerd. Hoewel er een verband tussen postcapsulotomie VF verbetering en

nastaar ernst werd gevonden, werd er geen verband tussen postcapsulotomie VF verbetering en nastaar morfologie gevonden. Gezichtsscherpte en strooilicht verslechteren met toenemende nastaar ernst. Het verband tussen nastaar ernst en logMAR is curvilineair, daarentegen is het verband tussen nastaar ernst en log(s) lineair. Het lineaire verband tussen nastaar ernst en log(s) illustreert dat het functionele effect van geringe nastaar al vastgesteld kan worden met een strooilichtmeting, terwijl er geen effect vastgesteld kan worden met een gezichtsscherpte test. Daarom werd geconcludeerd dat strooilicht gevoeliger is voor geringe nastaar dan gezichtsscherpte. Bovendien werd gevonden dat postcapsulotomie VF verbetering gerelateerd is aan precapsulotomie VF waarden: postcapsulotomie verbetering was het grootst in gevallen waarbij de precapsulotomie VF substantieel was aangedaan. De precapsulotomie log(s) waarde waarbij er een kans $\geq 50\%$ bestaat op een functioneel significant behandelingseffect, was 1.44. De precapsulotomie log(s) waarde waarbij er een kans $\geq 50\%$ bestaat op het uitblijven van een behandelingseffect, was 1.22. Deze precapsulotomie log(s) waarden zouden gebruikt kunnen worden als klinische richtlijn bij de besluitvorming of capsulotomie wel of niet geïndiceerd is. Er kan geconcludeerd worden, dat strooilicht een waardevolle, additionele indicator zou kunnen zijn voor gepaste capsulotomie indicatiestelling.

In **Hoofdstuk 6**, werd lichtverstrooiing door nastaar preparaten, afkomstig van menselijke donor ogen, gedocumenteerd in een in-vitro setting. De preparaten waren van het fibrotische en regeneratieve type. De gevonden optische eigenschappen, namelijk de hoek- en golflengte afhankelijkheid, van licht dat wordt verstrooid door nastaar, laten zien dat het lichtverstrooiende effect van kleine nastaar deeltjes de overhand heeft boven het effect van grotere nastaar deeltjes. Desalniettemin duiden de lichtverspreidende eigenschappen niet alleen op de aanwezigheid van kleine, verstrooiende deeltjes, maar ook op de aanwezigheid van grotere deeltjes, zoals staafvormige fibrotische nastaar structuren en parelvormige regeneratieve nastaar structuren, die het licht breken. Er werd gevonden dat de ratio tussen kleine, lichtverstrooiende nastaar structuren en grotere, lichtbrekende nastaar structuren tussen de beide nastaar typen verschilt: in fibrotische nastaar is de ratio ten gunste van kleine, verstrooiende structuren, en in regeneratieve nastaar is de ratio ten gunste van grotere, brekende structuren. Derhalve werd geconcludeerd dat fibrotische nastaar een groter effect zou kunnen hebben op strooilicht (grote hoek domein) dan op gezichtsscherpte (kleine hoek domein). Het tegengestelde zou het geval kunnen zijn bij regeneratieve nastaar: regeneratieve nastaar zou een groter effect kunnen hebben op gezichtsscherpte dan op strooilicht.

In **Hoofdstuk 7**, werden de verstrooiingsintensiteit en de optische eigenschappen van lichtverstrooiing door geïsoleerde gebieden van het lenskapsel geregistreerd, en vergeleken met die in een jong, gezond oog. Verstrooiingsintensiteiten die gevonden werden in geïsoleerde kapsel gebieden varieerden van een factor 10 onder (heldere kapsel gebieden) tot

een factor 10 boven (nastaar gebieden) de normaal waarde van een jong, gezond oog. Het bereik van de in-vitro strooilichtwaarden (verstrooiingsintensiteit) kwam overeen met in-vivo strooilichtwaarden bij pseudofaken. De hoekafhankelijkheid van lichtverstrooiing door heldere kapselgebieden was zwakker dan dat in een normaal oog, terwijl het in andere kapselgebieden sterker was. De golflengte afhankelijkheid toont aan, dat er geconcludeerd kan worden dat lichtverstrooiing door kleine deeltjes belangrijk is in nastaar. Daarnaast werd in kapselgebieden met nastaar bij kleine visuele hoeken een gecombineerd toenemende hoekafhankelijkheid en afnemende golflengteafhankelijkheid gevonden, hetgeen de aanwezigheid van lichtbrekende nastaar structuren met een afmeting groter dan de golflengte van licht impliceert. Ondanks dat kleine lichtverstrooiende deeltjes het meest belangrijk zijn in nastaar, kan er daarom ook geconcludeerd worden dat grotere lichtbrekende nastaar structuren toenemend belangrijk worden bij kleine visuele hoeken.

In **Hoofdstuk 8**, werd de strooilichtmeting als aanvullende screeningsmethode voor oogheelkundige geschiktheid na refractieve chirurgie bestudeerd, in kandidaten voor veeleisende beroepsgroepen. Er werd stilgestaan bij mogelijke afkapwaarden voor het onderscheid tussen geschiktheidskwalificatie en diskwalificatie: een strenge limiet van $\log(s) \geq 1.26$ (gemiddelde van beide ogen), te gebruiken in de meest veeleisende beroepsgroepen, en een minder strenge limiet van $\log(s) \geq 1.46$ (gemiddelde van beide ogen), te gebruiken in minder veeleisende beroepsgroepen. De strenge limiet correspondeert met een 2-voudige strooilicht toename, en de minder strenge limiet correspondeert met een 3.2-voudige strooilicht toename, in vergelijking met een jong, gezond oog. Het toepassen van de factor 2 limiet op de huidige populatie van kandidaten, met een voorgeschiedenis van refractieve chirurgie en een ongecorrigeerde gezichtsscherpte in de verte van ≤ 0.00 (logMAR), zou resulteren in een diskwalificatie cijfer van 4%. Er werd stilgestaan bij methodologische vereisten voor strooilichtmeting: herhaalbaarheid was goed, systematische verschillen waren afwezig en de kans op aangedane waarden veroorzaakt voor meetvariabiliteit was klein.

Abbreviations

AC	Anterior capsule
ACO	Anterior capsule opacification
BAT	Brightness acuity tester
BCVA	Best corrected visual acuity
CC	Compensation comparison
CCD	Charge-coupled device
CDVA	Corrected distance visual acuity
CI	Confidence interval
CIE	Commission Internationale de l'Eclairage
CS	Contrast sensitivity
DC	Direct compensation
Deg.	Degrees
EPCO	Evaluation of posterior capsule opacification
ESD	Expected standard deviation
ETDRS	Early treatment diabetic retinopathy study
IOL	Intraocular lens
I_{total}	Total amount of light passing through the specimen
I_{θ}	Amount of light collected at scatter angle θ
LASIK	Laser-assisted in situ keratomileusis
LEC	Lens epithelial cell
Log(CS)	Logarithm of contrast sensitivity
log(s)	Logarithm of the straylight parameter s
logMAR	Logarithm of the minimum angle of resolution
Nd:YAG	Neodymium-doped Yttrium Aluminum Garnet
NEI	National Eye Institute
PBS	Phosphate-buffered saline
PC	Posterior capsule
PCO	Posterior capsule opacification
PMMA	Polymethylmethacrylate
PRK	Photorefractive keratectomy
PSF	Point spread function
Q	Quality
R	Range
RC	Repeatability coefficient
RK	Radial keratotomy

RM SD	Repeated-measures standard deviation
ROI	Region of interest
s	Straylight parameter s
SD	Standard deviation
UDVA	Uncorrected distance visual acuity
VA	Visual acuity
VF	Visual function
VFQ	Visual function questionnaire
VFQ-25/NL	Dutch consensus translation of the 25-item visual function questionnaire
θ	Scatter angle
θ^a	Angular dependence of intraocular straylight; exponent a
λ^b	Wavelength dependence of intraocular straylight; exponent b

PhD portfolio

PhD student:	M.C.J. van Bree	Promotor:	Prof.dr. J.C. van Meurs
Institution:	Rotterdam Ophthalmic Institute (ROI)	Supervisors:	Dr. T.J.T.P. van den Berg
PhD period:	December 2007 – June 2012		Dr. N.J. Reus Drs. B.L.M. Zijlmans

PhD training

	Year	Workload
General courses		
- Statistische begrippen in de medische literatuur – deel 1, Pfizer	2008	3 hours
- Statistische begrippen in de medische literatuur – deel 2, Pfizer	2008	3 hours
- Good clinical practice, ICH-training en advies	2008	8 hours
- Methodologie van patientgebonden onderzoek en voorbereiding van subsidieaanvragen – CPO minicursus, EMC	2009	8 hours
- Principles of Research in Medicine and Epidemiology, NIHES	2009	28 hours
- Biomedical English Writing and Communication, EMC	2010	28 hours
Specific courses (e.g. Research school, Medical Training)		
- Lens Opacities Classification System (LOCS III), L.T. Chylack	2010	24 hours
Seminars and workshops		
- Science day, Rotterdam Ophthalmic Institute	2008-2010	8 hours
- Science day, Rotterdam Ophthalmic Institute (oral presentation)	2011	16 hours
- 2nd Research Course in Ophthalmology & Visual Science, NIN	2010	8 hours
- 4e Themadag Oog en Werk, Amersfoort	2010	8 hours
- NIOIC symposium, Nijmegen	2010	8 hours
- Weekly Ophthalmology seminars, Rotterdam Eye Hospital	2007-2012	1 hour
- Monthly Scientific seminars, Rotterdam Eye Hospital	2007-2012	2 hours
- Monthly Scientific seminars, Rotterdam Ophthalmic Institute	2009-2012	1 hour
(Inter)national conferences		
Oral presentations / poster contributions		
- ESCRS annual meeting	2008	24 hours
- NOG annual meeting (oral presentation)	2008-2012	36 hours
- ARVO-NED annual meeting (oral presentation)	2009	16 hours
- ARVO annual meeting (oral presentation)	2009	80 hours
- ARVO annual meeting (poster contribution)	2011	76 hours
- SOE (poster contribution)	2010	24 hours
- Oogheelkundige Fysica dag, ROI (oral presentation)	2011	32 hours
- Oogheelkundige Fysica dag, NIN (oral presentation)	2011	32 hours
- Scientific seminar, ROI (oral presentation)	2010	12 hours
- Scientific seminar, ROI (oral presentation)	2011	12 hours

List of publications

- **van Bree MC**, Kruijt B, van den Berg TJ. Real-world scenes captured through posterior capsule opacification specimens: simulation of visual function deterioration experienced by PCO patients. *J Cataract Refract Surg* 2013;39(1):144-7.
- **van Bree MC**, Zijlmans BL, van den Berg TJ. Effect of neodymium:YAG laser capsulotomy on retinal straylight values in patients with posterior capsule opacification. *J Cataract Refract Surg* 2008;34(10):1681-6.
- **van Bree MC**, van den Berg TJ, Zijlmans BL. Posterior capsule opacification severity, assessed with straylight measurement, as main indicator of early visual function deterioration. *Ophthalmology* 2012;in press.
- **van Bree MC**, van der Meulen IJ, Franssen L, et al. Imaging of forward light-scatter by opacified posterior capsules isolated from pseudophakic donor eyes. *Invest Ophthalmol Vis Sci* 2011;52(8):5587-97.
- **van Bree MC**, van der Meulen IJ, Franssen L, et al. In-vitro recording of forward light-scatter by human lens capsules and different types of posterior capsule opacification. *Experimental Eye Research* 2012;96(1):138-46.
- **van Bree MC**, van Verre HP, Devreese MT, et al. Straylight values after refractive surgery: screening for ocular fitness in demanding professions. *Ophthalmology* 2011;118(5):945-53.

Dankwoord

Hoewel ik de inhoud van de andere hoofdstukken van dit proefschrift graag wil aanbevelen, realiseer ik me dat deze laatste alinea's door velen als enige, of toch zeker als eerste, gelezen zullen worden. Dat is begrijpelijk: het weerspiegelt de aard van het traject leidend tot de overige hoofdstukken. Een traject waar ik tevreden en met ontzettend veel plezier op terug kan kijken. Iedereen die er getuige van is geweest wil ik bedanken voor de belangstelling en betrokkenheid. Enkele personen zijn voor de totstandkoming van dit proefschrift onmisbaar geweest en wil ik in het bijzonder bedanken.

Tom, als co-promotor ben jij het dichtst bij dit promotietraject betrokken geweest. Van zó dichtbij dat ik eigenlijk beter kan zeggen dat je het traject met me meeliep. Een soort Tom-Tom die de route aangeeft, maar dan feilloos. Je moedigde me aan, of eigenlijk liep je alvast vooruit en probeerde wat van mijn verwachte aankomsttijd af te snoepen. Je efficiëntie hielp daar enorm bij: beantwoorden van mijn mailjes deed je meestal dezelfde dag, of anders toch zeker de ochtend erna zo rond 08:00 uur. Excuses voor al die keren dat ik van dat laatste zo handig gebruik heb weten te maken door 's avonds een berichtje achter te laten. TomTom had ook oog voor nuttige plaatsen langs de route: de studie in Brussel en het in-vitro project bij jou in het Nederlands Instituut voor Neurowetenschappen (NIN). Daarnaast waren er in het NIN vele manuscript sessies die bepalend waren voor de voortgang: met een soort vanzelfsprekendheid lag er 's ochtends bij aankomst een met rode pen gecorrigeerd manuscript op me te wachten. Door mij gereviseerde A4tjes verdwenen direct weer in jouw kamer waar ze in dezelfde sessie nog een 2^e, 3^e, correctieronde ondergingen (dezelfde pen, iets minder rood effect). Al die keren dat het tot mijn opluchting gelukt was om een inzichtelijk plotje uit de data te destilleren en jij er direct de merkwaardigheden uit haalde. Daarmee begon het wetenschappelijke proces pas echt. Parallel daaraan liep (loopt) mijn eigen leerproces waarvan de onbewust onbekwame fase al snel overging in een (nogal ongemakkelijke) bewust onbekwame fase (stelling 8). De bewust bekwame fase? Wie weet..... In ieder geval kan het leerproces doorgaan met de stapel data die nog klaarligt. Tom, ontzettend bedankt voor je gedrevenheid, expertise, kritische blik, bijsturing, geduld en betrokkenheid. Ook je betrokkenheid op persoonlijk vlak waardeer ik ontzettend. Ik heb het dan ook als bijzonder fijn ervaren dat je haarscherp doorzag wanneer er iets speelde dat voor mij belangrijk was.

Bart, jij bent vanaf het allereerste begin betrokken geweest bij dit project. Ik kwam bij je voor een 'oudste' coschap oogheelkunde. Met dat coschap wilde ik in de kliniek ontdekken of het vak nu echt iets voor me zou zijn. Omdat ik me er niet van bewust was dat een oudste coschap in het Oogziekenhuis een wetenschapscomponent heeft, was ik nogal verrast toen je vertelde dat er een strooilicht onderzoek op de plank lag waar ik mee van start kon.

Je loodste me mee naar het kamertje met de strooilightmeter, terwijl ik alleen maar kon denken 'dit is niet de bedoeling'. Maar uiteindelijk gingen mijn en jouw idee bij het coschap prima samen. Bedankt voor de kennismaking met dit, bij nader inzien, interessante onderwerp. Bedankt ook voor je improvisatievermogen op de dinsdagochtenden tijdens het laser spreekuur, wanneer ik weer eens net een patient teveel includeerde en daarmee de planning om zeep hielp. Met je ontspannen kijk op de zaken en relativiseringsvermogen hield je me op momenten dat het niet vlot liep, een spiegel voor.

Nic, in de eindfase van een manuscript mocht ik gebruikmaken van jouw frisse blik. Je optimisme en enthousiaste reacties waren een enorme stimulans. Je inzichten waren waardevol voor zowel de inhoud als de leesbaarheid van menig manuscript.

Prof.dr. van Meurs en Netty, bedankt voor jullie interesse en vinger aan de pols. Jullie enthousiasme tijdens de voortgangsgesprekken onttaarde vaak in een scala van mogelijke nieuwe onderzoeksopzetten ('zet je even een protocol op papier?'). Prof.dr. van Meurs, bedankt voor uw snelle acties wat betreft de 'hora est' aangelegenheden, toen met de start van mijn opleiding en het aankomend moederschap, mijn onrust om het boekje af te krijgen toenam.

Graag wil ik de leden van de promotiecommissie hartelijk bedanken voor de tijd en aandacht die ze aan mijn proefschrift hebben besteed.

Mijn bijzondere dank gaat uit naar de patienten van het Oogziekenhuis en hun begeleiders, de cataractgroep en de laserafdeling/poli OK voor bijdrage aan de dataverzameling. Cornea Bank Amsterdam, hartelijk dank voor de humane donor bulbi.

Luuk, Joris en Ivanka, wat ontzettend fijn dat ik de in-vitro studie van jullie mocht overnemen. Luuk, bedankt voor de gezelligheid tijdens de manuscript sessies. Maar ook voor het inwerken met de bijbehorende tips en trucs; zonder jou zat ik nu nog cuvetten te poetsen. Joris, bedankt voor alle keren dat je als razendsnelle troubleshooter beschikbaar was voor de goniometer. Ivanka, bedankt voor je interesse en enthousiasme op afstand. Bastiaan, met jouw elegante MacGyver-achtige vindingrijkheid werden de opnamen uit Hoofdstuk 3 een succes.

Hedwig, hartelijk dank voor de mooie dataset die jullie in het Militair Hospitaal Koningin Astrid verzamelden, en voor de prettige samenwerking aan het 'Brussel manuscript'.

Collega's in het Rotterdams Oogheelkundig Instituut, bedankt voor de goede sfeer en nuttige tips. Josine, Myrthe, Eva, Toine, Linda, Elsbeth, Sankha en 'de nieuwe garde' bedankt voor de gezellige lunches aan de grote tafel. Na de lunch op tijd weer aan de slag gaan was

een beproeving. Leuk dat we ook de opleidingsjaren in het Oogziekenhuis met elkaar zullen delen, ik kijk er naar uit!

Josine, wat was ik bevoorrecht met jou als kamergenoot! We konden urenlang uiterst geconcentreerd in stille werken, waarbij ik vele door jou gehaalde kopjes thee koud liet worden. Nuttige adviezen gingen over en weer, met af en toe wat gemopper (meestal van mijn kant) als het even tegen zat. Ik koester de bijzondere gesprekken over belangrijke zaken in het leven en bewonder je oprechtheid en onverstoobarheid enorm. Fijn om je als paranimf ook tijdens de verdediging naast me te hebben.

Nichtje Mariëlle, ploeggenoten Nienke, Martine en Cox, hoe herkenbaar waren jullie promotie perikelen. Bedankt voor de leuke koffiemomenten. Mariëlle, ik heb grote bewondering voor de manier waarop jij je door het afgelopen jaar hebt heengeslagen. Met al je daadkracht konden we op dezelfde dag naar de drukker.

Een goede balans tussen werk en ontspanning doet wonderen. Ploeggenoten van de Maas en Leonidas D24, het is heerlijk inspannend ontspannen met jullie. Kitty, Renee, Camilla, Mechteld, Jackelien, Eveline, Susanne en Ester bedankt voor jullie aanhoudende interesse en fantastische, jarenlange vriendschappen. Ester, met een promotietraject achter de rug adviseerde je me om goed na te denken voordat ik aan dit traject begon. Het heeft me niet ontmoedigd, maar maakte wel dat ik voorbereid was op de iets minder leuke momenten.

Ton en Annelies, doordat de laatste weken van mijn zwangerschap en promotietraject samenvielen met de eerste weken van mijn opleiding, hebben jullie mijn zwangere buik minder vaak kunnen zien dan gehoopt. Weet dat jullie enthousiasme over het grootouderschap en de betrokkenheid bij Careen voor ons ontzettend waardevol zijn.

Lieve papa en mama, jammer dat er maar 2 paranimfen mogelijk zijn. Maar op gegeven moment komt er een tijd van ontspannen achteroverleunen, wetende dat je het als ouders fantastisch hebt gedaan. Dat moment is aangebroken. Als wij voor Careen hetzelfde kunnen betekenen, dan zijn we dik tevreden!

Gezinnetje Beekers, lieve Bregje, weet dat ik stiekem onder de indruk ben van de manier waarop je, ogenschijnlijk moeiteloos en zonder enige twijfel, trouw bent aan je prioriteiten in het leven.

Wat voor team? Het leukste team! Het beste team! Youp, wat ben ik ontzettend gelukkig met het team dat we samen vormen. 'Dit is waar het om draait.' Jouw integriteit, onvoorwaardelijke hulp, uitzonderlijk probleemoplossend vermogen en scherpe oog voor wat voor het

team belangrijk is, zorgt voor de fijnste thuisbasis die ik me kan wensen. Ik ben ontzettend trots en dankbaar dat je met de komst van Careen de overstap maakte van 'X5 naar Lijn 5', van McKinsey naar de niet minder uitdagende RET, om zo het team voldoende flexibiliteit te geven. Ik hoop met jou en ons heerlijke kindje stokoud te worden.

About the author

Maartje was born on October 29th 1979 in Tilburg. After graduation from the Cambreur College secondary school in Dongen, she studied Psychology at Maastricht University, and ultimately started medical school in 2000 at Erasmus University Rotterdam. During medical school she worked at the 'Star Medical Diagnostic Center' in Rotterdam, and participated in research projects at Erasmus Medical Center: (1) the Generation R Study, a prospective cohort study from foetal life until young adulthood in a multi-ethnic urban population, designed to identify early environmental and genetic causes of normal and abnormal growth, development and health, and (2) Integrated Primary Care Information, a post marketing surveillance on drugs and research based on data from the electronic patient records of Dutch general practitioners. In 2001 she joined the student rowing club 'A.R.S.R. Skadi' in Rotterdam and started rowing on a national level until 2004, when she started her internship. She completed a scientific internship in The Rotterdam Eye Hospital. In July 2007 she obtained her medical degree and started working as a resident at the Cardiac Surgery Department at Haga Hospital in The Hague. From December 2007-December 2008 she started her research on retinal straylight at The Rotterdam Eye Hospital, which was continued as a PhD project at the Rotterdam Ophthalmic Institute from December 2008-June 2012. In July 2012 she started her residency in Ophthalmology at the Rotterdam Eye Hospital.

